Stories from the wall: Envelope-associated functions in bacteria. Focus on cell wall synthesis, protein secretion & signal transduction machineries.

Antoine P. Maillard

Stories from the wall:

Envelope-associated functions in bacteria

Focus on cell wall synthesis, protein secretion & signal transduction machineries.

Mémoire en vue d'obtenir l'Habilitation à Diriger des Recherches

UFR de Chimie-Biologie – Université Grenoble Alpes

Antoine Maillard

Bacterial Pathogenesis & Cell Responses, dir. Ina Attrée

Biology of Cancer & Infection, dir. Jean-Jacques Feige

Interdisciplinary Research Institute in Grenoble, dir. Jérôme Garin

Soutenue publiquement le mercredi 22 mai 2019 devant le jury composé de :

Mme le Prof. Sophie BLEVES, rapportrice
Mme le Dr. Françoise JACOB-DUBUISSON, rapportrice
M. le Dr. Jean-Michel JAULT, rapporteur
Mme le Prof. Christelle BRETON, présidente
Mme le Dr. Cécile BREYTON, examinatrice
Mme le Dr. Ina ATTREE-DELIC, examinatrice

La inspiración existe, pero tiene que encontrarte trabajando.

Pablo Picasso (1881 – 1973)

Acknowledgements - Remerciements

Mes premiers remerciements vont aux membres de mon jury d'habilitation, tout particulièrement aux deux rapportrices et au rapporteur qui ont accepté de consacrer leur expertise et une part appréciable de leur temps à l'évaluation de mon travail. Votre implication à tous m'honore et m'oblige.

Mme le Pr. Christelle Breton a été le guide et le censeur de mes démarches en tant que directrice de l'Ecole doctorale de chimie et des sciences du vivant de l'Université de Grenoble. Christelle Breton a présidé le jury de thèse de Widade Ziani dont j'étais co-encadrant. Dans toutes ces circonstances, j'ai bénéficié d'une écoute à la fois rigoureuse, opérationnelle et, m'a-t-il semblé, bienveillante : je suis très reconnaissant à Christelle Breton d'avoir accepté la présidence de ce jury d'habilitation.

Mme le Pr. Sophie Bleves a une expérience riche et diversifiée des systèmes de sécrétion et de la virulence bactérienne. Par ses travaux en effet, Sophie Bleves a contribué / contribue / contribuera certainement encore à caractériser les voies de sécrétion de type 2, 3, 5, 6… Rencontre récente, je suis heureux que Sophie Bleves ait accepté de juger mon travail en tant que rapportrice et l'en remercie chaleureusement.

Mme le Dr. Françoise Jacob-Dubuisson a baptisé les systèmes TPS, dont j'étudie désormais un exemple. Un travail intense, des collaborations fructueuses et des approches diversifiées ont, malgré les spécificités de FHA du bacille de la coqueluche, rendu ce modèle incontournable pour qui tente de comprendre la fonction d'export de ces machines. Un autre volet majeur de ses recherches, que je connais moins, porte sur un système à deux composants, régulateur majeur de la virulence de *Bordetella pertussis*. Je suis honoré que Françoise Jacob-Dubuisson ait accepté de juger mon travail en tant que rapportrice et l'en remercie infiniment.

M. le Dr. Jean-Michel Jault fait partie de ceux qui m'ont accueilli à l'Institut de Biologie Structurale. Pendant les premières années, Jean-Michel Jault a suivi les progrès du projet Cnr à travers réunions et discussions au sein du Laboratoire des Protéines Membranaires. Sa grande culture, sa disponibilité et sa bienveillance s'exercent maintenant à Lyon et je le remercie vivement d'avoir accepté d'évaluer mon travail en tant que rapporteur.

Mme le Dr. Cécile Breyton est elle-aussi une collègue de l'IBS. Il m'avait été donné de citer son travail sur le système Sec avant même de la rencontrer. Cécile Breyton a suivi les avant-derniers progrès du projet Cnr en tant que membre du Comité de suivi de thèse de Widade Ziani. Je lui suis très reconnaissant d'avoir accepté de participer à mon jury d'habilitation.

Mme le Dr. Ina Attrée-Delic dirige le groupe de recherches Pathogenèse Bactérienne et Réponses Cellulaires dont je fais partie depuis août 2016. Son accueil chaleureux, sa confiance et ses encouragements sont autant de raisons de lui exprimer ma profonde reconnaissance, qui va donc bien au-delà de sa participation à ce jury.

J'ai eu la chance de croiser ou d'accompagner quelques personnes que je suis heureux de pouvoir remercier ici. Certaines ont contribué de près ou de loin à façonner le chercheur que je suis, faisant un métier de ce qui était une vocation. D'autres ont joué un rôle plus ponctuel. Je fais confiance aux personnes concernées pour restituer la reconnaissance, l'affection ou l'admiration que je leur porte.

Merci à ceux qui m'ont fait grandir au début de ma carrière : Yves Gaudin, Michel Arthur et Franck Duong.

Merci à Jean-Jacques Feige, Jérôme Garin et Eva Pebay-Peyroula qui m'ont fait confiance et m'ont accueilli dans leurs laboratoires / instituts de recherches.

Merci à Thierry Vernet et Franck Fieschi pour leur accueil et leur générosité quand j'ai manifesté mon intérêt pour travailler à l'Institut de Biologie Structurale.

Merci à Michel Morange, Michel Goldberg, Dominique Anxolabéhère, Claude Nespoulous, Anne Wisner, Gilles Rivière, Michael Domanski, Eric Guittet, Anne Flamand, Félix Rey, Ghada Ajlani, Bruno Robert, Stéphane Mesnage, Jean-Emmanuel Hugonnet, Claudine Mayer, Régis Villet, Anne-Charlotte Sentilhes, Meriem Alami, Dominique Belin, Nhâm Nguyen, Florence Baudin et Rob Ruigrok. *(les vies d'avant)*

Merci à Richard Kahn, Eric Girard, Juliette Trepreau, Widade Ziani, Isabelle Petit-Härtlein, Eve de Rosny, Stephan Lacour, Annie Kolb, Jacques Covès, Kouloud Mahroug et Loïc Grandvuillemin. Merci aussi à Eric Forest. *(cnr)*

Merci à Juan-Carlos Fontecilla-Camps, Yvain Nicolet, Anne Volbeda, Patricia Amara, Claudine Darnault, Lydie Martin, Monika Spano, Franck Borel, David Cobessi, Xavier Vernède et Jean-Luc Ferrer. *(go metallo !)*

Merci à Caroline Mas, Michel Vivaudou (XL !!!), Christophe Moreau, Jean Revilloud, Isabel Ayala, Lionel Imbert, Michel Thépaut, Céline Julian-Binard, Corinne Vivès, André Zapun, Claire Durmort, Cécile Morlot, Jérôme Dupuy, Nicole Thielens, Christine Ebel, Hugues Lortat-Jacob et Jacques Neyton.

Merci à mes désormais-'collaborateurs de l'IBS Daphna Fenel, Guy Schoehn, Jean-Marie Teulon, Jean-Luc Pellequer, Quentin Bertrand et Andrea Dessen, pour nos échanges : si ExlA a une forme, nous la découvrirons !

Merci à mes collègues du laboratoire de Biologie du Cancer et de l'Infection pour leur bon accueil. Je n'en cite que quelques-uns : Nadia Alfaidy, Sabine Bailly, Nadia Cherradi, Claude Cochet, Odile Filhol-Cochet, Laurent Guyon et en particulier Isabelle Vilgrain pour ses conseils de biochimie (!) et ses dons de matériel. Nos réunions hebdomadaires sont une véritable invitation à l'introspection biologique pour le microbiologiste que je suis !

Merci à Belinda Champagne, Amandine Morand et Anaëlle Dumazer dont le sérieux et l'implication ont été ou sont bien utiles pour étudier ExlA.

Bravo à Sylvie Elsen, Philippe Huber, Stéphanie Bouillot, Eric Faudry, Mylène Robert-Genthon, Viviana Job, Michel Ragno, François Cretin, Petar Panchev, Claire Bama et Marie-Pierre Mendez, ainsi qu'à Pauline Basso, Emeline Reboud, Alice Berry, Vincent Déruelle, Tuan-Dung Ngo, Stéphane Pont, Julian Trouillon et Manon Janet-Maître qui, avec Ina, font ou ont fait de l'équipe Pathogenèse bactérienne et réponses cellulaires un labo si riche et si vivant !

Il n'y a pas que la science qui avance !

Je pense très fort à mes parents, mes sœurs, mon frère, leurs conjoints et leurs enfants.

Je pense aussi aux amis que l'on fait et à ceux que l'on retrouve, autour du bac à sable ou quelques centaines de kilomètres plus loin.

A tous, je dis : c'est miraculeux de vous (re)trouver !

Ce manuscrit est dédié à…

Anne

Mathilde

Charles

Summary

Abbreviations

ASD	anti-sigma domain
AT	autotransporter
ATP	adenosine triphosphate
CD	circular dichroism
CDF	cation diffusion facilitator
CL	cardiolipin
cryoEM	cryo-electromicroscopy
DDM	β-D-dodecylmaltoside
DTSSP	3,3'-dithiobis(sulfosuccinimidyl propionate)
ECF	extra-cytoplasmic function
EM	electromicroscopy
EPR	electron paramagnetic resonance
FHA	filamentous hemagglutinin
GFP	green fluorescent protein
GNAT	Gcn5-related N-acetyl transferase
IM	inner membrane
LPS	lipopolysaccharide
MS	mass spectrometry
OM	outer membrane
PA	phosphatidic acid
PBP	penicillin-binding protein
PC	phosphatidylcholine
PE	phosphatidylethanolamine
PFT	pore-forming toxin
PG	peptidoglycan
PI	phosphatidylinositol
PL	phospholipid
PMF	proton-motive force
POTRA	polypeptide transport-associated
PS	phosphatidylserine
PVDF	polyvinylidene fluoride
RBC	red blood cell
RND	resistance nodulation and cell division
RP	RNA polymerase
SDS	sodium dodecylsulfate
SPase	signal peptidase
SRP	signal recognition particle
TnS	type n secretion
TnSS	type n secretion system
TA	teichoic acid
TAT	twin-arginine translocase
TF	trigger factor
TG	transglycosylase
TIC	transcription intiation complex
TM	transmembrane
TP	transpeptidase
TPS	two-partner secretion
TPSS	two-partner secretion system
UM5K	UDP-MurNAc-pentapeptide

List of figures

CV

Antoine MAILLARD

Born in Paris on may, 15th 1973 – 45 years old.

Father of two – 9 and 7 years old.

Biochemist with a strong interest for structural and genetic approaches in microbiology.

Researcher at the CEA research center in Grenoble since october 2007.

antoine.maillard@cea.fr

Lab **Biologie du Cancer et de l'Infection** CEA / DRF / IRIG / DS / BCI / PBRC

Team **Pathogenèse Bactérienne & Réponses Cellulaires** 17, avenue des Martyrs

Tel +33 4 38 78 35 74 38054 Grenoble cedex 9

Education

12/01 Doctorat de Biochimie from the Université Pierre et Marie Curie – Paris 6 grade TH

Jury: MM. MORANGE (president), LE MAIRE, DUBUISSON & GAUDIN (supervisor)

NB: written congratulations from the jury have been forbidden at Paris 6 starting september 2001

12/00 - 09/01 Military duty – scientist at the CEA research center in Saclay – DBJC – SBFM.

09/97 DEA de Structure, Fonction & Ingénierie des Protéines – Paris 6 grade AB

Dir. A. CHAFFOTTE, M. DESMADRIL, M. GOLDBERG, J. JANIN, M. MORANGE

06/96 Maîtrise de Biochimie – Paris 6 grade AB

Major in biochemistry & biophysics (3rd/210) (dir. C. MARION)

Optional modules: Molecular biology of Eukaryotes (dir. M. MORANGE)
In vitro genetics (dir. B DUJON)
Interactions between plants and microorganisms (dir. G BOMPEIX)

06/95 Licence de Biochimie – Paris 6 grade AB

Major in biochemistry & molecular biology (11th/188) (dir. P. SARTHOU)

Mandatory modules of Organic chemistry (dir. A. MARQUET) and Classical genetics.

06/90 Baccalauréat C (Math & Physics grade AB, followed by 3 years Math Sup & Math Spé Bio)

Research experience

08/16 - present Institut de Recherche Interdisciplinaire de Grenoble (IRIG)

team Bacterial pathogenesis & cellular responses – Ina ATTREE

Pseudomonas aeruginosa virulence.

10/07 - 07/16 Institut de Biologie Structurale – Grenoble

team Heavy Metal & Signaling – Jacques COVES

Transmembrane signaling in response to an extracellular stress agent in proteobacteria.

10/06 - 09/07 Institut de Virologie Moléculaire et Structurale – Grenoble

dir. Florence BAUDIN

Structure and function of the NS1 protein from type A influenza virus.

06/04 - 09/06 Duong lab – University of British Columbia – Vancouver

dir. Franck DUONG

Molecular dynamics of *Escherichia coli* translocon SecYEG during protein translocation.

04/02 - 05/04 Laboratoire de Recherche Moléculaire sur les Antibiotiques - INSERM – Paris

dir. Michel ARTHUR

Structure & function of UDP-MurNAc-pentapeptide:aminoacyl-transferases of *Firmicutes*.

10/97 - 12/01 Laboratoire de Virologie Moléculaire et Structurale - CNRS - Gif-sur-Yvette

dir. Yves GAUDIN

Identification of elements contributing to the folding of rabies virus envelope protein.

08/96 - 09/97 Unité des Venins - Institut Pasteur – Paris

dir. Cassian BON & Anne WISNER

Cloning, expression, molecular modeling of 3 related proteins from *Crotalinae* snake venom.

04/96 - 05/96 Laboratoire de Dynamique du Génome - Institut Jacques Monod – Paris

dir. Martine SIMONELIG

Screening of a human genomic bank with a gene from *Drosophila melanogaster*.

06/95 - 08/95 Unité de Biochimie et Structure des Protéines - INRA - Jouy-en-Josas

dir. Claude NESPOULOUS

Spectroscopic study of the effect of lipids and detergents on the structure of cryptogein, a fungus toxin.

Skills

Biochemistry: chromatographic & electrophoretic separation, immunoprecipitation, enzymology

Biophysics: basics in UV /CD / FTIR spectroscopies, equilibrium & sedimentation ultracentrifuge

Molecular Biology: PCR cloning, directed mutagenesis, recombinant expression

Cell Biology: cell culture, cell transfection, immunofluorescence

Bioinformatics: databases and their dedicated tools (KEGG, PATRIC, NCBI, Uniprot, MiST, PDB…)

Softwares: Excel (VBA programming), UCSF Chimera, Swiss PDB viewer, BioEdit, Jalview…

Languages: fluent english ; german spoken, read & written.

Financial support

*Personal applications in **bold** type:*

01/11 - 12/13	Région Rhône-Alpes – CIBLE funding (project #1910)
10/07 - present	**Researcher position at the CEA**
10/06 - 09/08	ANR *via* the CNRS
08/05 - 09/06	University of British Columbia
08/04 - 07/05	**INSERM via the INSERM-CIHR agreement**
06/04 - 07/04	University of British Columbia
10/03 - 05/04	Association Biologie Infection
04/02 - 09/03	A.C.I. « Nouvelles Cibles Thérapeutiques » from the Ministry of Research
12/00 - 09/01	*Military duty*
11/00	CNRS
11/97 - 10/00	**Ph.D. funding from the Ministry of Research**
04/97	**DEA fellowship from the Ministry of Research**

Honors

01/06 Cecil Green award

Back then, the Cecil Green award for Academic research and Scientific communication was awarded once a year by the Principal of Green College (GC) to selected resident members for their contribution to the academic life of the College. A residential unit, GC is also an academic unit from the Faculty of interdisciplinary studies at the University of British Columbia. The mission prescribed to GC by its founder, Cecil Green, is to bring together academics from various backgrounds such as to promote knowledge and foster ideas & friendship.

Publications

19 articles, 1 book chapter

Please note the code below:
● joint first coauthors
* corr. author
names of the students I co-supervised & my own.

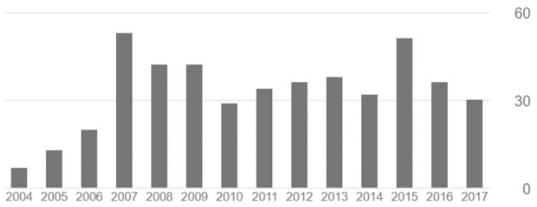

Citations per year from 2004 to 2017:

2007 = Cnr project starts

2015 = Covès team down

2016 = joined the Attrée team

Research articles

[17] Maillard AP● & Künnemann S●, Grosse C, Volbeda A, Schleuder G, Petit-Härtlein I, de Rosny E, Nies D, Covès J. (2015) Response of CnrX from *Cupriavidus metallidurans* CH34 to nickel binding. *Metallomics* 7 622-31 cited ***6*** times as of march 20th 2019 (Google Scholar)

[16] Ziani W● & Maillard AP●, Petit-Härtlein I, Garnier N, Crouzy S, Girard E, Covès J. (2014) The X-ray structure of NccX from *Cupriavidus metallidurans* 31A illustrates potential dangers of detergent solubilization when generating and interpreting crystal structures of membrane proteins. *J. Biol. Chem*. 289 31160-72 cited ***6*** times

[15] Maillard AP*, Girard E., Ziani W, Petit-Härtlein I, Kahn R., Covès J. (2014) The crystal structure of the anti-σ factor CnrY in complex with the σ factor CnrH shows a new structural class of anti-σ factors targeting extracytoplasmic function σ factors. *J. Mol. Biol*. 426 2313-27 cited ***26*** times

[14] Trepreau J, Grosse C., Mouesca J.-M., Sarret G., Girard E., Petit-Haertlein I, Kuennemann S., Desbourdes C., de Rosny E, Maillard AP, Nies D., Covès J. (2014) Metal sensing and signal transduction by CnrX from *Cupriavidus metallidurans* CH34: role of the only methionine assessed by a functional, spectroscopic, and theoretical study. *Metallomics* 6 263-73 cited ***12*** times

[13] Trepreau J, de Rosny E, Duboc C, Sarret G, Petit-Haertlein I, Maillard AP, Imberty A, Proux O, Covès J. (2011) Spectroscopic characterization of the metal-binding sites in the periplasmic metal-sensor domain of CnrX from *C. metallidurans* CH34. *Biochemistry* 50 9036-45 cited ***9*** times

[12] Trepreau J, Girard E, Maillard AP, de Rosny E, Petit-Haertlein I, Kahn R, Covès J. (2011) Structural basis for metal sensing by CnrX. *J Mol Biol.* 408 766-79 cited ***27*** times

[11] Pompidor G, Girard E, Maillard A, Ramella-Pairin S, Bersch B, Kahn R & Covès J (2009) Biostructural analysis of the metal-sensor domain of CnrX from *Cupriavidus metallidurans* CH34 *Antonie van Leeuwenhoek* 96 141-8 cited ***8*** times

[10] Pompidor G, Maillard AP, Girard E, Gambarelli S, Kahn R & Covès J (2008) X-ray structure of the metal-sensor CnrX in both the apo- and copper-bound forms FEBS Lett. 582 3954-58 cited ***17*** times

[9] Villet R, Fonvielle M, Busca P, Chemama M, Maillard AP, Hugonnet J-E, Dubost L, Marie A, Josseaume N, Mesnage S, Mayer C, Valéry J-M, Ethève-Quelquejeu M, Arthur M (2007) Idiosyncratic features in tRNAs participating in bacterial cell wall synthesis. *Nucleic Acids Res.* 35 6870-83 cited ***35*** times

[8] Maillard AP, Lalani S, Silva F, Belin D, Duong F (2007) Deregulation of the SecYEG translocation channel upon removal of the plug domain. *J. Biol. Chem*. 282 1281-7 cited ***64*** times

[7] Tam PC● & Maillard AP●, Chan KK, Duong F. (2005) Investigating the SecY plug movement at the SecYEG translocation channel. *EMBO J*. 24 3380-8. cited ***121*** times.

[6] Maillard AP● & Biarrotte-Sorin S●,Villet R, Mesnage S, Bouhss A, Sougakoff W, Mayer C, Arthur M. (2005) Structure-based site-directed mutagenesis of the UDP-MurNAc- pentapeptide-binding cavity of the FemX alanyl transferase from *Weissella viridescens*. *J Bacterio*l. 187 3833-8 cited ***31*** times.

[5] Biarrotte-Sorin S● & Maillard AP●, Delettré J, Sougakoff W, Arthur M, Mayer C. (2004) Crystal structures of *Weissella viridescens* FemX transferase and its complex with UDP-MurNAc-pentapeptide: insights into FemABX family substrate recognition. *Structure (Camb.)* 12 257–267 cited ***66*** times.

[4] Biarrotte-Sorin S● & Maillard AP●, Delettré J, Sougakoff W, Blanot D, Blondeau K, Hugonnet J-E, Mayer C, Arthur M. (2003) Crystallization and preliminary X-ray analysis of Weissella viridescens FemX UDP-MurNAc-pentapeptide:L-alanine ligase. *Acta Crystallogr. D Biol. Crystallogr*. 59 1055-7 cited ***2*** times

[3] Maillard A, Domanski M, Brunet P, Chaffotte A, Guitet E, Gaudin Y. (2003) Spectroscopic characterization of two peptides derived from the stem of rabies virus glycoprotein. *Virus Res*. 93 151-8 cited ***11*** times

[2] Desmézières E, Maillard AP, Gaudin Y, Tordo N, Perrin P. (2003) Differential stability and fusion activity of Lyssavirus glycoprotein trimers. *Virus Res*. 91(2)181-7 cited ***26*** times

[1] Maillard AP, Gaudin Y. (2002) Rabies virus glycoprotein can fold in two alternative, antigenically distinct conformations depending on membrane-anchor type. *J. Gen. Virol*. 83 1465-76 cited ***25*** times

Review articles & book chapter

[3] Reboud E●, Basso P●, Maillard AP●, Huber P, Attrée I. (2017) Exolysin Shapes the Virulence of *Pseudomonas aeruginosa* Clonal Outliers. *Toxins* 9 364

[2] Maillard AP, Chan K, Duong F. (2005) Preprotein Translocation through the Sec Translocon in Bacteria. Landes Bioscience - Springer / edited by Jerry Eichler

[1] Maillard AP, Gaudin Y. (2001) Les changements de conformation des glycoprotéines fusogènes virales. Cahier des Ecoles Physique et Chimie du Vivant n°3 Membranes biologiques : 71-78

Scientific communications

Invited seminars at international conferences:

VAAM annual meeting, Marburg, mar. 1st 2015 – chair: Pr. Dr. T. MASCHER
Metal sensing and transmembrane signaling by the CnrYXH complex from *Cupriavidus metallidurans*.

5th International IMBG meeting, Autrans, sep. 20th 2012 – chair: Dr. J. COVES
Metal sensing and transmembrane signal transduction *via* the CnrYXH pathway in *Cupriavidus metallidurans* CH34.

Invited seminars:

Institut de Biologie Structurale, sep. 27th 2007 – host: Dr. J. COVES
Dynamique du transporteur SecYEG au cours de la translocation des préprotéines à travers la membrane cytoplasmique.

Institut Pasteur de Lille, nov. 23rd 2006 – host: Dr. C. LOCHT
Dynamique du transporteur SecYEG au cours de la translocation des préprotéines à travers la membrane cytoplasmique.

Migenix Inc., Vancouver, aug. 2nd 2006 – host: Dr. D. DUGOURD
The envelope of viruses and bacteria: a biochemist grip.

Laboratoire de Recherche Moléculaire sur les Antibiotiques, oct. 10th 2005 – Dr. M. ARTHUR
Canal ouvert, canal fermé: dynamique du translocon SecYEG d'*E. coli*

Posters at international conferences:

Ziani W, Girard E, Petit-Härtlein I, Kahn R, Covès J, Maillard AP. (2013) Transmembrane signaling *via* ECF-type σ factors: CnrY-mediated inhibition of CnrH in *Cupriavidus metallidurans* CH34 typifies an emerging class of minimal size antisigmas. FEMS 5th Congress of microbiologists. SIGNALLING/282. Leipzig

Ziani W, Maillard A, Girard E, De Rosny E, Petit-Haertlein I, Coves J. (2014) Metal-induced transmembrane signal transduction by CnrYXH from Cupriavidus metallidurans CH34: interaction between CnrX and CnrY in the periplasm. International Congress on Bio-Inorganic Chemistry. S391. Grenoble

Maillard AP, Gaudin Y. (2002) Rabies virus glycoprotein can fold in two alternative, antigenically distinct conformations depending on membrane-proximity. XIIth IUMS International Congress of Virology. V1128. Paris

Maillard A, Dominguez Del Angel V, Lee W-H, Arocas V, Bon C, Wisner A (2001) Cloning, expression and molecular modeling of botrocetin, the von Willebrand factor coagglutinin component from *Bothrops jararaca* venom. XVIIIth Congress of the International Society of Thrombosis and Haemostasis. P234. Paris

Teaching & mentoring students

Stereochemistry & organic chemistry

02/07 – 05/14 UFR Chimie-Biologie at Univ Grenoble-Alpes / **CHI120** module
Every year: 20h to 30h teaching classes & practicals to 1st year students.

Technician trainees

07/11 – 10/11 Kouloud Mahroug (Lycée Professionnel Louise Michel, Grenoble)
10/08 – 06/10 Mathias Alcoz (SFP, Moirans)
10/07 – 06/09 Stéphanie Ramella-Pairin (SFP, Moirans) – shared supervision

Undergraduate students

01/19 – 01/19 Jennifer Riondet – L3 tainee (Univ Grenoble Alpes)
06/17 – 07/17 Belinda Champagne – L3 trainee (Univ Grenoble-Alpes)
06/14 – 07/14 Loïc Gandvuillemin – L3 trainee (Univ Grenoble-Alpes)
04/08 – 06/08 William Stafford – L3 trainee / ERASMUS (Univ Grenoble-Alpes)

Graduate students

03/19 – 08/19 Anaëlle Dumazer – M2 trainee (ENSCM)
04/18 – 06/18 Amandine Morand – M1 trainee (Univ Grenoble-Alpes)
10/11 – 09/14 Widade Ziani – PhD student (Univ de Grenoble-Alpes) – shared supervision
04/14 – 07/14 Christopher Arthaud – M1 trainee (Univ de Grenoble-Alpes)
10/08 – 09/11 Juliette Trepreau – PhD student (Univ Grenoble-Alpes) – shared supervision
09/03 – 05/04 Régis Villet – PhD student (Univ Paris 6) – shared supervision
01/03 – 07/03 Anne-Charlotte Sentilhes – M2 trainee (Univ Paris 7) – shared supervision

Teaching or mentoring the general public

07/13 Stage de 3ème
One-week observation internship, mentoring Thibaut Fousse.

10/10 Grenoble Science Fair
Presenter of a protein discovery workshop (structure, function & diversity).

10/09 Grenoble Science Fair
Designer and producer of the slideshow used to introduce proteins to the public visiting the Institut de Biologie Structurale. Presenter to highschool students.

12/08 Stage de 3ème
One-week internship, mentoring Aurélien Cassebras.

04/06 Greater Vancouver Regional Science Fair 2006
The Greater Vancouver Regional Science Fair is a festive public event celebrating the scientific method and its learning by children and teenagers. University scientists are offered to volunteer and as a member of the jury, I was assigned five projects in the junior section, i.e. five children / teenagers who presented their own experiment. Reasoning, experimental set-up and analysis, novelty were the appreciation criteria. Our prime mission of course was to make constructive remarks to everyone, and ranking was performed by judges at round tables to mark a project for a prize.

11/05 Green College, University of British Columbia, Green Speaker Series
'Getting across the border of the bacterium *E. coli*: the journey of a macromolecule.'

Service to the Community

Conseil d'Unité of the Institut de Biologie Structurale

01/15 – 07/16 Elected substitute personnel representative.
01/12 – 12/14 Elected personnel representative. Deputy to the Conseil de Direction of ex CEA / DSV.
01/08 – 12/10 Elected personnel representative. Deputy to the Conseil de Direction of ex CEA / DSV.

Conseil de Pôle of the COMUE Université de Grenoble – Alpes
New body with counseling role to the COMUE members, even though it is still very much focused toward the university. It gathers ~20 elected representatives from 3 colleges. Decision making body for the IRS call for research projects of the COMUE, consulting body for human ressources (sabbatical applications…).

11/15 – 10/20 Elected personnel representative
11/14 – 10/15 Appointed personnel representative at the first instance of the Conseil

1.7.3 SFBBM-SFB joint congress organization

The organization of the SFBBM-SFB joint 2011 congress was a one year-long project, coordinated by Christine Ebel and whose preparation involved ~20 scientists to various extent including Jean-Michel Jault and Cécile Breyton. With occasional help, my personal involvement covered:

- communication: design of the announcement poster with CNRS communication service, mailing preparation, banner and bag design. I also coined the title that was finally attached to the event.
- booklet design & print
- outreach for 2000 € subsidies
- abstract selection for the session « Integrative & structural biology »
- administration: design the solution that helped our technical assistant in the main room (not a professional) to be paid by the SFBBM

Abstract

Bacterial cells are enclosed within an envelope that displays several layers: the cytoplasmic membrane, the periplasmic space or equivalent and the peptidoglycan-based cell wall, made complete with teichoic acids or an outer membrane. The bacterial envelope serves as a physical scaffold, a selective diffusion barrier and a functional hub altogether. By electing projects on peptidoglycan synthesis, protein translocation and signal transduction, I have made my research experience relate to all of these properties. My present project aims at understanding how the exolysin that is the main virulence factor of *P. aeruginosa* clonal outliers and a pore-forming toxin, acquires its functional properties upon secretion and achieves function upon target membrane encounter. This somehow sounds like an echo of my predoctoral research, when I investigated fungal or snake toxins and a viral membrane-fusion protein. I have always been attracted to questions revolving about structure:function relationships. In my experience, it feels even better when there's a border to cross.

Introduction

- How do toxins trigger dysfunction?
- What does toxin-induced dysfunction unravel about the target?

Having stated my interest for research in this way while talking with my professors, MM. Morange, Goldberg and Chaffotte, I got soon persuaded to contact the head of the Venom unit at the Pasteur Institute in Paris, where I was to spend the next 13 months as an intern for my master's degree. The project that I took there aimed at understanding how bothrojaracin, a C-type-lectin-like toxin from the *Viperidae* snake *Bothrops jararaca* venom inhibits thrombin, a pivotal blood coagulation factor. Homology modeling eventually allowed to define patches of charged residues that would occlude thrombin exosites, yet there was so much more to this project! For example the fact that totally new functions were associated to the C-type lectin fold through heterodimerization *via* a swapped interface was a thrilling example of how evolution generated a plethora of new target binding specificities through the parsimonious use of a pre-existing fold. Also, in those days of rising genomics, as part of the perspective section of a paper that was never submitted, I had drafted a project of screening for new hemostatic functions after high-throughput cDNA cloning of a library of C-type-lectin-like toxins, taking advantage of the conserved regulatory DNA sequences that flanked toxin genes. Consituting a portfolio of hemostatic proteins was appealing at a time when some thought that plasminogen activator from *Trimeresurus stejnegeri* venom would replace tissue plasminogen activator as a blockbuster thrombolytic drug. But the Venom unit was about to enter a phase of negociated shut-down that lasted 6 years and I was fortunate to perform my PhD elsewhere on solid ground.

August 2016, nineteen years later: toxin on my path again as I joined Ina Attrée's group to work on the newly described exolysin! After working on cryptogein, bothrojaracin and rabies virus membrane-fusion protein, for the fourth time in my career I work on a protein that is used by a predator or a pathogen to weaken a prey or break into a host. Considering how invasive these properties are, I find it funny that the rest of my time was mostly dedicated to the biogenesis and maintenance of a wall.

Living organisms all display an envelope which encloses a space under physiological control. Soft or hard, fully organic or mineral in part, with shape defined or not, the primary role of the envelope is to control energy dissipation so it can be used to build or maintain a living entity.

Bacterial cells are enclosed within an envelope that serves as a physical scaffold, a selective diffusion barrier and a functional hub altogether. By electing projects on peptidoglycan synthesis (**section 1**), protein translocation (**sections 2 & 4**) and signal transduction (**section 3**), I have made my research experience relate to all of these properties, which I am happy to bring together in this document.

1. Building up the wall

Bacterial cells are micrometer-large living entities with a prokaryotic organization, *i.e*. membrane-delimited intracellular compartment or nucleus have not been observed yet. Based on structural and sequence traits, *Bacteria* have been acknowledged as one of the three domains of life (Woese et al., 1990) yet their already established role in shaping *Eukarya*, whose mitochondria and plastid organelles are of alphaproteobacterial and cyanobacterial origin, respectively (Archibald, 2015), and their emerging role in physiological, not only pathogenic processes of multicellular organisms (Byrd et al., 2018; Gensollen et al., 2016; Man et al., 2017; Sonnenburg and Bäckhed, 2016) tend to draw more attention than ever on the pervasive influence of *Bacteria* in life as we know it.

Despite their contribution to *Eukarya* evolution, bacteria are often studied for the threat that they pose to health and farming activities (Fisher and Mobashery, 2016). This is how a strong interest has been developed towards the biogenesis of the peptidoglycan, which is an essential component of the bacterial cell wall, a distinctive feature of bacterial cells, a cue for innate immunity and a major drug target (Höltje, 1998; Nikolaidis et al., 2014; Ray et al., 2013; Typas et al., 2011; Zhao et al., 2017).

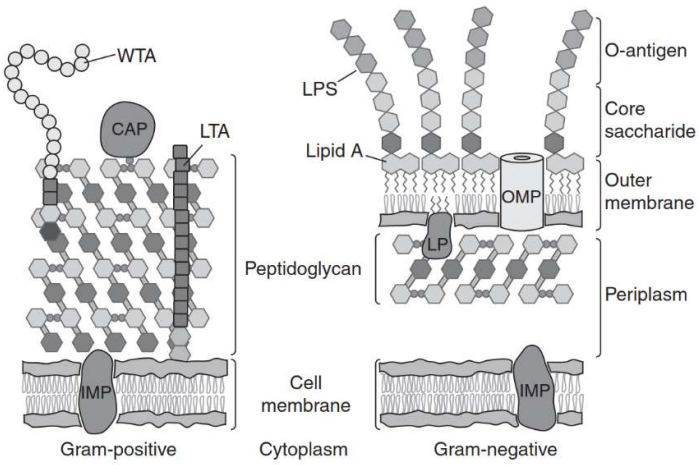

Figure 1. Depiction of Gram-positive and Gram-negative cell envelopes.

*(**Left**) Monoderm cell wall contains one lipidic membrane with a thick peptidoglycan layer and teichoic and lipoteichoic acids. (**Right**) Lipopolysaccharidic diderm bacteria are enveloped by two membranes with a thin peptidoglycan layer in-between.CAP covalently attached protein; IMP, integral membrane protein; LP, lipoprotein; LPS, lipopolysaccharide; LTA, lipoteichoic acid; OMP, outer membrane protein; WTA, wall teichoic acid. (from Silhavy et al., 2010)*

1.1. Layered structure of the bacterial cell envelope

Peptidoglycan is not alone: the bacterial envelope is a complex protective structure made of several layers which together achieve physical robustness and controlled permeability (Höltje, 1998; Morris and Jensen, 2008; Silhavy et al., 2010; Strahl and Errington, 2017). Essentially two organizational plans

have been selected and display a common base: the cytoplasmic membrane, the periplasmic space or its equivalent and the peptidoglycan-based cell wall, made complete with teichoic acids, as in monoderms, or an outer membrane as is the case for diderms (**Fig. 1**).

1.1.1. The inner membrane

In Gram-negative bacteria, the cytoplasmic membrane is called the inner membrane (IM). Like the eukaryotic plasma membrane for which the fluid mosaic model was coined (Nicolson, 2014), the bacterial plasma membrane is made of a phospholipid bilayer (60%) with proteins (40%) embedded, anchored or bound in various ways (Kuhn et al., 2017; Zückert, 2014).

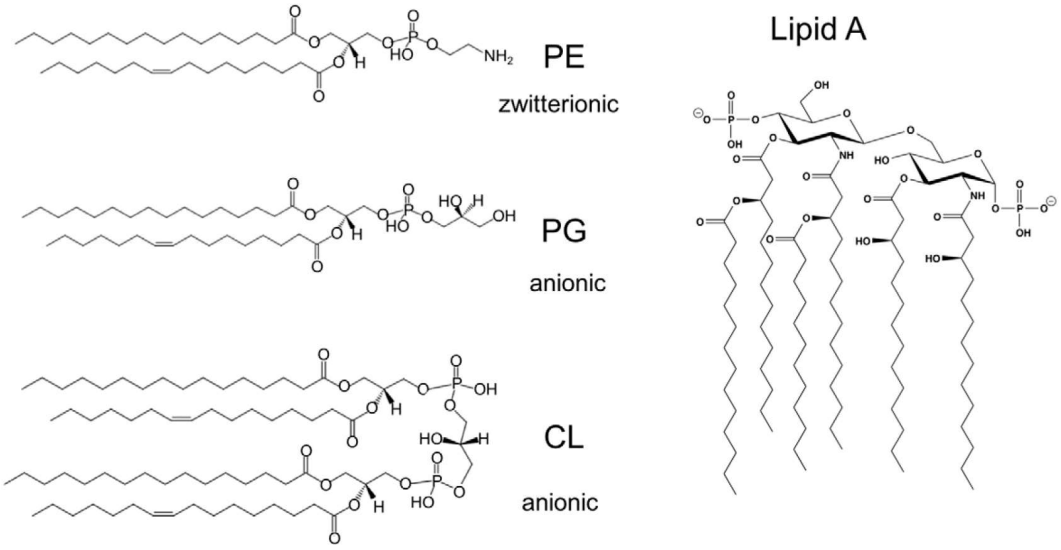

Figure 2. Major membrane lipids of* E. coli *K-12.

The structures of the most abundant membrane lipids of E. coli *K-12 are depicted. (**Left**) The zwitterionic phospholipid phosphatidylethanolamine (PE; ~75% of total lipid by weight) as well as the anionic phospholipids phosphatidylglycerol (PG; ~20%) and cardiolipin (CL; ~5%) are the major lipids of the IM. They are also found in similar proportions in the inner leaflet of the OM. (**Right**) The asymmetric OM bilayer consists of LPS whose lipid A moiety makes the outer leaflet of the OM. (modified from May and Silhavy, 2017)*

The phospholipids (PL) are produced in the cytosol by a machinery that is very conserved among bacteria (and from which it has actually spread to plants and protozoans by gene transfer, Zhang and Rock, 2008). Lipid composition of membranes (**Fig. 2**) may be regulated in response to environmental changes, with respect to lipid head-group, acyl chain length and degree of acyl chain saturation (Zhang and Rock, 2008). PL composition not only affects the physicochemical properties of the membrane but

may also drive the localization of proteins (Strahl and Errington, 2017). Finally, specific protein:lipid interactions have been shown to contribute to protein topology or function (Bogdanov et al., 2014; Gold et al., 2010; Hertle et al., 1997).

In bacteria (and in energetic eukaryotic organelles), the cytoplasmic membrane is energized with a proton gradient across the plasma membrane. This proton gradient is maintained by the respiratory chain ATPase and is called the proton-motive force (PMF). This source of energy entails two components, $\Delta\psi$ and ΔpH, which relate to the electric and the chemical gradients, respectively. PMF is used to fuel transport of small molecules and of proteins across the cytoplasmic membrane (see **section 2.1.3**) and across the outer-membrane as well (see **section 1.1.4**).

1.1.2. The periplasm

The periplasm was originally defined in diderm bacteria to account for the space between the IM and the outer membrane (OM). Some pictures occasionally showed a peptidoglycan layer detached from the OM. The periplasm is made accessible to small molecules from the extracellular milieu *via* major porins, whose production is regulated in response to environmental changes, sometimes also upon antibiotic exposure.

The periplasm is the compartment where all proteins from the general secretion pathway fold, unless they need to be maintained in a competent state to translocate across the OM. Soluble proteins SurA, FkpA and Skp are the general chaperones in *E. coli* periplasm while Spy and other chaperones seem to play more specific roles (Goemans et al., 2014). DegP contributes to periplasm homeostasis by playing a dual role, both as a chaperone and a temperature-dependent protease (Krojer et al., 2008a, 2008b; Meltzer et al., 2008; Spiess et al., 1999). Finally, lipoproteins of the OM are shuttled from the IM by the protein LolA (**Fig. 3**).

The periplasm is devoid of energy and chaperones cannot promote folding by ATP-regulated interactions (Clare and Saibil, 2013; Mas and Hiller, 2018). Instead, a protein like Spy uses loose electrostatic binding to help client proteins to fold (Clark and Elcock, 2016).

What about monoderm bacteria? In the recent years, evidence has been published that *S. aureus, B. subtilis* and probably monoderms as a whole display a periplasmic space in-between their cytoplasmic membrane and peptidoglycan (Matias and Beveridge, 2006, 2008). Lipoteichoic acids fill the periplasmic compartment of monoderms which is very different from the periplasm in diderms. Still, in support of the comparison, SurA homolog PrsA is a membrane-tethered chaperone that contributes to secretion (Lin et al., 2018; Wahlström et al., 2003).

1.1.3. The peptidoglycan

The peptidoglycan is bacteria's very own protective structure. This gigantic molecule called murein is built outside the cell by periplasmic transglycosylases and transpeptidases from units synthesized in the cytoplasm and the inner leaflet of the IM (see below). This exoskeleton forms a so-called sacculus that helps withstanding osmotic pressure around all bacterial cells, with the exception of some intracellular bacteria (Otten et al., 2018).

As a distinct physical barrier, the PG comprises anywhere between a few to dozens of so-called layers, depending on bacterial source and growth state (Höltje, 1998). For example, its thickness has been estimated to 2-to-5 layers in *E. coli* depending on the growth phase (Leduc et al., 1989) but as little as a single layer was observed in a cryoelectromicroscopy study (Gan et al., 2008). In monoderm bacteria where PG is in contact with the outside, it is functionalized by the covalent attachment of proteins (Jacobitz et al., 2017).

Under selective conditions, it is possible to maintain so-called L-forms of monoderm or diderm bacteria that are devoid of murein: these can also occur naturally, e.g. under the pressure of PG-targeting antibiotics to which they are resistant (Errington et al., 2016). L-forms were used to solve a long-time question: by inactivating the gene *murC* of the PG precursor synthesis pathway and the restoring it, Kawai et al. (2014) were able to show that no template is necessary and a rod-shape is self-determined in *B. subtilis* by the balanced activities of the elongasome and divisome PG synthetic machineries (see below).

1.1.4. The outer membrane

In diderm bacteria, the OM bilayer is attached to PG by the so-called Braun's lipoprotein, Lpp (Braun and Rehn, 1969) on the periplasmic side. As a result, OM proteins may bind PG, e.g. OmpA (Wang et al., 2016). The OM is an asymmetric bilayer whose inner leaflet is made of the same PL as the IM and whose outer leaflet is assembled from lipopolysaccharides (LPS), a distinctive feature (**Fig. 2**), toward the outside. OM asymmetry is vital to bacteria (Malinverni and Silhavy, 2009; Sutterlin et al., 2016)

LPS is synthesized at the IM, shuttled to the outer leaflet of the OM and assembled in tight arrays by the Lpt pathway. LPS is a major contributor to OM impermeability, sugar moieties keeping hydrophobic molecules away and the lipid cores keeping hydrophilic molecules outside. Indeed, increased antibiotic sentivity is associated with LPS defect in the OM (Sutterlin et al., 2014 for an example). It is also called the endotoxin as the strong immune response it provokes, sometimes causes a septic shock.

The OM is functionalized with proteins that are inserted by the essential β-barrel assembly machine (BAM) (Noinaj et al., 2017) or the translocation and assembly module (TAM) (Stubenrauch and Lithgow, 2019).

Finally, no more energy is stored in the OM than in the periplasm. Still, processes taking place at the OM can be energized using the PMF at the IM. Such is the role of the TonB:ExbB:ExbD complex in the IM, which provides energy through the periplasm to TonB-dependent transporters, a family of β-barrel transporters bearing a semi-conserved 5-residueTonB-box near the N-terminus (Noinaj et al., 2010).

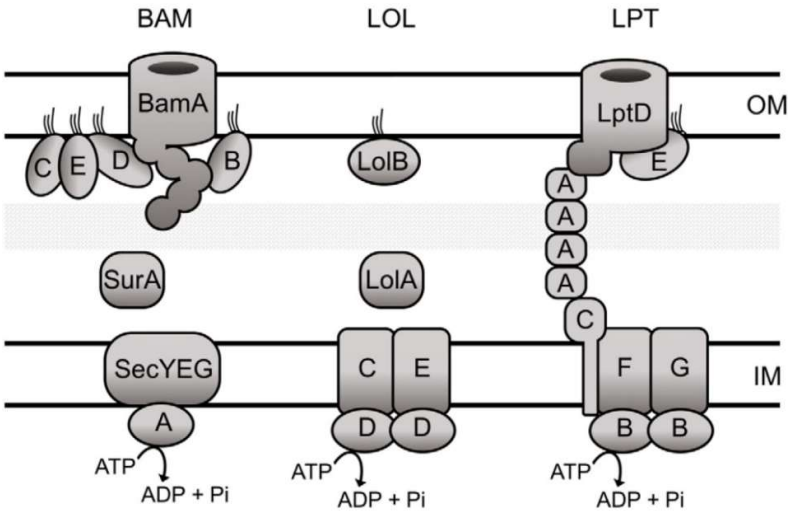

Figure 3. OM biogenesis machinery.

*Depicted are the components of three essential cellular machines required for outer membrane (OM) biogenesis. β-barrel proteins and lipoproteins are made initially in the cytoplasm in precursor form with a cleavable signal peptide that directs these precursors to the Sec machinery for translocation across the IM. Chaperones, e.g. SurA deliver β-barrel outer membrane proteins to the β-barrel assembly machine (**BAM**) for insertion into the OM. For OM lipoproteins, after the signal sequence is removed and lipids are attached to the amino-terminal cysteine residue, the **Lol** machinery delivers them to the OM. The LipoPolysaccharide Transport (**LPT**) pathway transports LPS from its site of synthesis in the IM to the cell surface* via *a hydrophobic conduit formed by oligomerized **LptA**. (modifed from Konovalova et al., 2017)*

1.1.5. Surface polysaccharides

Sugars make a quantitative contribution to the bacterial envelope. They are found in permanent structures like PG, LPS (Bertani and Ruiz, 2018) and TA (van der Es et al., 2017) as well as diversified glycan moieties of proteins that make so-called S-layers (Schäffer and Messner, 2017). All of these are assembled from the same initial cytoplasmic building block that is divergently modified and flipped across the IM upon completion.

Surface-exposed polysaccharides can modulate the immune response of the host like has been found e.g. in *P. aeruginosa* (McCarthy et al., 2017).

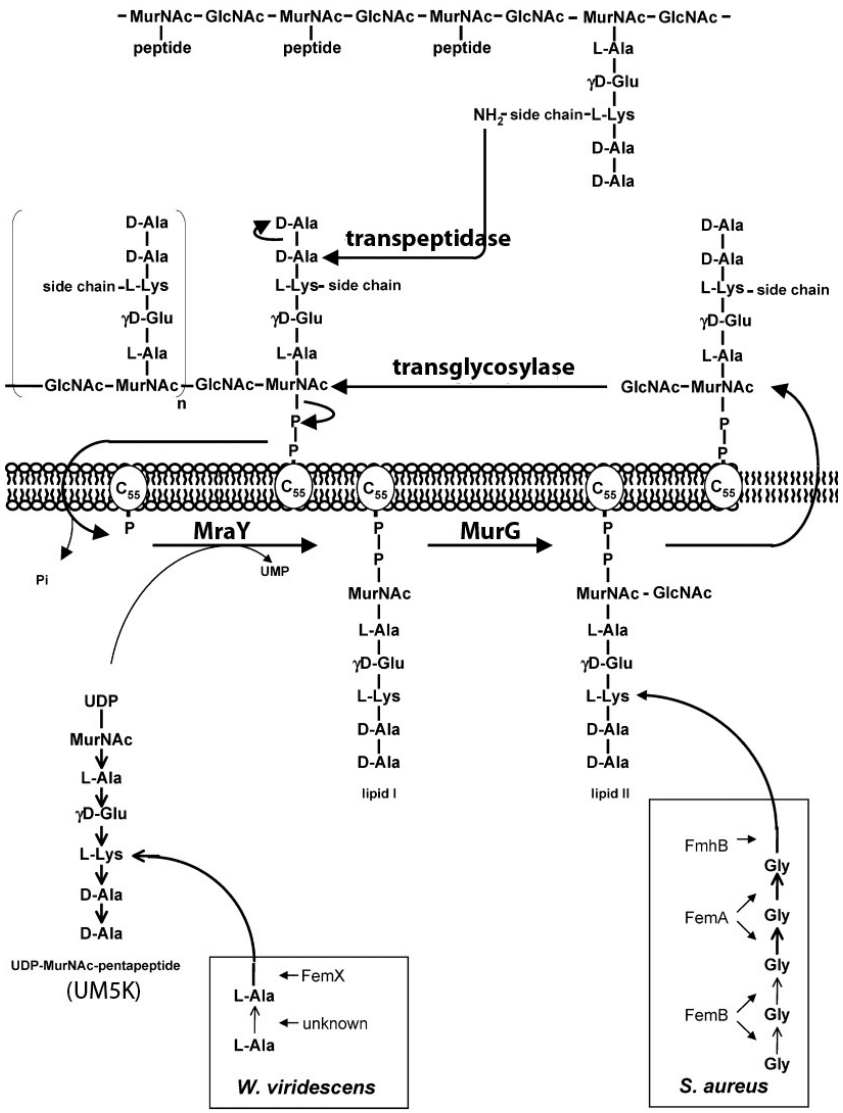

Figure 4. Peptidoglycan synthesis in W. viridescens and S. aureus

The peptidoglycan is the result of the polymerization of a pentapeptide dinucleotide subunit by transpeptidation and transglycosylation reactions. Conserved features of the pentapeptide stem linked to the D-lactyl group of MurNAc include (i) alternate amino acids of the L and D configuration, except for the C-terminal residues (D-alanyl-D-alanine), (ii) presence of a diamino acid residue at the third position (L-lysyl, L-ornithyl, or meso-diaminopimelyl), and (iii) linkage of the latter residue to the side chain carboxyl group of the second residue (γ-D-glutamyl). The linear pentapeptide stem is assembled in the cytoplasm by the stepwise addition of amino acids and of the dipeptide D-Ala-D-Ala onto UDP-MurNAc by the Mur synthetases to form the UDP-MurNAc-pentapeptide precursor. Unlike Fem transferases, Mur synthetases catalyze amide or peptide bond formation by a mechanism involving ATP-dependent activation of carboxyl groups via formation of acyl phosphates. The membrane-associated steps of peptidoglycan synthesis are initiated by the transfer of the phospho-MurNAc-pentapeptide moiety from the nucleotide to the lipid carrier undecaprenyl-phosphate to form lipid intermediate I (undecaprenyl-P-P-MurNAc-pentapeptide). Following addition of GlcNAc to form lipid intermediate II (undecaprenyl-P-P-MurNAc[pentapeptide]-GlcNAc), the complete disaccharide-peptide subunit is translocated to the cell surface and delivered to the peptidoglycan polymerization complexes containing the essential glycosyltransferase and D,D-transpeptidase activities. Insets show side chain synthesis by Fem transferase in W. viridescens and S. aureus. The arrows indicate the direction of the CO → NH peptide bonds. C55 , undecaprenyl lipid carrier.

1.2. Making the peptidoglycan mesh

The PG is built from a highly conserved disaccharidic-pentapeptidic brick whose pieces are brought together by the Mur ligases on the inner leaflet of the cytoplasmic membrane (**Fig. 4** for details). After the brick has been assembled and flipped to the outer leaflet by flippases such as FtsW or RodA in *E. coli*, it gets incorporated into the PG mesh by transpeptidase (TP) and transglycosylase (TG) activities that are brought together in multienzyme complexes of two sorts, depending on whether they make PG at the division septum (divisome) or in the lateral cell wall (elongasome). Both machineries perform a similar function and display the same essential set of complementary actors that work to rearrange PG as the bacteria grows: (i) one penicillin binding protein (PBP) that carries both TP and TG activities (class A PBP), (ii) a specific lipoprotein partner of this enzyme that was shown to amplify its efficiency (Caveney et al., 2018; Greene et al., 2018; Typas et al., 2010, 2011), (iii) one PBP carrying a morphogenesis module and TP activity (class B PBP), (iv) hydrolytic enzymes (v) one flippase and (vi) scaffolding proteins (**Fig. 5**).

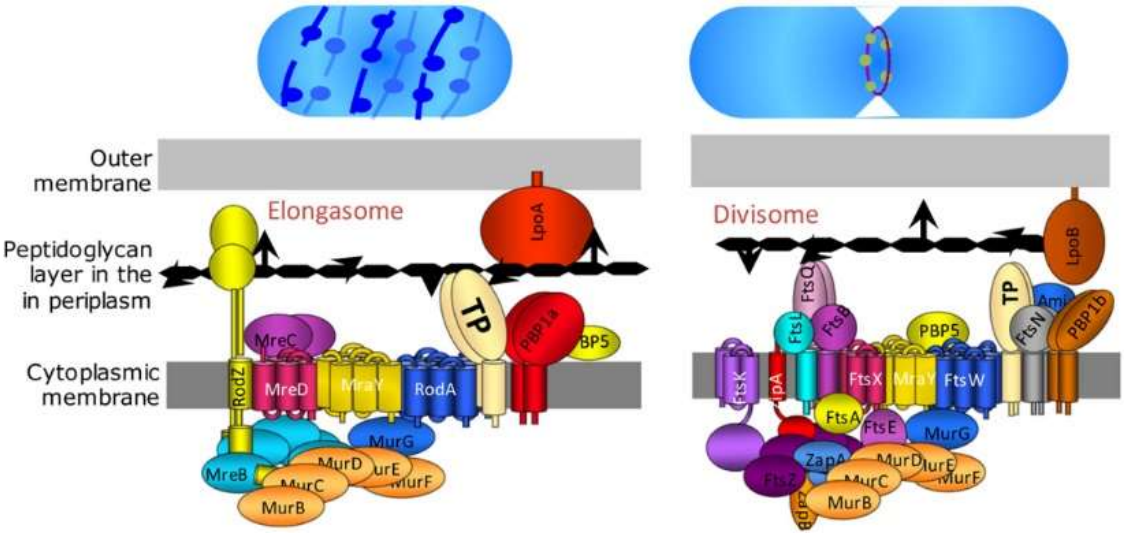

Figure 5. Complexes responsible for PG synthesis in E. coli during lateral cell-wall growth and division.

Peptidoglycan polymerization involves two complexes, the divisome and the elongasome, responsible for septum formation and lateral cell-wall elongation, respectively. These complexes include all the biosynthetic and hydrolytic enzymes required for the incorporation of new subunits into the expanding peptidoglycan net, as well as cytoskeletal proteins, MreB and FtsZ, acting as trailing guides. (reproduced from Hugonnet et al., 2016)

As a result of the coordinated activities of the PG synthetic machineries, the PG mesh is made of glycan strands running circumferentially (Gan et al., 2008; Tocheva et al., 2013; Turner et al., 2018; Verwer et al., 1978) that are cross-bridged by peptide moieties. Peptide cross-bridges have been extensively

characterized using partial digests and mass spectrometry, unraveling an unexpected flexibility in ways cross-linking is achieved, which sometimes causes antibiotic resistance (Mainardi et al., 2008).

Most often, peptide bridges are forged by PBPs that catalyze the condensation between the carboxyl end of the 'acyl donor' peptide and the amino function on the side chain of the 'receiver' peptide (**Fig. 3)**. The majority of firmicutes produce PG precursors containing an additional side chain linked to the -amino group of a diamino acid residue at the third position of the pentapeptide stem (Schleifer and Kandler, 1972). The addition of glycine and of L-amino acids is performed by a unique family of nonribosomal peptide bond-forming transferases that use aminoacyl~tRNA as substrate (Hegde and Shrader, 2001; Plapp and Strominger, 1970a). These transferases differ by the type, position, and number of amino acids incorporated into the side chain and by the PG precursor used as substrate (Rohrer and Berger-Bächi, 2003). Most FemABX enzymes are loosely bound to the cytoplasmic side of the inner membrane where they modify the lipid II precursor of PG. In contrast, *Weissella viridescens* FemX had been shown to use UDP-Mur-N-Ac-pentapeptide as a substrate, on which it adds the first of the two alanyl residues present in the PG (Plapp and Strominger, 1970a, 1970b).

The interest in FemABX enzymes has been boosted when it was observed that the inactivation of non essential enzymes of the FemABX family restored methicillin susceptibility in methicillin-resistant *S. aureus* (Strandén et al., 1997). Acquired resistance in firmicutes is mostly due to the production of so-called low-affinity PBPs that display a narrow substrate specificity: the addition of a complete side chain to the PG precursors is essential for β-lactam resistance mediated by such low-affinity PBPs in *Staphylococcus aureus* (Rohrer and Berger-Bächi, 2003) but also *Streptococcus pneumoniae* (Filipe et al., 2001; Hakenbeck, 2001) and *Enterococcus faecalis* to a lesser extent (Bouhss et al., 2002). Transferases of the Fem family are therefore considered as potential targets for the development of novel antibiotics which would rehabilitate β-lactam antibiotics against β-lactam-resistant bacteria (Kopp et al., 1996).

1.3. Focus on FemABX enzymes, that make the PG branching peptide in firmicutes

The *Weissella viridescens* FemX transferase ($FemX_{Wv}$) has been selected as a model enzyme to elucidate kinetic and structural properties of FemABX enzymes because it catalyzes the transfer of L-Ala onto the cytoplasmic precursor UDP-N-acetyl-muramyl-pentapeptide (UDP-MurNAc-pentapeptide, UM5K) (Hegde and Shrader, 2001; Plapp and Strominger, 1970a), in contrast to other members of the Fem family, which preferentially (Bouhss et al., 2002) or exclusively (Plapp and Strominger, 1970b; Schneider et al., 2004) transfer amino acids to membrane bound peptidoglycan precursors. The research program on $FemX_{Wv}$ has been started by Michel Arthur who purified the

enzyme from a batch of *W. viridescens* and cloned the corresponding gene (Bouhss et al., 2001). Working in collaboration with structural biologists and synthesis chemists, I helped advance the structure:function characterization of FemX (Biarrotte-Sorin et al., 2003, 2004; Maillard et al., 2005; Villet et al., 2007)

1.3.1. Preliminary characterization of *W. viridescens* FemX catalytic mechanism

W. viridescens FemX is a 336 residue-long soluble protein. Kinetic studies by others have revealed an ordered mechanism involving (i) sequential binding of UDP-Mur-NAc-pentapeptide with a lysyl side chain at position 3 in the pentapeptidic stem (UM5K) and Ala~tRNA, (ii) transfer of L-Ala to the ε-amino group of L-Lys in the pentapeptide stem, and (iii) release of the tRNA and UDP-MurNAc-hexapeptide reaction products (Hegde and Blanchard, 2003; Hegde and Shrader, 2001). Site-directed mutagenesis had yielded identified Asp108 as a candidate for the catalytic base, as the Asp108Asn substitution decreased the catalytic efficiency (V/K) of the enzyme 230-fold, primarily due to a 60-fold decrease in k_{cat} (Hegde and Blanchard, 2003).

We developed our own enzymatic assay by quantifying the transfer of ^{14}C labelled alanine to UM5K: the UDP-N-acetylmuramic-hexapeptide (UM5K-Ala) product was separated from unreacted alanine by paper chromatography and radioactive spots corresponding to both reacted and unreacted alanine were located by autoradiography, cut out and quantified with a scintillation counter (Maillard et al., 2005). A coupled reaction was set up to ensure a constant supply of the short-lived Ala~tRNA substrate: the tRNA was completely acylated (90%) during the entire 10 minutes reactions, as judged by direct determination of ^{14}C Ala~tRNA. Our results were comparable to those already published (Hegde and Blanchard, 2003), with for a slightly higher k_{cat} (1,600 versus 660 min^{-1}) and a lower Km for Ala~tRNA (1.6 versus 15 µM), which we explained by the use of an extensively purified tRNA preparation as opposed to crude *in vitro* transcription reaction products. Also, the amount of acylated tRNA at steady state was not reported in the first study.

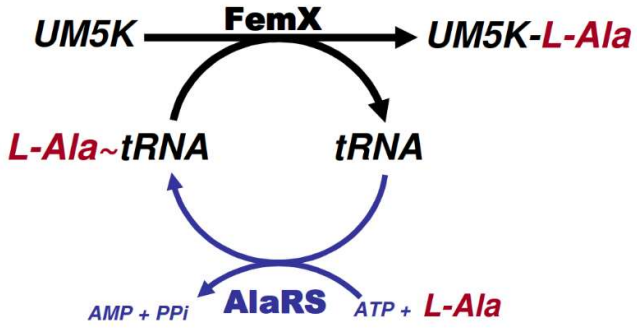

Figure 6. Coupled enzymatic assay set-up to detect and measure FemX activity.

Paper chromatography followed by scintillation counting allowed to quantify the incorporation of ^{14}C Ala into ^{14}C UDP-MurNAc-hexapeptide (UM5K-L-Ala). See text.

1.3.2. Use of truncated substrates allowed to raise a first imprint of FemX catalytic site

FemX first substrate is UM5K. By assessing FemX activity with purified precursors and break-down products of its natural substrate after chemical or enzymatic cleavage, I have identified the chemical groups that are important for FemX:UM5K interaction (**Table 1**). This seemed to show that the phosphate groups of the UDP nucleotide and the last two aminoacyl residues of the pentapeptide were instrumental in substrate binding (Maillard et al., 2005).

Truncated substrates	**Code name**	**FemX activity**
Ala-Glu-Lys-Ala-Ala	pentapeptide	not detected
P-MurNAc-Ala-Glu-Lys-Ala-Ala	P-MurNAc-5K	0.02%
P-P-MurNAc-Ala-Glu-Lys-Ala-Ala	PP-MurNAc-5K	0.15%
UMP-P-MurNAc-Ala-Glu-Lys-Ala-Ala	UM5K	100%
UMP-P-MurNAc-Ala-Glu-Lys-Ala	UM4K	0.03%
UMP-P-MurNAc-Ala-Glu-Lys	UM3K	not detected

Table 1. Relative activity of FemX towards truncated substrates

1.3.3. FemX crystal structures in the apo and PG precursor-bound forms

The FemABX family was structurally undefined as we started collaborating with Claudine Mayer (Université Paris 6) and her PhD student Sabrina Biarrotte-Sorin. Protocols allowing quantitative production, selenomethionine incorporation and purification for *W. viridescens* FemX have been established and our collaborators eventually crystallized FemX *apo* and UM5K-bound forms (Biarrotte-Sorin et al., 2003).

W. viridescens FemX structure was obtained at 1.7 Å resolution, showing two domains packed together in a globular object. As had been reported for *S. aureus* FemA (Benson et al., 2002), structural similarity with the acetyltransferases of the Gcn5-related N-acetyl transferase (GNAT) superfamily, which catalyze the transfer of the acetyl group from acetyl coenzyme A to a primary amine (Vetting et al., 2005), was also detected for FemX (Biarrotte-Sorin et al., 2004). Structural deviations between the C-termini of FemX domains and genuine GNAT enzymes coincided with divergence already described for the GNAT fold (Dyda et al., 2000). FemABX enzymes are not the only case of GNAT domain duplication , but the particularity of FemX is that the folding pattern of domain 1 starts with C-terminal residues. A closer look suggested that the FemABX family probably results from a complex evolutionary scenario involving gene duplication, circular permutation and domain insertion. Cirular permutation is considered as a rare event (Vogel and Morea, 2006).

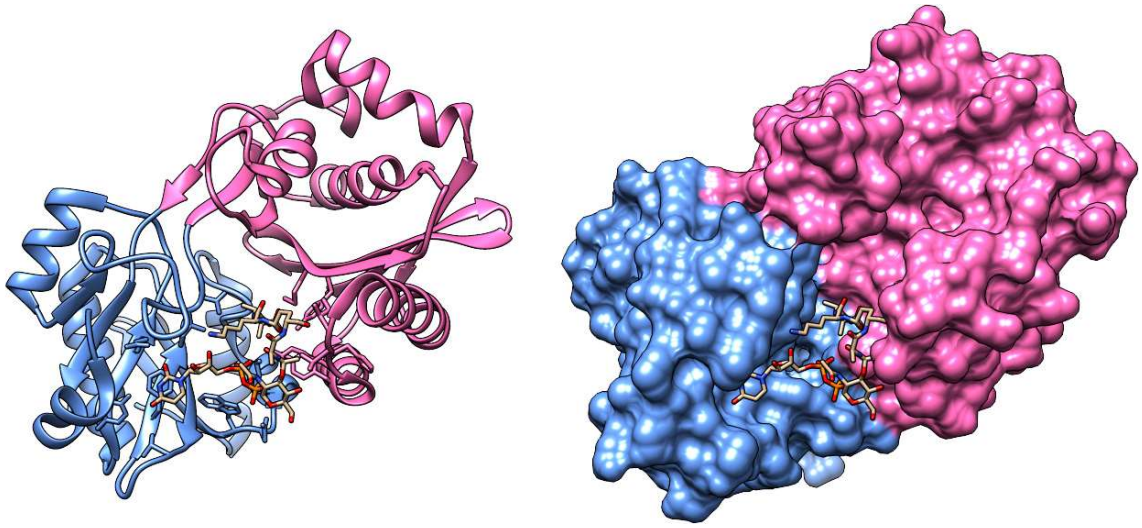

***Figure 7. Ribbon representation of FemX in complex with the UDP-MurNAc-pentapeptide**.*

GNAT-related domains are colored in blue (domain 1) or pink (domain 2). The UM5K is shown as ball-and-stick

New to the field was the structure of a FemABX enzyme in complex with its first substrate, at 1.9 Å resolution. UM5K is bound into a cleft at the interface of the two domains, mostly in contact with domain 1 (**Fig. 7**) inducing minor structural differences to FemX if any (0.2 Å root mean square deviation). Notable differences were observed for Lys36 through stabilization of its amino group in the complex and for Tyr215 and Tyr256 whose hydroxyl groups are displaced by 0.9 and 2.1 Å, respectively as they shift from a mutual interaction to UM5K binding (**Fig. 8**). UM5K displays a unique bent structure (**Fig. 7**), the UDP-MurNAc moiety being clearly stabilized by polar and stacking interactions with the protein (Bmean 22.3 Å²) whereas the pentapeptide showed a higher degree of flexibility (Bmean 50.0 Å²).

1.3.4. Partial characterization of FemX active site by site-directed mutagenesis.

Mutagenesis was performed in three phases, based on the more and more precise informations unraveled. First, conserved positions in multiple sequence alignments within the FemABX family have been mutated: Lys305Met has been the most promising hit identified with this approach as it behaved like the wild type during purification but had a ~4000-fold depressed activity. Yet results obtained with other mutants showed that a 3 log inactivation was very partial (unpublished). Second, when a structural homology with the GNAT superfamily has been recognized, I have tested a hypothetic functional similarity between both catalysts by superimposing individual FemX domains on the model

GNAT Esa1 (Yan et al., 2000) and mutated FemX residues that aligned with Esa1 catalytic residues. Mutating these positions only yielded marginal effects (unpublished).

Finally, when the structure of FemX in complex with its first substrate has been determined, a census of all chemical groups of FemX interacting with UM5K has been made. These residues belonged to both domains and their systematic mutagenesis pointed at Arg211 and Lys36, whose mutation to methionine inactivated the enzyme. Both residues take part into a hydrogen-bonds network that involves many groups of the substrate (Biarrotte-Sorin et al., 2004).

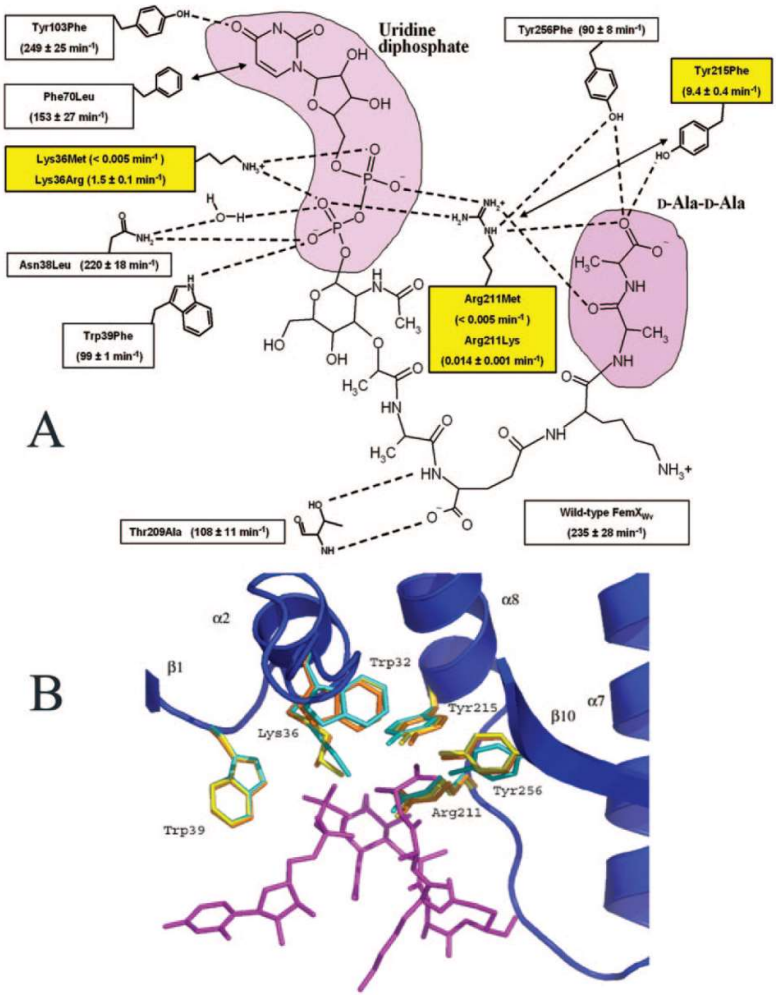

Figure 8. Structure of the UDP-MurNAc-pentapeptide-binding cavity of FemX$_{Wv}$.

(A) Schematic representation of the nine FemX$_{Wv}$ residues in contact with the substrate through hydrogen (dashed lines) or stacking (arrows) interactions. The estimates of the transferase activity (v/E) were obtained for the mutant proteins with a single amino acid substitution as described in the text. (B) Close view of the superimposition of the FemX$_{Wv}$ UDP-MurNAc-pentapeptide-binding cavity in the structures of the apo wild-type enzyme (4), UDP-MurNAc-pentapeptide:apo wild-type enzyme complex (4), and Lys36Met mutant protein (this work). The bound substrate and secondary structures of FemX$_{Wv}$ are colored in magenta and dark blue, respectively. The FemX$_{Wv}$ side chains of Trp32, Lys36, Trp39, Arg211, Tyr215, and Tyr256 are colored in yellow for the apo wild-type enzyme, in cyan for the complex, and in orange for the Lys36Met mutant.

Three lines of evidence indicate that a complex hydrogen bond network involving Lys36, Arg211 and, to a lesser extent, Tyr215 is critical for the transferase activity of FemX$_{Wv}$. First, Lys36Met and Arg211Met substitutions depleted (47,000-fold) activity below detectable levels (**Fig. 8**). Second, comparison of the CD spectra and crystal structures in the case of the Lys36Met substitution indicated

that conformational changes in the mutant proteins cannot account for the loss of activity. Thus, changes in the chemical nature of the residues at positions 36 and 211 were responsible for the loss of activity. Third, analysis of substrate analogs indicated that a loss of the phosphate end or of the C-terminal D-Ala residue severely depleted $FemX_{Wv}$ activity (**Table 1**). Together, these results indicate that hydrogen interactions between two residues of $FemX_{Wv}$ (Lys36 and Arg211) and two regions of UM5K (phosphate groups and D-Ala residues) constrain the substrate in a bent conformation which is essential for activity.

In spite of their essential role in activity, Lys36 and Arg211 are not highly conserved in members of the Fem family. Looking for concerted residue-changes in multiple sequence alignments in order to reach out beyond UM5K binding site was unsuccessful (Biarrotte-Sorin et al., 2004).

1.3.5. Conclusion

As no catalytic residue was identified, the burning question remained intact… The mechanism of aminoacyl transfer from Ala-tRNA~Ala to UM5K has been identified when the structure of a complex between FemX and a synthetic peptidyl-RNA conjugate mimicking a bisubstrate reaction intermediate was determined (Fonvielle et al., 2013). Structural comparison with FemX:UM5K complex showed little change in protein structure except for a loop that folded back onto the PG precursor and, significantly, in the first three residues of the pentapeptide stem mimick. This movement suggested a rotation of the acyl acceptor lysyl residue toward the tip of the Lys305 side chain, which was proven to carry the catalytic base.

Taking a step back, my work on FemX completed my PhD experience to make me a biochemist, comforting my keen interest in structure-function relationships. Working with Michel Arthur also pulled me in the field of microbiology, which I enjoy very much up to now.

2. Gating the cytoplasmic membrane

Cells are enclosed in a lipidic cytoplasmic membrane which primarily acts as a diffusion barrier for aqueous solutes. Isolation is no long term option, and the entry or detection of such molecules is achieved by membrane-embedded proteins: transporters and receptors control material and information fluxes.

This section is about the universally conserved Sec protein channel of the general secretion pathway. I joined Franck Duong's project and helped settling his new laboratory at the University of British Columbia where my work contributed to substantiate functionally relevant intramolecular motions of the channel (Maillard et al., 2007; Tam et al., 2005).

2.1. Introducing the essential Sec translocase

Secretion by the Sec translocase is the fate of proteins with an aminoterminal signal peptide (Blobel and Dobberstein, 1975). The so-called general secretion pathway is universally conserved among living organisms but the definition and functional characterization of its components was spear-headed by *S. cerevisiae* and *E. coli* models, owing to the accessibility of biochemical reconstitution (Wickner and Schekman, 2005) and the unsurpassed exploratory power of genetic screens (Bieker et al., 1990). Fifteen years ago, model objects from archaea and other sources have emerged that supported the structural characterization of SecYEG / SecYEβ / Sec61αγβ machineries (Rapoport et al., 2017).

2.1.1. The SecYEG translocon at the atomic scale

Biochemical, biophysical and electrophysiological studies have established that the Sec complex serves as the channel through which preproteins traverse the membrane. The structures of SecYEG (~75 kDa) and SecYEβ complexes, respectively from *E. coli* and the archaea *Methanococcus jannaschii*, provided new insights into the translocation mechanism (Breyton et al., 2002; Van den Berg et al., 2004).

The SecY subunit consists of two subdomains, transmembrane segments TM1–TM5 and TM6–TM10, arranged like a claw and related to each other by a two-fold pseudo-symmetry axis. The essential SecE-subunit docks its TM helix across the interface of the two SecY subdomains, clamping them together.

The proposed translocation channel, in the center of the SecY-subunit, is constricted by a ring of six hydrophobic amino acid residues halfway across the membrane plan, that delineate a 5-8 Å diameter pore. The ring is proposed to seal the channel in dynamic manner during translocation as it should widen enough, probably by shifts in the helices forming the channel, to allow the passage of a

polypeptide chain. On the periplasmic side, the channel is filled by a short distorted helix (TM2a, termed the plug) that is contributed by a loop, right against the hydrophobic ring. Movement of the plug would yield a continuous aqueous channel through which preproteins could be translocated.

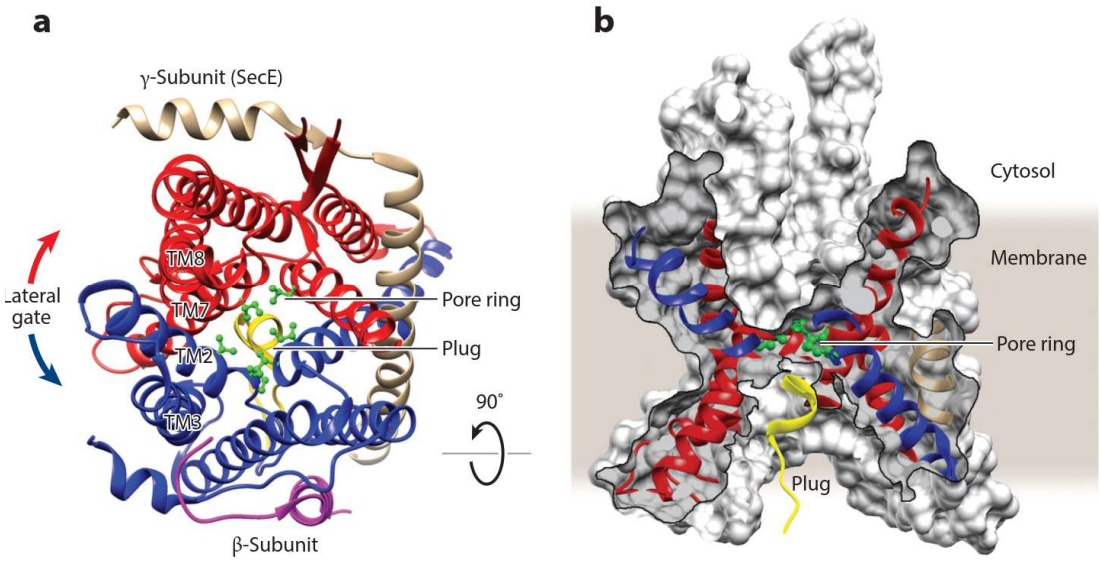

***Figure 9. Crystal structure of the idle SecY channel from Methanocaldococcus jannaschii (PDB code 1RH5)**.*

*(a) View from the cytosol. The N- and C-terminal halves of the α-subunit (**SecY**) are shown in blue and red, respectively, the β-subunit in purple, and the γ-subunit (**SecE**) in beige. The plug domain is in yellow, and the pore ring residues are shown as green sticks and balls. Transmembrane (TM) segments forming the **lateral gate** are labeled. (b) Cutaway side view of a space-filling model of the channel in the membrane. (reproduced from Rapoport et al., 2017)*

The small Secβ subunit (SecG-like subunit) is peripherally attached and makes limited contacts with SecY, which is consistent with its non-essential role in translocation. The groove between the transmembrane domains TM2 and TM7, lying at the edges of the two SecY halves is open to the lipid bilayer and was hypothesized to form a lateral gate for the release of TM segment of the membrane proteins.

2.1.2. Sec substrate at the gate - role of the signal peptide

Several cofactors of protein targeting or folding have been shown to bind on the ribosome, close to the exit channel. The trigger factor (TF) chaperone, the signal recognition particle (SRP) and the motor ATPase of the Sec machinery SecA, all scan nascent polypeptidic chains as they emerge from the channel, sometimes reaching for their substrate inside the channel (Kuhn et al., 2017). (**Fig. 9**)

Aminoterminal signal peptides that target presecretory proteins to the Sec translocon are 15-to-30 residue long, seldom longer, and typically display successively a short positively charged region (n region) followed by a central hydrophobic core (h) and a leader peptidase cleavage site (c). These traits, especially the size and hydrophobic character of the h region, determine whether the presecretory proteins will be targeted to the co-translational, SRP-dependent pathway, that picks the more hydrophobic signal peptides from integral membrane proteins, or to the post-translational, SecA-dependent pathway, which is prevalent. (Kuhn et al., 2017; Owji et al., 2018; Tsirigotaki et al., 2017)

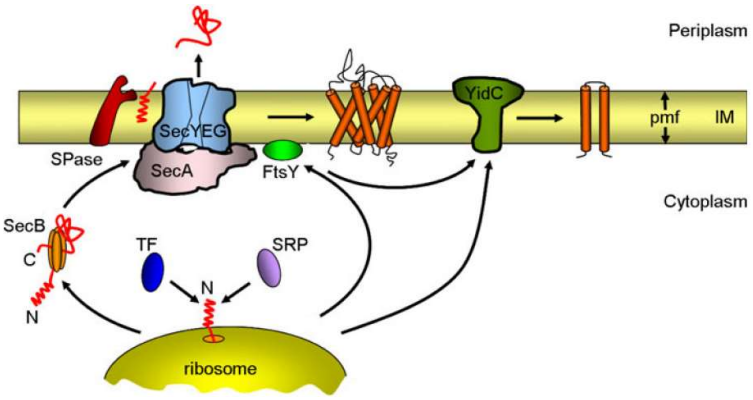

Figure 10. Schematic overview of bacterial inner-membrane protein biogenesis.

*Newly synthesized proteins are targeted to the Sec complex either by the signal recognition particle (**SRP**) as soon as they emerge from the ribosome tunnel (co-translational translocation, mainly inner-membrane proteins) or by the tetrameric **SecB** chaperone after translation (post-translational translocation, mainly secretory and outer-membrane proteins). Trigger factor (**TF**) competes with SRP for the binding of the nascent protein. Proteins destined for the inner (IM) or outer membrane are transported into or across the inner membrane through the Sec complex. The complex consists of the **SecYEG** protein-conducting channel and the ATPase motor **SecA**. The signal peptidase (**SPase**) cleaves the signal sequence from preproteins at the outer face of the inner membrane. A few membrane proteins insert into the inner membrane via **YidC**. For simplicity, SecYEG is shown without its accessory components (**SecDFYajC** and YidC). pmf proton motive force. (reproduced from Facey and Kuhn, 2010)*

The physico-chemical properties of signal peptides are essential for the interaction with the translocon and thus to initiate preprotein translocation (Owji et al., 2018). Insertion of the signal peptide into SecY channel at an early stage of translocation has been thouroughly analyzed with photoreactive probes, showing that opposite sides of the h region contact SecY segments TM2 and TM7, while each residue of the signal peptide could also be cross-linked to phospholipids (Martoglio et al., 1995; Plath et al., 1998). This picture took shape with *M. jannaschii* SecYEβ structure, where TM2 and TM7 delineate the proposed lateral gate and are accessible from the lipidic and cytoplasmic sides of the membrane.

Signal peptide binding to the translocon also involves specific charged residues in SecY loops. Charge-reversal mutations indicated that these conserved amino-acyl residues functionally interact with the n region of signal peptides and impose a hairpin loop conformation inside the channel (Puziss et al., 1992). This was illustrated in the recent structure of a substrate-engaged SecY, obtained by fusing proOmpA signal peptide to SecA and crosslinking the chimera to SecYEG (Li et al., 2016).

Synthetic signal peptide addition to the cytoplasmic side of reconstituted *E. coli* membrane bilayers has been shown to open aqueous pores detectable by transmembrane conductivity measurements (Simon and Blobel, 1992). The structure of the SecY channel in its closed state shows that the plug domain shall move away and the N- and C-terminal halves of SecY shall move apart for the channel to open and accommodate the signal peptide. A shutter-like movement of the TM segments could also contribute to adjust pore size as the polypeptide chain moves through. Earlier experiments actually support the first of these motions and have been instrumental in the design of my project (Harris and Silhavy, 1999, see **section 2.2**).

2.1.3. Powering protein translocation through the SecYEG channel

Sec-mediated translocation can be coupled to protein translation as it takes place at the ribosome during cotranslational translocation or it can be coupled to ATP hydrolysis by SecA in the preferred, post-translational translocation pathway.

The SecYEG-bound SecA ATPase activity is stimulated by a translocation-competent preprotein. This activity, termed SecA translocation ATPase, is responsible for preprotein translocation. *In vitro* reconstitution shows that the initiation step requires ATP binding but not its hydrolysis. This initial event leads the signal peptide and attached polypeptide to cross the channel in a loop-like configuration such as it can be processed by signal peptidase at the periplasmic face of the membrane. Continued translocation then requires ATP hydrolysis which causes the release of bound preprotein from SecA. New cycle of ATP binding and hydrolysis results in the stepwise translocation of preprotein domains.

The mechanism by which the energy of ATP binding and hydrolysis at SecA is converted into the movement of preproteins across the membrane has given rise to one of the most surprising stories in the field: the cyclic, ATP-driven membrane insertion of SecA (Economou and Wickner, 1994), where proteolysis protection and epitope accessilibility in different translocation states were interpreted as a piston motion of SecA, inserting into the membrane as it would push the substrate through. Several papers contributed new details to the story but some crystal structures now show how SecA docks to SecYEG, binding two large cytoplasmic loops of SecY C-terminal half and a short loop of the N-terminal half. This has replaced indirect, complex experiments with structure-informed, defined mechanistic studies, from which controversy is not absent either (Allen et al., 2016; Bauer et al., 2014; Catipovic et al., 2019).

In bacteria, the cytoplasmic membrane is energized with the PMF (**section 1.1.1**). PMF strongly stimulates post-translational SecYEG translocation. Its mechanism of action is still unknown. Altogether, the PMF has been suggested to optimize signal peptide orientation, to confer electrophoretic mobility to the translocating polypeptide as SecA cyclically detaches, to modulate SecA binding to SecY, to be used by the SecDF subunit of the translocase to pull sequences from the periplasm (Denks et al., 2014 for a review).

2.1.4. Additional subunits make the translocase holo-enzyme

In contrast to SecA, SecY and SecE, SecG is not essential for cell viability. This short bacterial protein is made of two TM segments with a short apolar cytosolic linker in-between. SecG is not needed for the high-affinity binding of SecA to SecYE, *i.e*. it is not essential to translocation, but it readily stimulates SecA activity. The *in vivo* contribution of SecG is clearly observed when SecA function is impaired by mutations, low temperature, absence of SecDF, absence of acidic phospholipids or at low transmembrane PMF (Nishiyama et al., 1994).

Figure 11. Components and hypothetical organization of the holotranslocon.

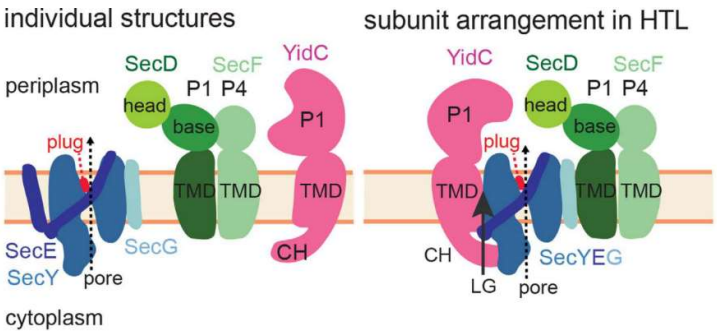

Cryo-EM reconstruction at 14 Å of E. coli holo-translocon (HTL) and subcomplexes was used to allocate density to specific components. (left) individual components of the holotranslocon: SecY marine, SecE dark-blue, SecG cyan, SecD green, SecF light-green, YidC magenta. (right) Periplasmic domains of YidC, SecD and SecF are labelled P1, P1 and P4 respectively. (Botte et al., 2016)

The core SecYE also associates with the SecDFyajC heterotrimeric membrane protein complex (Duong and Wickner, 1997). SecDFyajC is limited to prokarya, sometimes appearing as a single fusion protein. It has been shown to promote translocation in otherwise limiting conditions, e.g. SecG depletion. At low translocation rate, it has been shown the SecDFyajC complex allows the accumulation of preprotein translocation intermediates which clear the channel upon membrane energization with the PMF. This result has suggested that SecDFyajC uses PMF to boost translocation. This hypothesis still stands after structures of SecDF have been published (Tsukazaki, 2018).

A later addition to the holotranslocase is the protein YidC, a homolog of the mitochondrial Oxa1p. Oxa1p was first considered as an alternative pathway to insert proteins in the membrane, before *E. coli* YidC was found to cross-link with the same substrate that was translocating through SecYEG (Scotti et al., 2000)

The oligomeric state of SecYEG, SecA and YidC have all been controversial. Controversies about the oligomeric state of the translocase have evolved, as more and more structures showed monomers of the elements of the translocon (Rapoport et al., 2017). For these transporters, like has been noted for others at another time (Veenhoff et al., 2002), questions remain regarding a possible function for the dimers observed in the membranes (Breyton et al., 2002; Deville et al., 2011; Schulze et al., 2014; Spann et al., 2018).

2.2. Focus on SecY : dynamics of the main protein channel in the inner membrane

January 2004, the crystallographic structure of an archaeal translocon at 3.2 Å resolution was published (Van den Berg et al., 2004). Comparison with *E. coli* SecYEG structure at 8 Å resolution (Breyton et al., 2002) and multiple sequence alignments suggested that it is representative of the Sec translocon in the three domains of life. The channel component SecY looks like an hourglass with a hydrophobic constriction halfway through. It was hypothesized that this is actually the channel, plugged by a short helix (TM2a) on the periplasmic side (**Fig. 9**).

Right after *M. jannashii* SecYβ structure was published (Van den Berg et al., 2004), several groups put to test the functional relevance of the crystal structure by probing e.g. the translocation path or channel opening (Cannon et al., 2005; Junne et al., 2006; Li et al., 2007; du Plessis et al., 2009; Tam et al., 2005). My project aimed at exploring the dynamics of the SecYEG channel, using the hottest structural data and the large body of literature on SecYEG function, to capture translocation intermediates with cross-links that could be correlated in intensity with translocase activity.

2.2.1. Demonstration of a plug-open intermediate of the channel during translocation

The proposed mechanism of channel gating seemed to be supported by an earlier *in vivo* crosslinking experiment in which it was shown that cysteines introduced into the plug domain of SecY and at the C-terminal end of SecE can form a disulfide bridge (Harris and Silhavy, 1999). These two cysteines stand 20 Å apart in the closed channel structure, so that the observed crosslink was explained by the movement of the plug out of the center of the channel and toward the periplasmic side of the membrane (Van den Berg et al., 2004). The ‘plug hypothesis’ was further supported by the localization

of signal sequence suppressor (*prl*) mutations in the constriction of the channel (*prlA4*) or in the plug (*prlA3*) (Osborne and Silhavy, 1993).

The original SecY-F67C and SecE-S120C cysteine mutations described by Harris and Silhavy (1999) were taken as starting point. Cysteine-dependent covalent association between SecY and SecE was readily observed under nonreducing gel electrophoresis conditions (**Fig. 12, lanes 5 and 6**). Native gel electrophoresis showed that the dimeric SecYEG complex could be dissociated into monomers after detergent extraction, even though the SecY and SecE subunits were crosslinked (**Fig. 13, right**). This result showed that the crosslink between SecY–F67C and SecE–S120C occurs within a single SecYEG protomer.

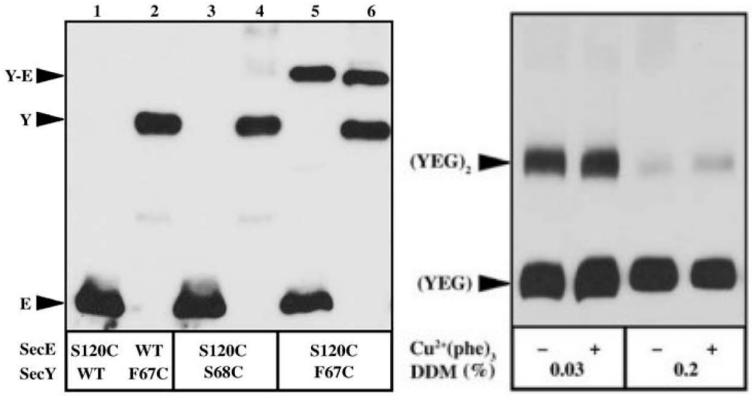

Figure 12. Crosslinking between SecY plug and SecE.

*The cysteine mutations SecY-F67C (*prlA3*) and SecE-S120C were introduced together into constructs encoding HA-tagged SecE or HA-tagged SecY. Inner membrane vesicles (IMVs) were prepared from induced cells and analyzed by SDS-PAGE and Western blotting. (**Left**) non-reducing PAGE of IMVs (1 mg total protein) enriched for the cysteine-mutagenized SecYE(HA)G (odd lanes) or SecY(HA)EG (even lanes.). Immunostaining was performed with anti-HA antibodies. (**Right**) Blue-Native PAGE of the detergent-solubilized SecYEG complex. SecYEG is monomerized at 0.2% ß-D-dodecylmaltoside (DDM). $Cu^{2+}(phe)_3$: copper phenanthroline, oxidative agent.*

Spontaneous disulfide formation between SecY–F67C and SecE–S120C could be a direct effect of the F67C mutation on the translocon (Duong and Wickner, 1999) or an indirect consequence of F67C phenotype, which consists in upregulated translocation activity. Moving the Cys mutation to a neighboring position abolished the spontaneous SecY–SecE crosslinks (**Fig. 12, lanes 3 and 4**) and restored wild type level translocation activity altogether (**Fig. 13A**).

The translocase activity of the Sec complex seemed to correlate with the location of the SecY plug domain. This dynamics was further evidenced when the SecY–S68C/SecE–S120C IMVs were incubated in oxidative conditions and SecY–SecE cysteine crosslinks were detected as well (Tam et al., 2005). This

suggests that the plug possess intrinsic mobility so that the two cysteines SecY–S68C and SecE–S120C are trapped in a disulfide bridge as they get closer in an oxidative environment.

SecY-plug movement is promoted during preprotein translocation

The plug hypothesis was directly assessed by mixing IMVs enriched for the SecY–S68C/SecE–S120C complex with translocation ligands and ATP. The results showed that the progress of preprotein translocation into the IMVs was concomitant with the appearance of the SecY–SecE cysteine crosslinks (**Fig. 14B, right**), and with kinetics comparable to that of the translocation reaction itself (**Fig. 14A**). Moreover, the concentration of preprotein substrate available was shown to determine a dose-response effect on SecY–SecE crosslinking (**Fig. 14C**) and the SecY–SecE cross-linking reaction had similar requirements as the translocation reaction itself (**Fig. 14D**). These observations directly supportes the hypothesis that the SecY plug relocates toward SecE–S120 during preprotein translocation. Under the same conditions, the IMVs enriched for the SecY–F67C/SecE– S120C complex did not show a translocation-dependent increase of the SecY–SecE crosslinks (**Fig. 14B, left**), which was interpreted as a saturation effect associated to the SecY–F67C mutation, which upregulates translocation.

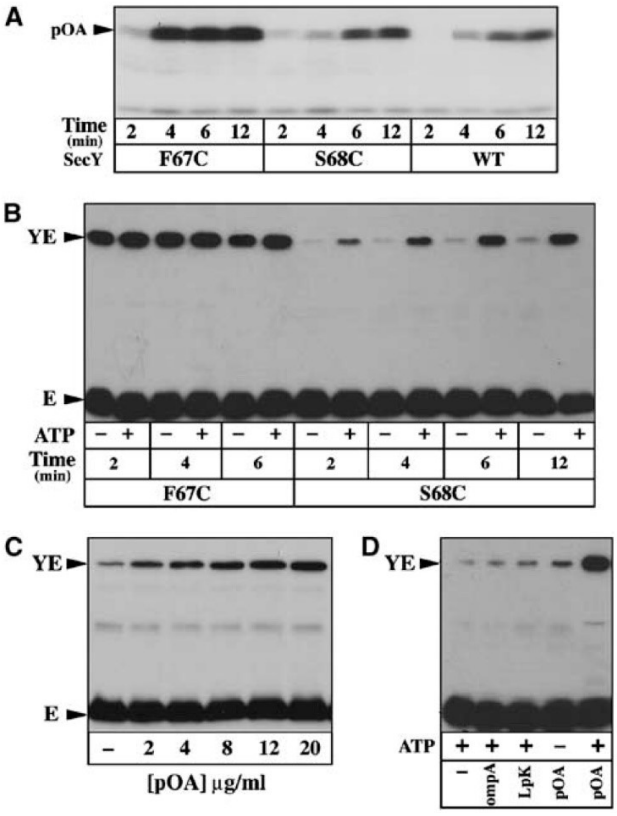

Figure 13. SecY-plug movement during preprotein translocation.

*(**A**) IMVs enriched for the WT or cysteine-mutagenized SecYEHAG complexes were tested for their translocase activity using the preprotein substrate [125I]proOmpA, as described in Materials and methods. (**B**) IMVs were incubated in the same conditions as in (A), but using unlabeled proOmpA. Unreacted cysteines were blocked with NEM (8 mM, 5 min, RT) prior to IMV solubilization and analysis by SDS–PAGE and Western blotting with anti-HA antibodies. (**C, D**) IMVs were incubated in the same conditions as in (B), but using the indicated concentration of proOmpA, or using a preprotein substrate with a deleted (OmpA) or altered (LpK) signal peptide.*

Further correlation between the translocase activity of the Sec complex and SecY plug relocation towards SecE-S120 was obtained by combining the double cysteine construct with translocation-enhancing factors *secG* and *prlA4*. SecG, a nonessential subunit, strongly stimulates the rate of

preprotein translocation (Nishiyama et al., 1994). PrlA4 is SecY-I408N, the most active variant of SecY and a mutant within the pore ring (Osborne and Silhavy, 1993; Van den Berg et al., 2004). As expected, SecG deletion correlated with diminished cross-linking whereas concurrent SecY-S68C/I408N mutations exacerbated crosslinking (Tam et al., 2005).

The open state of the channel increases the translocase potential of the Sec complex

Results obtained so far allowed to verify that plug relocation was a function of SecY translocase activity. The reciprocal question was asked: could we determine translocase activity by stabilizing the open state of the channel? IMVs enriched with SecY–S68C/SecE-S120C were incubated with increasing concentrations of an oxidizing agent, then re-isolated and analyzed for their polypeptide translocation activity. The chemically induced crosslink led to a spectacular increase in translocase activity (**Fig.**), which plateaued at a level comparable to that obtained with the original SecY–F67C (*prlA3*) mutation (Tam et al., 2005). Thus, it is possible to enhance the preprotein translocation reaction *via* artificial stabilization of the open state of the channel.

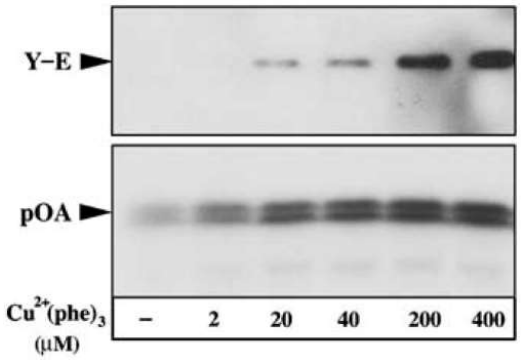

Figure 14. Stabilization of the plug in the open state increases the translocase activity.

IMVs enriched for the SecY–S68C/SecE–S120C complex were oxidized with copper phenanthroline $Cu_2(phe)_3$ at the indicated final concentration (5 min, RT), then re-isolated by ultra-centrifugation. The left lane (-) corresponded to IMVs treated with 1 mM DTT. After IMV resuspension, the amount of SecY–SecE crosslinks obtained was monitored by SDS–PAGE and Western blotting (top panel), while the translocase activity was measured using ^{125}I-proOmpA as substrate (8 min, 37°C; bottom panel).

This finding was further analyzed using other allelic forms of the Sec complex, including *prlA4* - for which an additive effect was found. This way, the phenotype of a double *prlA3* and *prlA4* mutation, which could not be combined *in vivo*, was measured (Tam et al., 2005).

Thus, structural and genetic data (Harris and Silhavy, 1999; Van den Berg et al., 2004) have inspired a thorough investigation of SecY internal dynamics during translocation, allowing us to identify a functional intermediate of the Sec complex. Switching the cysteine position from F67 to S68 has been instrumental to the demonstration that this intermediate is functionally relevant and has allowed to shed a new light on the interaction between different translocation enhancing factors.

2.2.2. Role of the plug in SecY-mediated translocation

Observing that the plug domain has intrinsic mobility (**Fig. 12**) I wondered whether it could be ablated, and what would be the phenotype of a plug-less channel.

The plug domain is located in the first periplasmic loop of SecY, upstream TM2 of the lateral gate. (**Fig**. **9**). It is often connected to TM1 and TM2 by loops with conserved hinge motifs. Based on a structure-informed alignment of SecY sequences (Van den Berg et al., 2004), I designed two plug-less channels: one with a strict truncation of the plug domain (SecYΔ8) and one with the segment between the hinge motifs missing (SecYΔ33). This was done in order to minimize the possibility that the missing plug be replaced by residues from an adjacent loop, which was actually observed in the crystal structure of a plug-less mutant of the archaeal translocon published later (Li et al., 2007).

The functionality of plug-less SecY channels was assessed genetically in two ways by Dominique Belin and Filomena Silva (Genève): (i) complementation of the thermosensitive phenotype in a *secY24* background and (ii) complementation of the loss of a plasmid-borne copy of *secY* upon plasmid curation in a *secY* null background. In both assays, partial complementation was observed with the plug-less channels, as was the case with *prlA3*, that encodes SecY-F67C (Maillard et al., 2007).

Finally, the *secY* mutant genes were cloned along *secE* and *secG* and the production of plug-less SecYEG complexes was a success. SecY, SecE and SecG were produced at similar levels, regardless of the presence of the plug domain or not. Consequently, the plug-less mutants were correctly assembled in the membrane and plug-less channels were sealed, since overproduction was not deleterious to the cells (Maillard et al., 2007).

Plug-open channels have been found to reproduce a Prl phenotype with respect to enhanced activity and PMF-dependency bypass (Tam et al., 2005). The same effect was demonstrated after plug ablation: plug-less channels behaved like PrlA3 containing channels. This was assessed quantitatively in a proOmpA translocation assay (Maillard et al., 2007)., and SecA partial proteolytic resistance, stronger in Prl phenotypes (**Fig. 15**).

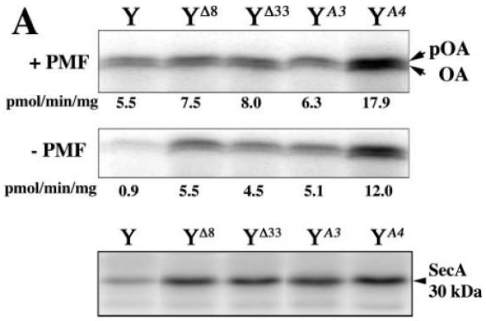

Figure 15. In vitro activity of the plug-less translocation channel.

*(**Top**) Translocation of ^{125}I-labeled proOmpA (pOA) into IMVs enriched for the indicated SecYEG complex in the presence or absence of PMF. OA, OmpA. (**Bottom**) SecA membrane insertion was measured using urea-stripped IMVs. The reaction was initiated in the presence of proOmpA and ATP (1mM) for 10min at 37°C followed by the addition of AMP-PNP (4 mM) for 3 min.*

A similar conclusion was reached *in vivo* when the secretion of PhoA or the signal peptide-deficient MalE(T16K) were assessed. As determined by the extent of signal sequence cleavage, only 10% of the MalE(T16K) protein was exported during the radioactive pulse in cells expressing the wild-type SecYEG complex. In contrast, the export was strongly improved in cells expressing the plug-less SecYEG complexes, and almost reached the level observed in cells expressing the PrlA3 mutant complex (Maillard et al., 2007). Altogether, the results show that the ablation of the plug domain increases the activity of the SecYEG channel but reduces its selectivity.

The Prl phenotype of plug-less channels was further established by bringing evidence of a lower stability of those channels. Indeed, a fundamental distinction between wild-type and PrlA mutant channels resides in the strength of the SecYEG subunit associations (Duong and Wickner, 1999). Both plug-less SecYEG complexes were thus tested for the stability of their quaternary structure upon extraction from the membrane with DDM. DDM-solubilized SecYEG migrated as a population of monomers and dimers, like SecYEG complexes carrying the *prlA3* or *prlA4* mutation (**Fig. 16**). In contrast, complex instability was detected with the large SecYΔ33 deletion, for which much less SecYEG dimers was detected with a concomitant increase of dissociation products, migrating below the SecYEG monomer. The SecYΔ8 deletion also appeared to destabilize the SecYEG channel but to a lesser extent.

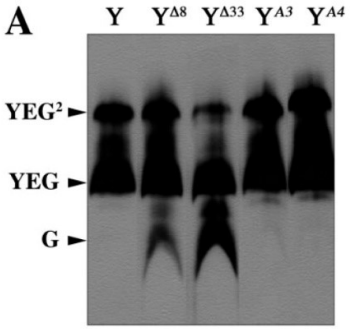

Figure 16. Stability of the plug-less translocation channel.

IMVs enriched for the indicated SecYEG mutant complex (1µg of total IMVs proteins) were solubilized with 0.1% DDM final, 30 min on ice, and the proteins were separated by linear gradient 4–13% BN-PAGE. After electrotransfer onto PVDF membrane, the Sec complex was immunostained with anti-SecG antibodies.

That the plug domain is essential neither for the function of the translocon nor for channel closure was provocative, but the Prl phenotype associated with plug displacement or plug removal clearly showed a direction.

Investigating plug dynamics again, I asked whether plug motion itself is essential for translocation and decided to reduce plug mobility by cysteine cross-linking. The crystal structure of the *M. jannaschii* SecY complex was used to design a plug-closed mutant of SecY in which positions 68 (plug) and 282 (TM7) have been replaced by cysteines such as to be able to link them with a disulfide upon oxidation.

The extent of disulfide crosslinking was monitored with trypsin cleavage of SecY, taking advantage of a cleavage site in the cytosolic loop between TM6 and TM7 (Brundage et al., 1990): successful crosslinking of S68C and S282C tethers both parts together, yielding a seemingly intact product in SDS-PAGE.

Membranes containing the SecYEG complex were oxidized with increasing copper phenanthroline prior being tested for crosslinking and protein translocation activity (**Fig. 17**). Progressive oxidation of the SecYEG complex led to a concomitant decrease of protein translocation efficiency (**Fig. 17A**). The translocation activity was reduced to a level comparable to that of wild-type membranes (*i.e.* containing only chromosomally encoded wild-type SecYEG) when the plug domain was quantitatively linked to residue Cys-282 of TM7 This reduction of translocation activity depended on the presence of both Cys-68 and Cys-282 in SecY (**Fig. 17B**). Thus, the mobility of the plug is essential to the mechanism of translocation.

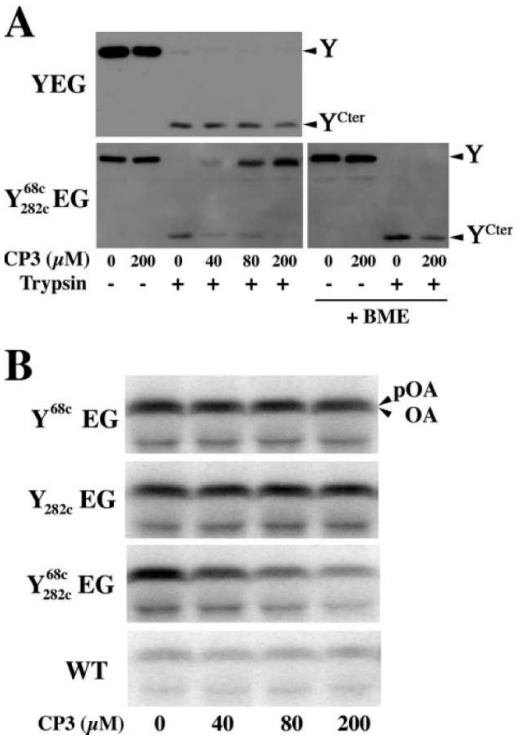

Figure 17. The movement of the plug is essential for protein translocation.

(Top) *In the presence of trypsin, the SecY protein is digested into two fragments, and the C-terminal fragment (14 kDa) is detected using an antibody recognizing the most C-terminal cytoplasmic loop of SecY. IMVs were oxidized with the indicated concentration of copper phenanthroline (CP3) and reisolated by ultracentrifugation. After trypsin digestion (30 min on ice, 1 mg/ml trypsin), samples were analyzed by 12% non-reducing SDS-PAGE and immunostained with antibodies against the C-terminal part of SecY (YCter).* ***(Top right)*** *To show that trypsin digestion and cysteine cross-linking had occurred, 2-mercaptoethanol (2 mM) was added to the samples before separation on the gel.* ***(Bottom)*** *Translocation activity of the IMVs oxidized in A was measured using ^{125}I-labeled proOmpA (pOA). Wild-type (WT) IMVs or IMVs enriched for the SecYEG complex containing only 1 cysteine residue at the indicated position were oxidized and analyzed in the same conditions. OA, OmpA.*

2.2.3. Conclusion

The crystal structure of the SecY complex represents the closed state of the channel where the so-called plug domain docks onto the constriction ring (Van den Berg et al., 2004). Translocation supposes plug displacement and constriction ring expansion to let polypeptides go through. The plug domain was found to be dispensable to channel gating, as it could be ablated in vivo, both in bacteria (Maillard

et al., 2007) and in yeast (Junne et al., 2006). Yet the experiments presented here, where the plug was locked into in an open state or into the closed state, clearly indicated that the movement of the plug is an essential subreaction associated with polypeptide transport across the membrane.

The function of the plug domain was not fully understood. Inspired by the large corpus of data available on SecY *prl* mutants, I could show a clear parallel between plug function and the phenotype of these mutants. Noteworthily, the structure has revealed that most *prl* mutations in secY are located at the pore and in the plug domain (Smith et al., 2005).

Various phenotypes are associated to *prl* mutations *in vivo* and *in vitro*: enhanced translocation rates, increased membrane affinity and insertion of SecA, diminished requirement for canonical signal peptides, reduced PMF dependence of translocation, facilitated translocation of folded domains, and for some signal peptides or TM segments, inversion of their membrane topology (Nouwen et al., 1996; Peters et al., 1994; Prinz et al., 1998; van der Wolk et al., 1998). It was proposed that these seemingly unrelated effects all derive from an enhanced conformational flexibility of the translocation channel (Duong and Wickner, 1999). Accordingly, the SecYEG complex is expected to be dynamic to let the polypeptide substrate move through or be released laterally into the lipid bilayer.

Because (i) the plug domain could be cross-linked to the middle part of TM7, which belongs to the lateral gate, and (ii) plug ablation weakened intermolecular interactions in SecYEG, it is possible that the plug domain in the closed state also interacts with the inner wall of the channel. This would stiffen and stabilize the channel in the closed state. Binding of the signal peptide between TM2 and TM7 (Plath et al., 1998) would prime plug displacement, thus interfering with plug-mediated stabilization of the closed state and inducing channel relaxation. In this model, the role of the plug is to regulate SecY dynamics (Maillard et al., 2007), which is a key feature of translocation (Tam et al., 2005).

3. Monitoring the envelope

The bacterial envelope is not a passive, protective shell around the cell. Being neither energized or fully under control, with peptidoglycan as its foremost component, the envelope is kin to a polder that the bacterial cell would have claimed over its surroundings. Envelope proteins not only serve maintenance or transport functions but also adhesion and motility or monitoring functions.

3.1. Prevalent signaling pathways in bacteria

In bacteria, signaling is dominated by two types of pathways: one-component and two-component signal transduction systems which account together for more than 95% of the signaling systems inventoried (Ulrich and Zhulin, 2010). Both are widespread, numerous and very diverse, with one-component systems prevailing by *ca*. one order of magnitude, suggesting that the two-component systems actually evolved from one-component systems, after Archaea and Bacteria branched apart (Ulrich et al., 2005; Wuichet et al., 2010). σECF constitute a third type of pathways that has been acknowledged quiet recently to take into account the various cues they respond to, as well as their widespread phyletic distribution; a classification was proposed (Staroń et al., 2009). Finally the LytTR domain which belongs to the repertoire of one-component and two-component systems has been found to be also associated with a new regulatory mechanism in what might be a fourth type of signaling pathways (Zou et al., 2018).

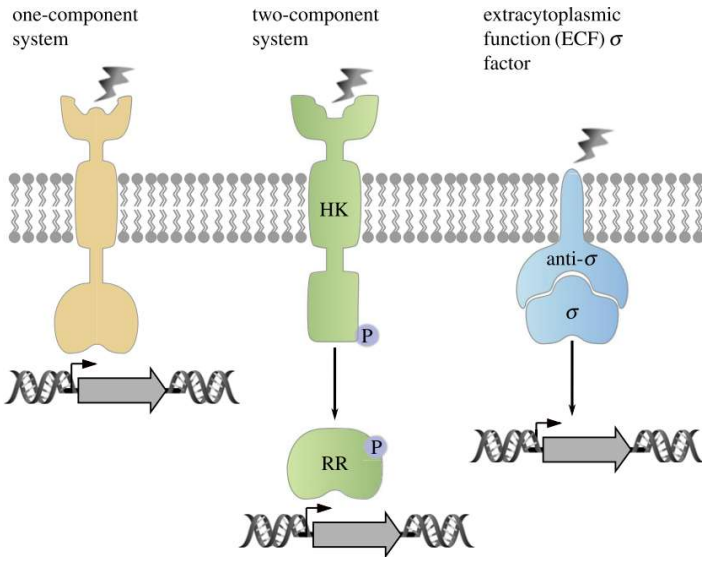

Figure 18. Schematic presentation of the major types of transmembrane signaling systems in bacteria.

One-component signaling systems, consisting of sensor and DNA-binding domain (yellow), two-component systems with a membrane-integrated histidine kinase (HK) and a response regulator (RR) (green), and extracytoplasmic function (ECF) sigma factors (σECF) that will be released from the anti-sigma factor (anti-σ) upon stimulus perception (blue). (reproduced from Jung et al., 2018)

3.1.1. One-component and two-component systems prevail

One-component systems rely on a single protein that carries one input domain and one effector domain. Most of them are soluble in the cytoplasm but some do work across the cytoplasmic membrane (**Fig. 18**). The input domain scans its environment for a stimulus whose perception triggers a conformational change that will regulate, directly or indirectly, the function of the output domain. The output domain is a DNA binding domain and the whole protein is a switchable transcription factor (Ulrich et al., 2005).

In two-component systems, the input and effector domains belong to distinct proteins, respectively called the sensor and the response regulator (Capra and Laub, 2012; Jacob-Dubuisson et al., 2018). Sensors are histidine kinases whose activity is reversibly switched from phosphatase to kinase by perception of the appropriate stimulus (Mascher et al., 2006). The autophosphorylation of a histidinyl residue starts a phosphorylation cascade that will eventually regulate the activity of the effector domain of the response regulator, which is a transcription factor in 70% of the cases (Zschiedrich et al., 2016).

3.1.2. ECF-type sigma factors

Most bacterial responses are regulated at the transcription initiation level. This reflects in the massive recruitment of DNA-binding domains in one-component and two-component systems. Transcription initiation is achieved by a distinct family of transcription factors, called σ factors, which are dissociable subunits of the bacterial RNA polymerase (RP). A third type of signaling systems has been acknowledged in which the availability of the σ factor is controlled from the outside by a signaling cascade: the extracytoplasmic function σ factors (σECF) (Staroń et al., 2009).

Bacteria possess several σ factors that control the transcription of different sets of genes and compete to bind the α2ββ'ω core of the RP (Gruber and Gross, 2003). Most σ factors belong to the σ70 family: they show related transcription initiation mechanisms and display two to four of the typical domains named σ1 through σ4 (**Fig. 19**). The simplest of σ70 factors only display domains σ2 and σ4 connected by a linker that is unrelated to σ3: this is the signature of the σ ECF, which form a large, diversified subfamily (Lonetto et al., 1994).

Sequence profiling has allowed sorting σECF in an open classification of more than 40 subgroups that reflect stimulus and promoter specificities (Staroń et al., 2009). Sigma factor availability is regulated by specific anti-σ factors (anti-σ) and proteins building regulatory networks around them (Hughes and Mathee, 1998; Sineva et al., 2017). For most σECF, regulatory networks reach across the cytoplasmic

membrane, allowing their cytoplasmic availability to reflect a particular condition sensed in the envelope. Indeed, in all elucidated cases, cytoplasmic availability is tuned by the conditional destruction of a transmembrane antisigma factor (Sineva et al., 2017).

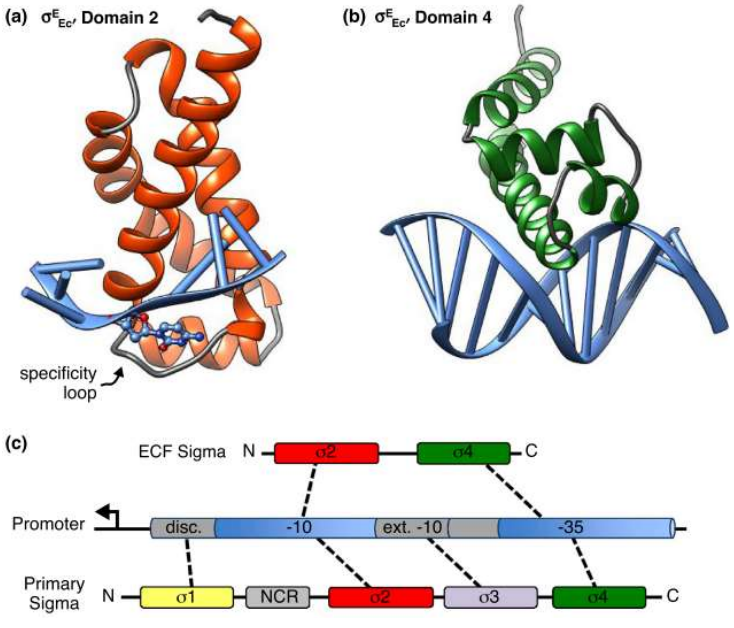

Figure 19. Promoter recognition by sigma factors.

*(**a**) Domain σ2 bound to the nontemplate strand of the -10 promoter element. The loop that determines binding specificity forms a pocket for the cytosine base, shown in ball and stick format, that is flipped out from the single stranded DNA helix. (**b**) Domain σ4 bound to the -35 promoter element. (**c**) Domain organization of σECF and primary σ factors (σ70) are compared. Interactions between individual σ factor domains and the promoter are indicated by dashed lines. NCR is the non-conserved region of primary σ factors. Disc., discriminator motif. ext. -10, extended -10 motif. (modified from Sineva et al., 2017).*

Most of the model σECF investigated so far have led to similar discoveries regarding both regulation by regulated intramembrane proteolysis and structure. Indeed, in half the subgroups, the corresponding antisigma factors display a similar 70-residue-long structural motif, called ASD for antisigma domain, in combination with diverse sensory modules (Campbell et al., 2007). Still a remarkable variety of mechanisms is expected (Mascher, 2013) and alternative structural scaffolds do exist for antisigma factors. The story that follows lifted the veil on such a scaffold and the events that take place upstream in the signaling pathway.

3.2. Focus on CnrYXH-mediated signaling across the inner membrane

The β-proteobacterium *Cupriavidus metallidurans* CH34 has been first isolated from the sludge of a decantation tank in a Belgian zinc factory (Mergeay et al., 1985). It has known a circumvoluted taxonomic history, changing names and affiliations, up to twice the same year, until *Cupriavidus* was acknowledged as the valid genus name (Vandamme and Coenye, 2004). *C. metallidurans* is best known for its resistance to millimolar-range concentration of numerous heavy metal ions, thanks to efflux,

complexation or reducing precipitation (Janssen et al., 2010). Not surprisingly it is selected in metal-rich anthropic sites, including mine ores (Reith et al., 2009) and the international space station (Rob van Houdt, personal communication). Probably for the same reason, *C. metallidurans* has recently emerged as a threat in the hospital (Langevin et al., 2011; Vandamme and Coenye, 2004).

Heavy metal efflux (HME) resistance nodulation and cell division (RND) pumps are the major players in *C. metallidurans* resistance to heavy metals. Redundant HME-RND transporters with somewhat overlapping specificities expel surplus cations from the periplasm while inner membrane exporters, e.g. from the cation diffusion facilitator (CDF) superfamily, detoxify the cytoplasm (von Rozycki and Nies, 2009). Resistance genes are induced following the detection of heavy metal cations in the periplasm, which happens mostly by two-component systems but not exclusively (Grosse et al., 2004, 2007).

The cobalt and nickel resistance (*cnr*) determinant of *C. metallidurans* CH34 belongs to the 170 kb plasmid pMOL28 and displays two operons (Grass et al., 2000; Liesegang et al., 1993; Tibazarwa et al., 2000). The effector operon *cnrCBAT* encodes the RND pump CnrCBA and the CDF transporter CnrT. The regulatory operon *cnrYXH* encodes three proteins that regulate *cnr* expression, including the σECF factor CnrH that will be described in much detail below. As we began, the *cnr* determinant had but one known ortholog, *nccYXHCBAT* that was deemed responsible for nickel cobalt and cadmium resistance in *C. metallidurans* 31A (Schmidt and Schlegel, 1994). Such systems are usually annotated as *cnr*/*ncc* in data bases. Noteworthily, it is no trivial task to determine metal specificity: in absence of an appropriate exchange experiment or an individual assessment, one may consider that *cnr* and *ncc* are essentially interchangeable.

Some data on *cnr* can help picture how tricky assessing metal specificity can be. Even though Zn(II) has been shown repeatedly not to induce *cnr* expression (Grass et al., 2000; Monchy et al., 2007; Tibazarwa et al., 2000; Trepreau et al., 2011), unregulated expression of the *cnrCBAT* operon has been associated to high-level of Zn(II) resistance (Collard et al., 1993), showing that at least in this case, response selectivity is determined at the induction step, not the extraction step. Also, when *cnr* expression was used as a sensor of Ni(II) and Co(II) bioavailability, it was found to be 100 fold more sensitive to Ni(II) than Co(II) (Tibazarwa et al., 2001).

The regulation of *cnr* expression has been first investigated with genetics (Grass et al., 2000; Tibazarwa et al., 2000). Deletion, truncation and fusion experiments have helped establishing a model in which CnrH would be sequestered at the plasma membrane by the anti-sigma factor CnrY, whose action would be neutralized upon sensing of excess Ni(II) or Co(II) in the periplasm by CnrX. The presence of both proteins, CnrY and CnrX, seems to be essential for CnrH to be sequestered in the absence of a cue

(Grass et al., 2005). This can be correlated to the following sequence features: CnrX is made of a membrane-embedded periplasmic domain that carries a conserved zinc peptidase HExxH motif (Cerdà-Costa and Gomis-Rüth, 2014) and CnrY is the only bitopic protein of the system *i.e.* the only physical link between the periplasm and the cytoplasm (**Fig. 19a**).

Due to its minimal size, the mere chemical nature of the regulating cue, the novelty of both CnrX and CnrY for which only one homolog was known as we began, and possible applications involving biosensing (bioremediation) and sigma factor inhibition (antibiotic development), I considered the CnrYXH system to be ideal to investigate transmembrane signaling and got hired by the CEA to do so.

3.2.1. Molecular basis of CnrH inhibition by CnrY

A co-founder of the σECF subfamily, CnrH, shares 28% identity and 51% similarity with *E. coli* RpoE (Lonetto et al., 1994). CnrH is regulated by a complex of two transmembrane proteins: the periplasmic sensor CnrX and the anti-σ factor CnrY (Grass et al., 2000; Tibazarwa et al., 2000). At rest, CnrH is sequestered by CnrY whose 45-residue-long cytosolic domain is one of the shortest anti-σ-domains. Upon Ni(II) or Co(II) ions detection by CnrX in the periplasm, CnrH is released by an unknown mechanism (Fig. 1a). The complex between CnrH and the cytosolic portion of its minimal-size anti-σ CnrY has been characterized. This work has unraveled structure:function relationships in a new group of anti-σs and delivered several new insights regarding the regulation of σ factors of the σ70 family by their anti-σ factors.

The coproduction of the cytosolic domain of CnrY (CnrYc) and a strep-tagged derivative of CnrH supported the purification of the complex which eventually crystallized after uncontrolled proteolysis at the C-terminus of CnrYc. Crystals diffracted to 1.75 Å and the structure was determined by Richard Kahn and Eric Girard, using single wavelength anomalous diffraction of a Gd:DO3A derivative. As a result of conformational freedom in the linker connecting CnrH domains, three polypeptide chains were resolved in the asymmetric unit: CnrH σ2 and σ4 domains plus CnrYc.

Structure of the CnrH:CnrYc complex

In CnrH:CnrYc, an L-shaped CnrYc binds a globular CnrH whose domains σ2 and σ4 are packed against each other, their fold being preserved. CnrYc fits in a remarkable hydrophobic groove running at the surface of σ2 and extending into a hydrophobic pocket on σ4. As much as 40% of CnrYc molecular surface are buried in the complex (1245 Å²) and CnrYc folds into a well-defined α-helix (H1′) that fits into σ4 hydrophobic pocket. The peptide further extends along the hydrophobic groove of σ2 with no canonical structure except for a short helical turn (H2′) (**Fig. 20g**). The most prominent feature of CnrYc

is a hydrophobic knob made of V4, W7 and L8 side chains, that protrudes into σ4 hydrophobic pocket and contributes as much as quarter of the interface.

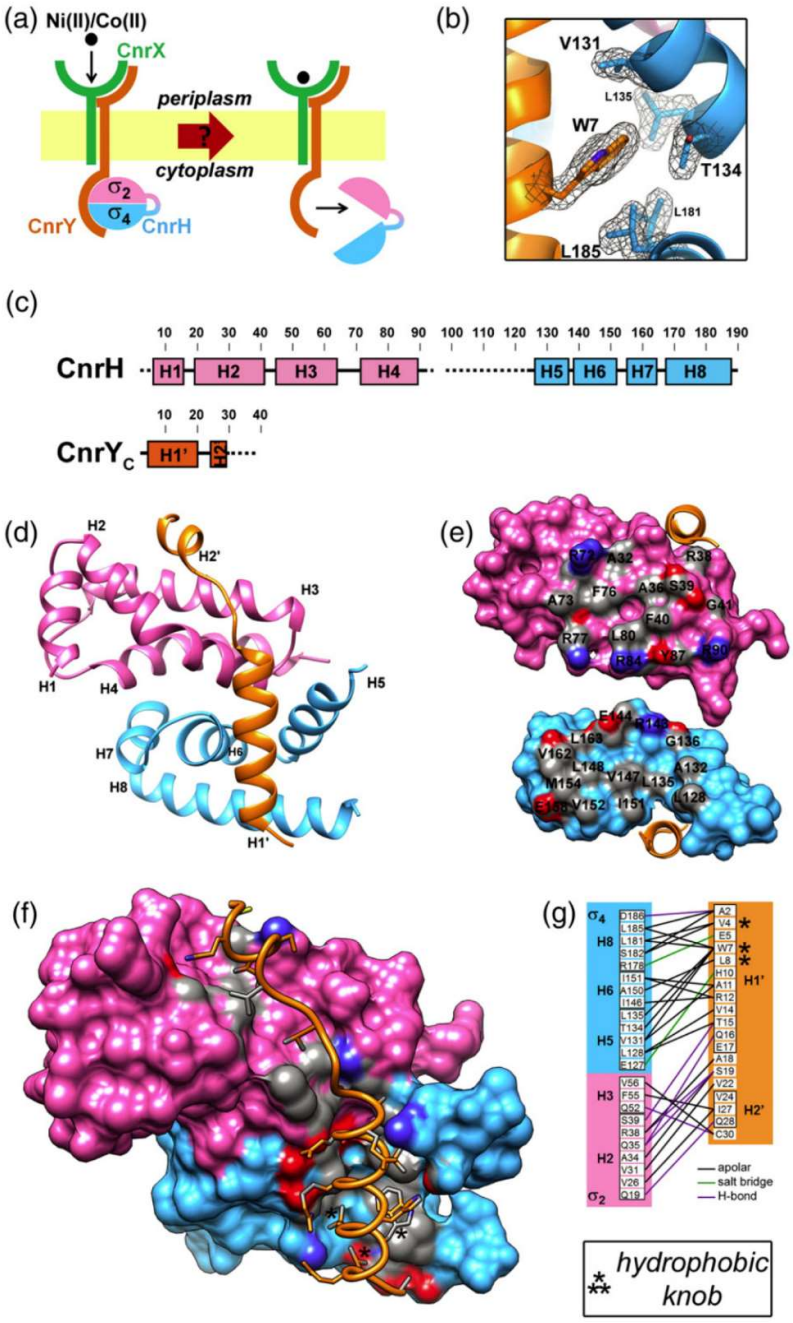

Figure 20. CnrY embraces the closed conformation of CnrH.

(a) CnrYXH signaling cascade involves Ni(II) or Co(II) binding to the sensor CnrX (green), which induces the anti-σ factor CnrY (orange) to release CnrH (σ_2 in pink, σ_4 in blue). CnrH drives the transcription of cobalt and nickel resistance genes. (b) $2F_O$-F_C electron density map near CnrY residue W7, contoured at 1 σ. (c) Diagram representation of CnrH and CnrYc fragments present in the crystal with segments unresolved in the electron density pictured as dashed lines. See text for details. (d) Ribbon representation of CnrYc in complex with CnrH domains σ_2 and σ_4. Helices were tagged near their N-terminus. (e) Open book display of σ_2 and σ_4 molecular surfaces with atoms of the σ_2:σ_4 interface in CPK colors. CnrYc H1' (orange) is shown for orientation. Residues of σ_2 in contact with σ_4 (top) make a central hydrophobic patch surrounded by a rim of arginyl residues contributing apolar contacts (R38, R72, R77) and interdomain salt bridges (R72:E158, R84:E144). Likewise, most σ_4 residues in contact with σ_2 are hydrophobic (bottom). (f) CnrH:CnrYc interface atoms. Intermolecular atomic contacts are CPK colored on CnrH molecular surface and CnrYc stick representations. V4, W7 and L8 side chains (stars) form a hydrophobic knob that protrudes into σ_4 hydrophobic pocket. (g) CnrH:CnrYc interface residues. CnrH domains σ_2, σ_4 and CnrYc appear as pink, blue and orange boxes respectively. Only residues with atomic contacts shorter than 4.0 Å are displayed.

CnrYc occludes CnrH functional surfaces in the complex

To achieve σ factor functionality, each of the σ2 and σ4 domains binds simultaneously the RP core and promoter DNA in the transcription initiation complex (TIC). The TIC with CnrH as the σ factor was

modeled by domain-to-domain superimposition in order to examine CnrH inhibition by CnrY (Vassylyev et al., 2002). As expected from the high degree of conservation within the σ70 family (Sharp et al., 1999), only minor steric clashes could be observed. Domain σ2 binds both DNA (Feklistov and Darst, 2011) and the so-called β' coiled-coil domain, a major site of interaction on RP (Arthur et al., 2000): in CnrH:CnrYc, σ2 cannot take part in any of these interactions because CnrY residues 21–30 compete with the β' coiled-coil domain and CnrH σ4 conceals the DNA-binding surface of σ2 (**Fig**. **21b-c**). Domain σ4 binds the promoter −35 element via region 4.2 (Campbell et al., 2002) that is freely accessible in CnrH:CnrYc and it docks the β flap-tip helix at the same hydrophobic pocket where CnrYc binds (**Fig. 21b-d**). Although CnrYc H1' and the β flap-tip helix run antiparallel with each other, it is remarkable that CnrYc residues forming the aforementioned hydrophobic knob (V4, W7, L8) superimpose with conserved residues of the β flap-tip helix (**Fig. 21e**) that mediate σ4 function (Geszvain et al., 2004).

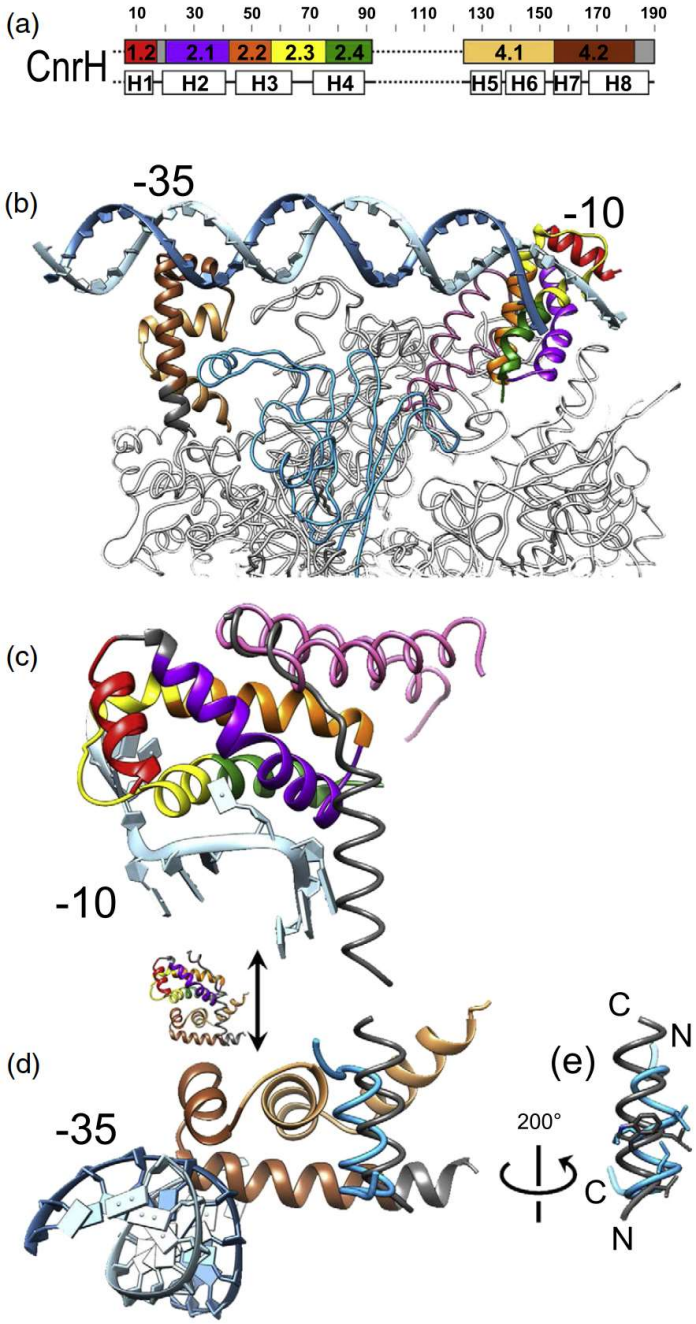

Figure 21. Molecular basis of CnrH inhibition by CnrYc.

(a) Diagram representations of CnrH show conserved σ^{70} regions as color-coded boxes (top), α-helices as bricks (bottom) and portions not determined in the electron density as dashed lines. (b) Model of CnrH within the transcription initiation complex. The RNA polymerase core (coil) contacts CnrH (ribbons) via the β' coiled-coil domain (pink) and the β flap tip helix (blue). The tips of the unresolved segment connecting CnrH domains stand 55 Å apart, which is compatible with the length of a 31-residue linker. (c) A close-up view at CnrH σ_2 shows that CnrYc helix H2' (grey) competes with the β' coiled-coil domain (pink) while CnrH σ_4 domain competes with the promoter -10 element. The latter is suggested by the double-arrow between panels (c) and (d) while the inset pictures CnrH:CnrYc. (d) A close-up view at CnrH σ_4 shows that CnrYc (grey) prevents σ_4 binding to the β-flap tip helix (blue) but not to the promoter -35 element. (e) CnrYc residues V4, W7 and L8 superimpose with conserved residues I777, L774 and L773 of the β-flap tip helix, respectively.

The relevance of these observations was comforted by assessing sequence conservation in CnrY-like proteins when it was found that sequence similarity was confined to the residues that occlude the RP-binding determinants of CnrH (**Fig. 22**). Because CnrY-like sequences bear no typical motif, they were collected using gene association within cnrYXH-like operons. CnrY-like sequences were systematically found upstream CnrX-like sequences, which indicates that CnrY is the protoype for an emerging family of CnrX-regulated anti-sigma factors (Maillard et al., 2014).

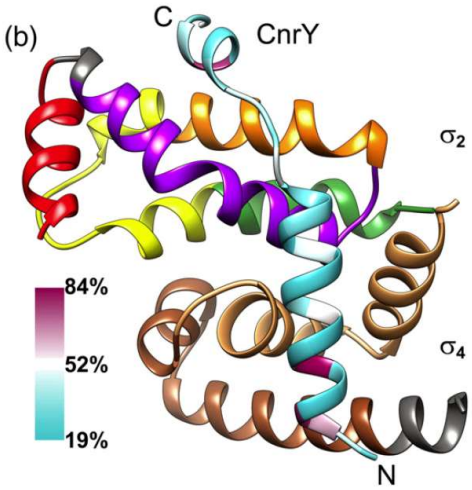

Figure 22. Sequence conservation analysis of CnrY-like proteins.

Mapping of CnrY sequence conservation on a ribbon representation of CnrH:CnrYc. Fourty-three sequences have been collected. CnrYc residues are colored from cyan to maroon as conservation increases (see color key) and CnrH conserved regions are colored as in Fig 2. CnrYc, partially occludes conserved regions 2.1 (purple), 2.2 (orange), 4.1 (sand) and 4.2 (brown) while the closed conformation of CnrH partially occludes regions 2.1, 2.3 (yellow), 2.4 (green), 4.1 and 4.2.

Finally, the prevailing role of the hydrophobic knob in CnrH inhibition by CnrY was demonstrated *in vivo* by Widade Ziani, PhD student, who used GFP as a reporter of CnrH-mediated transcription in the heterologous host *E. coli* and western blots to check protein production levels. The activity of structure-based variants of CnrY was measured: it was found that W7 & L8, the two largest residues of the knob actually formed a hot spot determining CnrY ability to sequester CnrH *in vivo*.

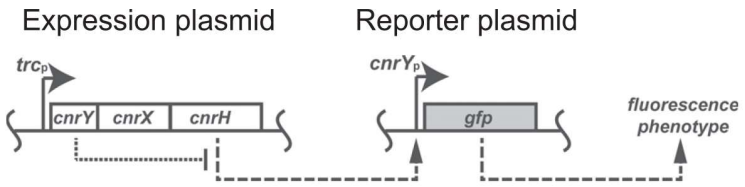

***Figure 23. Testing CnrY-dependent activity of CnrH in* E. coli.**

Design principle of the in vivo *functional assay. Compatible* E. coli *vectors carry the* cnrYXH *operon downstream an IPTG-inducible promoter and the* gfp *reporter gene downstream a CnrH-specific promoter. GFP fluorescence depends on CnrH functionality and it reflects the failure of CnrY to sequester CnrH when CnrY is present. (b) CnrH activity in the heterologous host* E. coli*. Overexpression of* cnrH *triggered high fluorescence intensity in* E. coli *cells thus demonstrating CnrH functionality in this host (counting from left, compare bars 1 and 2: and* cnrH*). CnrH activity was efficiently quenched when* cnrH *was expressed from the* cnrYXH *operon (compare bars 2 and 3:* cnrH *and* WT*). The positive control of CnrH activity when produced from* cnrYXH *was obtained by replacing CnrY cytosolic domain by an irrelevant sequence (FLAG tag) in* cnrYXH *(compare bars 3 and 4:* WT *and* FLAG*). Error bars depict standard deviation about the mean.*

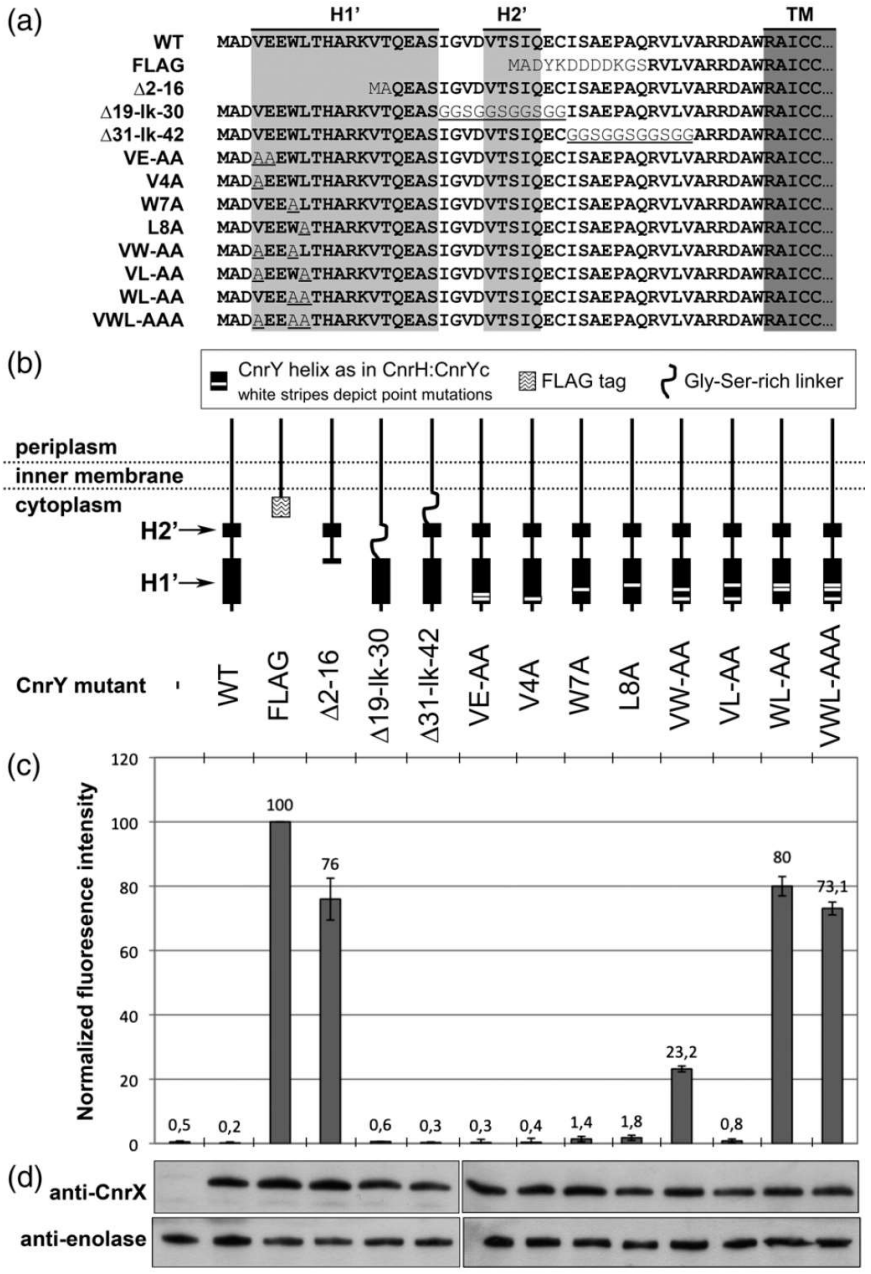

Figure 24. **In vivo *investigation of CnrY function pinpoints a hotspot in CnrH inhibitory binding.***

*(**a**) Partial sequence of the CnrY mutated proteins tested. Shaded are sequence portions aligned with helices H1' and H2' (light grey) and the cytosolic end of the transmembrane anchor (dark grey). As discussed in the text, the intrinsic stability of H1' and H2' is probably low and they are stabilized upon CnrY binding to CnrH. The sequence of wild type CnrY is in bold type whereas mutations are not; substitutions are underlined.*

*(**b**) Schematic representtation of the CnrY mutants tested. These are (left to right) wild type CnrY (*WT*); a CnrY derivative with a FLAG tag replacing the cytosolic domain (*FLAG*); a CnrY deletion mutant with residues 2 to 16 missing (*Δ2-16*); CnrY mutants where a linker was substituted to residues 19 to 30 (*Δ19-lk-30*) or residues 31 to 42 (*Δ31-lk-42*); point mutants of CnrY where V4, E5, W7, L8 have been changed to alanyl residues either alone (*V4A, W7A, L8A*) or in combination (all others).*

*(**c**) Fluorescence intensity was measured on live cells expressing either nothing (-, empty vector) or the* cnrYXH *operon encoding the CnrY construct specified above. The impact on CnrY function was maximized with the* WL-AA *double mutation; see text for details. Error bars depict standard deviation about the mean.*

*(**d**) The quantitative comparison of fluorescence measurements was comforted by ruling out a polar effect of* cnrY *mutations on downstream expression of* cnrXH*. Using antibodies directed against CnrX, the amount of recombinant proteins produced from each construct was assessed by western blotting.* E. coli *enolase was used as an internal control. The same washed-cell suspension was used to perform western analyses and fluorescence spectroscopy (panel c).*

A new structural class of anti-σECF

During the course of this work, structures of the σECF-like domain of PhyR in complex the anti-σ NepR have been published (Campagne et al., 2012; Herrou et al., 2012). PhyR is the response regulator of a two-component system (see **section 3.1**) that controls the general stress response in α-proteobacteria. CnrH:CnrYc was found to be structurally superimposable to PhyR:NepR despite both systems being otherwise unrelated. (**Fig. 25**). The high structural similarity of CnrYc and NepR in complex with their σ factor may result from convergent selection *via* binding to similar targets.

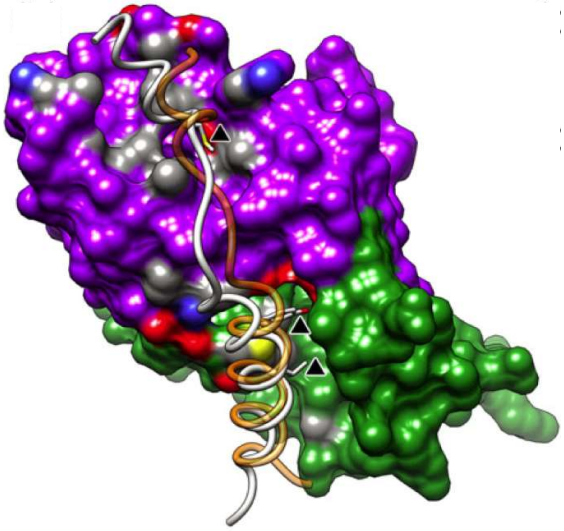

Figure 25. CnrY and NepR define a new structural class of anti-σs.

The σ-like domain of Sphingomonas sp. Fr1 PhyR [16] superimposed to CnrH with an rmsd of 2.45 Å over 121 Cα pairs. Consistently, CnrYc and NepR aligned over 24 Cα pairs with an rmsd of 2.57 Å as a result of this superimposition, thus indicating that both complexes are similar

The molecular surface of PhyR σ_2-like (purple) and σ_4-like (green) domains is shown with the backbone traces of $CnrY_C$ (transparent orange) and NepR (grey) running as coils. The side chains of three major determinants of PhyR:NepR interaction, NepR residues L32, Y36 and M48 are displayed as sticks and highlighted with triangles. Intermolecular atomic contacts are CPK colored on PhyR surface and on NepR-borne sticks.

This way of binding an σECF factor is distinct from the four-helix antisigma domain (ASD) discovered in *E. coli* RseA and *Rhodobacter sphaeroides* ChrR (Campbell et al., 2003, 2007). This new structural class is refered to as a class II ASD. The class II ASD is considerably shorter than other structurally characterized anti-σs, for example, RseA (70 residues), FlgM (80 residues) and Rsd (150 residues) [35]. The structure of CnrH:CnrYc shows that the minimal-size class II ASD achieves function by competition, not remodeling (Campbell et al., 2008) as CnrYc stabilizes a conformation of CnrH that cannot bind the promoter −10 element and occludes the RP core-binding determinants on σ2 and σ4.

Implications of targeting closed or open conformations of σ factors

CnrYc acts similarly as longer anti-σs, which suggests that these are minimum requirements for σ factor inhibition (**Fig. 26**). These requirements are satisfied in a variety of ways but it is remarkable that CnrY, NepR and FlgM share similar properties: (i) the lack of a hydrophobic core in CnrYc suggests that the cytosolic domain of CnrY is intrinsically unfolded, like NepR and the C-terminal region of Salmonella typhimurium FlgM (Campagne et al., 2012; Daughdrill et al., 1997; Herrou et al., 2012); (ii) CnrY and FlgM bind a closed conformation of σ that restrains promoter binding (Sorenson et al., 2004). This is in

contrast with RseA or ChrR whose ASD is sandwiched between the two domains of the σECF (Campbell et al., 2007) and with Rsd possibly doing the same (Patikoglou et al., 2007; Westblade et al., 2004; Yuan et al., 2008): these anti-σs compete directly for the DNA-binding determinants and the core-binding determinants as well (Campbell et al., 2008). Thus, anti-σs may be parted in two groups: those with a folded anti-σ domain that wedges between σ domains (RseA, Rsd) and those whose intrinsically unfolded anti-σ domain embraces a closed conformation of σ (NepR, FlgM). The diversity of anti-σECF is such that they are found in both. While the correlation between intrinsic disorder in the anti-σ and sequestration of a closed σ factor is only emerging, it is worth noting that folding upon binding can compensate for low-affinity (reversible) interactions in signaling events by promoting specificity and speed (Berlow et al., 2015; Uversky and Dunker, 2010): these may contribute to efficient-yet-labile σ factor sequestration.

Reconsidering the CnrYXH signaling pathway

Transmembrane signaling *via* σECF factors has been shown to involve regulated anti-σ proteolysis in all systems investigated to date (Sineva et al., 2017). All but *Bacillus subtilis* RsiV display the ASD and are no model for CnrY. On the other hand, similarity with NepR and FlgM supports new hypotheses

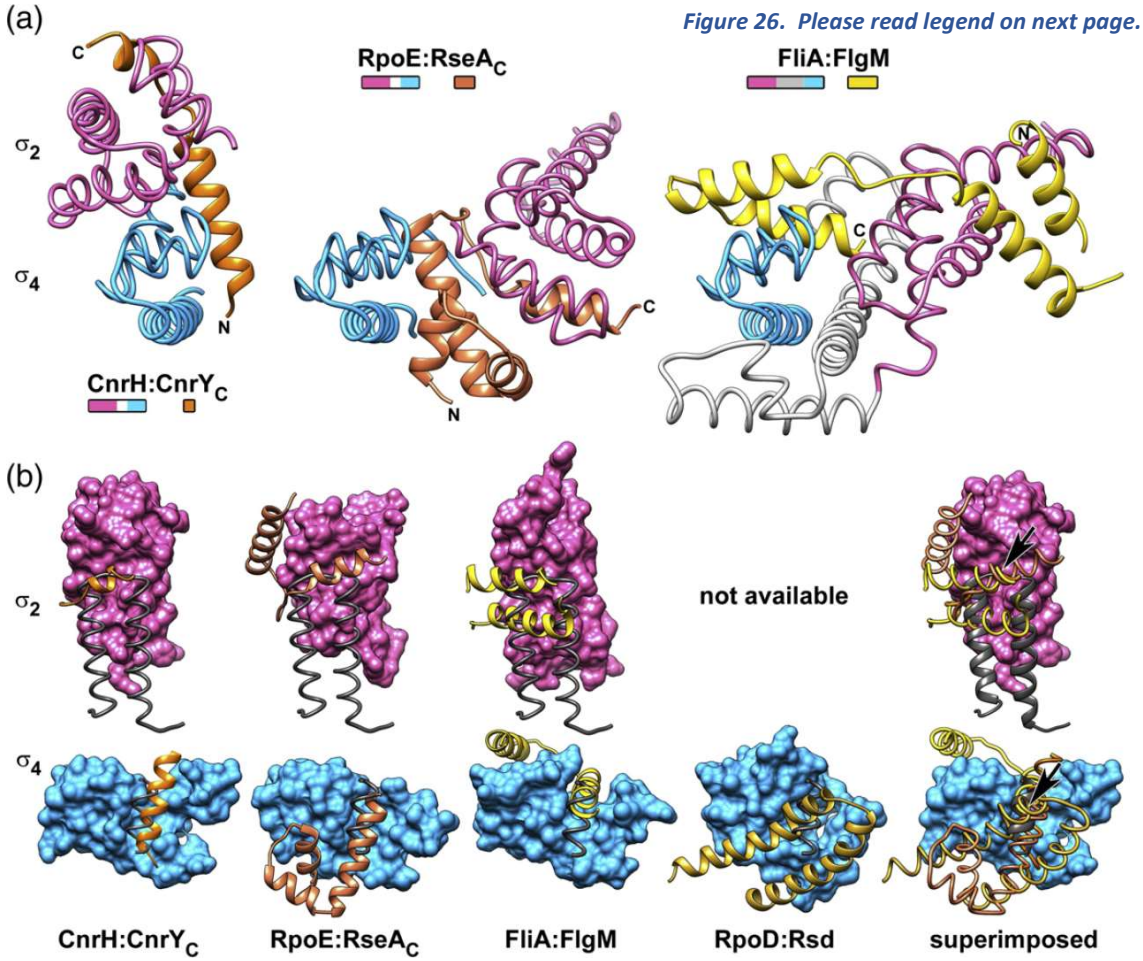

Figure 26. Please read legend on next page.

regarding CnrYXH function: the cytosolic release of CnrH from CnrY may be the consequence of (i) a partner-mediated switch, (ii) a conformational change, (iii) post-translational modification, (iv) regulated proteolysis or a combination thereof. A partner-mediated switch such as FlgM's relocation to the periplasm (Hughes and Mathee, 1998) is irrelevant because of CnrY membrane anchorage. A titration switch such as PhyR-mediated regulation of NepR is unlikely since all σECF detected in CH34 genome are functional (Grosse et al., 2007; Janssen et al., 2010) but the binding versatility of intrinsically unfolded proteins allows suggesting that CnrY might be titrated by a partner lacking σECF homology (Berlow et al., 2015; Uversky and Dunker, 2010). The structure of CnrH:CnrYc shows that CnrYc has no hydrophobic core to mediate a conformational change. It also shows that CnrH-bound CnrYc is accessible to the solvent from one end to the other, a property that is favorable to post-translational modification (two phosphorylation sites were predicted at Ser26 and Ser32 (Miller et al., 2009) or proteolysis.

Although this was not investigated *per se*, the existence of specific factors supporting Cnr operation in *C. metallidurans* CH34 is suggested by the observation that expressing the whole *cnr* determinant in *E. coli* failed to confer cobalt resistance (Nies et al., 1989) whereas CnrH is functional in *E. coli* (this study). The phylogenetic analysis of CnrY-like proteins also revealed that sequences from β- and α-proteobacteria cluster together (Maillard et al., 2014): this and the observation that the *cnr* determinant displays a distinct G + C content in *C. metallidurans* indicate that *cnrYXH* may have been acquired by horizontal gene transfer along with the resistance genes that they control (Monchy et al., 2007; von Rozycki and Nies, 2009). Therefore, the CnrYXH pathway may be incompletely described and examples from the literature suggest that additional factors be a kinase and/or proteinases (Barik et al., 2010; Mascher, 2013).

Figure 26. Comparison of CnrH:CnrY$_C$ to relevant σ:anti-σ complexes. *(on previous page)*

(a) CnrY$_C$ is a minimal size anti-σ. Left: the L-shaped CnrY$_C$ sequesters a compact conformation of the σ^{ECF} CnrH. Middle: the three-helix bundle of E. coli *RseA cytosolic domain (RseA$_C$, a typical ASD) is wedged in-between σ_2 and σ_4 domains of the σ^{ECF} RpoE[24]. Right:* A. aeolicus *FlgM sequesters a compact conformation of FliA which, unlike σ^{ECF}, also possesses a σ_3 domain[34]. To help with comparison, a similar orientation was devised for the domains σ_4 (blue) of all complexes by means of structural superimposition. Colored boxes depicting protein domains were drawn to scale. (b) Anti-σs constantly occlude the RNA polymerase binding determinants of domains σ_2 and σ_4 of their respective σ factor. The domains σ_2 (top) and σ_4 (bottom) of* C. metallidurans *CH34 CnrH,* E. coli *RpoE,* A. aeolicus *FliA and* E. coli *RpoD[36] have been superimposed onto relevant SigA domains from the* T. thermophilus *holoenzyme[19]. The β' coiled-coil (top) and the β-flap tip helix (bottom) appear in grey while the anti-σs appear in shades of orange. Overall superimposition allowed pinpointing a focal point in anti-σs' superimposed paths onto σ_2 and σ_4 domains (arrowheads). See Table 2 for relevant rmsd's.*

3.2.2. Molecular basis of metal sensing by CnrX

In *C. metallidurans* CH34, the Cnr phenotype depends on the expression of the *cnrCBAT* operon, which is under the control of CnrH, whose availability is controlled by a complex of two membrane proteins: the anti-σ factor CnrY and the periplasmic metal sensor CnrX (Grass et al., 2000, 2005; Tibazarwa et al., 2000). As we started, it was presumed that binding of Co(II) or Ni(II) to CnrX in the periplasm propagates a signal to CnrY thus leading to the cytoplasmic release of CnrH. The work of Juliette Trepreau, whose PhD training I co-supervised, consisted in a thorough investigation of structure:function relationships within the sensor domain of CnrX (CnrXs – residues 31 to 148, Pompidor et al., 2008, 2009). This eventually allowed to elucidate the first step of this transmembrane signaling pathway.

While CnrYXH regulates resistance to cobalt and nickel specifically in *C. metallidurans* CH34, a transcriptomic investigation of select metal responsive genes of this bacterium showed that other metal ions such as Cu(II), Cd(II), or Pb(II) could induce the expression of *cnr* while Zn(II) was inoperant (Monchy et al., 2007). This and an earlier report that showed that CnrYXH response to Ni(II) was 100-fold stronger than to Co(II) (Tibazarwa et al., 2001) prompted us to characterize as many CnrXs:metal complexes as possible by crystallography, in collaboration with Richard Kahn, Eric Girard then Anne Volbeda, and to correlate this to metal binding *in vitro* or function *in vivo*.

General architecture of CnrXs

CnrXs was first crystallized without any added metal after a purification scheme devoid of a metal chelator. The structure determined at 1.74 Å showed that CnrXs is a cradle-shaped homodimer where each protomer displays a short, four-helix bundle base, from which a long hairpin (H2 and H3) protrudes, whose tip reaches the bundle of the second protomer (**Fig. 27a**). Protomers also contact each other along helix H3. Two conformationally distinct dimers were present in the asymmetric unit and none of them was symmetrical, due to partial metalation with contaminating Cu(II) (Pompidor et al., 2008). Indeed, a 2-fold symmetry axis links the protomers of CnrXs dimer: this was best observed when Ni(II) or Co(II) was liganded into the metal binding site (Trepreau et al., 2011).

Metal binding by CnrXs

Although Cu(II) binding was artefactual, the metal binding site of CnrXs was clearly identified with the Cu(II) contaminated protein, as later results showed. Taking advantage of Cu(II) paramagnetic properties, the Cu(II) coordination sphere was probed with EPR spectroscopy in collaboration with Serge Gambarelli. This and the direct observation of CnrXs structure revealed an atypical type 2 Cu(II)

center with square equatorial 3N1O coordination and remote axial coordination by a sulfur atom contributed by a methionine, not a common ligand of Cu(II) (Pompidor et al., 2008).

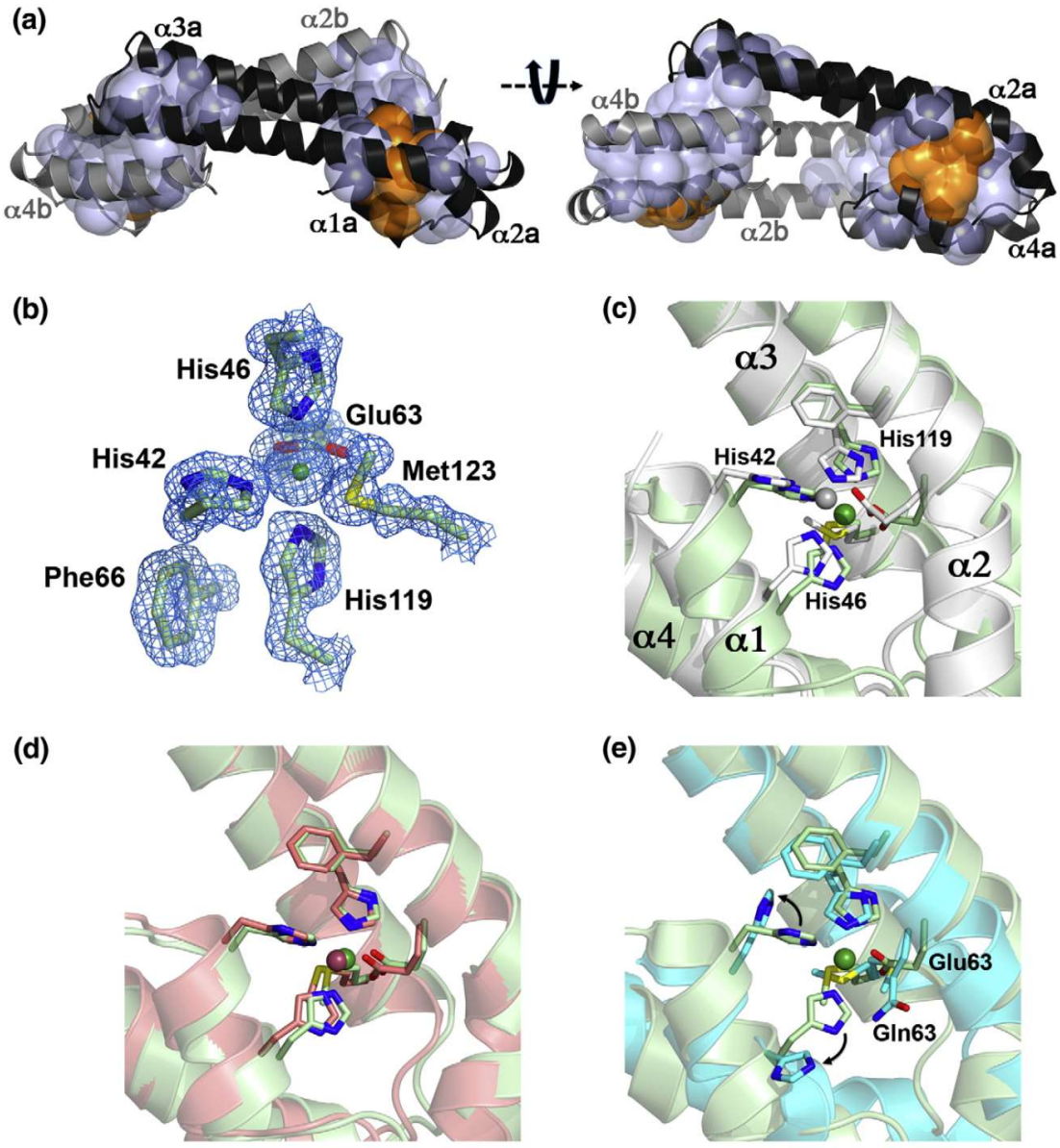

Figure 27. CnrXs dimer and close-up views of the metal-binding site with different bound metal ions.

*(**a**) The backbone structure is that of Ni-bound CnrXs. Protomer A, black; protomer B, gray. The intraprotomer and interprotomer hydrophobic interactions involving conserved residues are represented by light-blue spheres, and orange spheres correspond to the volume occupied by metal-binding sites. The two views are related by a 45°rotation. (**b**) 2Fo −Fc electron density map contoured at 1.5σ of the Ni-binding residues and the Ni ion. (**c**–**e**) Phe66 interacting with His119 is always included in the close-up views. (**c**) Superimposition of the 6-coordinate Ni-binding residues and of the 5-coordinate Zn-binding residues. (**d**) Superimposition of the Ni-binding and Co-binding residues. (**e**) Superimposition of the metal-binding residues in the presence of Ni or in E63Q-CnrXs. Note that two side-chain conformations are observed for Met123 in E63Q-CnrXs. The conformation of the side chains of the ligand residues is defined as "open" in E63Q-CnrXs and as "closed" in the metal-bound form. Color code for peptide backbone and side chains: Ni-bound, pale green; Co-bound, salmon; Zn-bound, white; E63Q-CnrXs, cyan. Color code for metal ions: Ni; green, Co, brown; Zn, gray.*

The metal binding site was confirmed as the structures of CnrXs in complex with stronger agonists were subsequently determined (Trepreau et al., 2011) (**Fig**. **27b**). Nitrogen ligands are provided by His42, His46 and His119, the imidazole of the latter being stabilized by π–π stacking with the phenyl ring of Phe66 from the hydrophobic core. The oxygen ligand of Cu(II) tetragonal 3N1O1S coordination sphere is supplied by the carboxylate group of Glu63, which also contributes a second oxygen ligand to the octahedral 3N2O1S coordination sphere of Ni(II) or Co(II) (Trepreau et al., 2011). The coordination sphere of Ni(II), Co(II) and Cu(II) is completed by the thioether sulfur of Met123 side chain. In conclusion, metal binding in the 13 kDa CnrXs protomer involves five strictly conserved residues from helices H1, H2 and H3 (Pompidor et al., 2008).

Metal sensing by CnrXs

Our understanding of CnrX function truly took shape when the structures of Ni(II), Co(II) and Zn(II)-bound forms of CnrXs have been determined. These structures were compared to each other and to the *apo* form of CnrXs, best represented by the E63Q metal binding site mutant, as it was found that CnrXs would bind substoichiometric amounts of trace metals in absence of a chelator (Pompidor et al., 2008; Trepreau et al., 2011).

CnrXs samples loaded with either Co(II) or Ni(II) prior to crystallization were virtually free of Zn(II) as judged by flame atomic absorption quantification and X-ray fluorescence spectra recorded just before diffraction data collection. Both Ni-bound and Co-bound forms contain one metal ion per protomer in a 3N2O1S coordination sphere (**Fig**. **27b,d**). The residues liganding Ni(II) or Co(II) are remarkably superimposable. Comparing Ni(II) and Co(II)-loaded sites to the same residues in the surrogate *apo* form (E63Q-CnrXs) showed that His119 side chain was invariant, unlike those of His42, His46, Glu63/Gln63 and Met123, which pointed outward in *apo* CnrXs. This suggests that His119 is a metal trap, possibly due to the stacking of its imidazole with the phenyl of Phe66.

Since a genuine *apo* form of CnrXs could not be obtained, it is very unlikely that this form be physiologically relevant. Hence the interest in the inactive, Zn(II)-bound form of CnrXs. Surprisingly, three Zn atoms were localized in Zn(II)-bound CnrXs: two in protomer A and one in protomer B. The single Zn(II) in protomer B was bound in a trigonal bipyramidal geometry with a 3N2O coordination sphere that essentially differs from that of the Ni or Co atom by the lack of contribution of Met123 (**Fig**. **27c**). This is considered as the relevant conformation of Zn(II)-bound CnrXs. In contrast, the metal-binding site observed in all other structures determined so far no longer exists in protomer A and was deemed irrelevant to CnrX physiology for several reasons, including sequence conservation issues (Trepreau et al., 2011).

The Zn(II)-loaded site of protomer B differs significantly from the activated, Ni(II) and Co(II)-loaded sites of CnrXs (**Fig 27c**). Owing to the fact that Zn(II) coordination sphere is satisfied by five, not six ligands, Zn(II) does not bind the sulfur atom of Met123 side chain. Thus the recruitment of Met123 to the metal-binding site is a marker of activation. The contribution of Met123 constrains the structural elements carrying metal binding residues, bringing H1 and H2 closer to H3 (**Fig 28a**). But this is not what helps CnrX to discriminate between Ni(II) and Co(II), a strong and a weak inducer, respectively (Tibazarwa et al., 2001).

At the core of CnrX function

The four-helix bundle defined by the N-terminal half of α2, the C-terminal half of α3, and the shorter helices α1 and α4 in each protomer is stabilized by a hydrophobic core (**Fig. 27a**). The residues involved in the hydrophobic core display a high degree of conservation in the members of the CnrX family (Trepreau et al., 2011). The hydrophobic core extends further to helix α4 and, across the dimer interface, to helices α2 and α3 of the opposite protomer. The two metal-binding sites, made by residues from α1, α2, and α3 in each protomer, form two discrete patches on each face of the dimer and lie surrounded by the hydrophobic core. As a consequence, the four-helix bundle not only accommodates the metal-binding site but also is a globular body on which the tip of α2–α3 hairpin from the partner protomer is docked (**Fig 28b,c**). This network of intraprotomer and interprotomer interactions allows metal-binding sites to tune the packing of CnrXs dimer as a function of the bound metal ion.

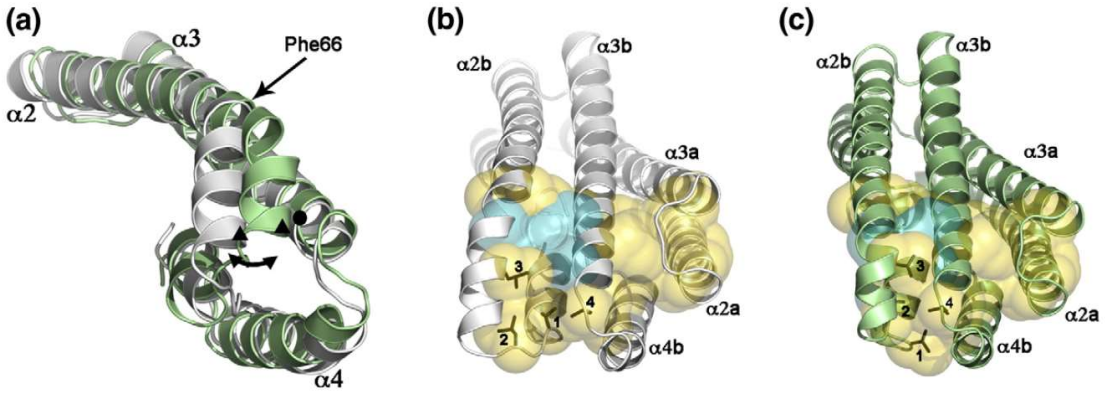

Figure 28. Comparison of metal-bound CnrXs conformations.

*(**a**) Superimposition of the protomer B backbone of Ni-bound and Zn-bound CnrXs in pale green and white, respectively. The straight arrow points to the location of Phe66 in α2, and the double arrow indicates the metal-dependent movement of the α2 N-terminal extremity. This movement is illustrated by the distance between the two positions of Glu55 (black triangles) and that of Met123 (black dot). (**b and c**) This movement brings together four conserved hydrophobic residues in a hydrophobic clip. These residues—Val49 (**1**), Leu51 (**2**), Leu59 (**3**), and Leu127 (**4**)—are displayed as brown sticks. The hydrophobic core (gold spheres) connecting the four-helix bundle in protomer B and the α2–α3 hairpin of the opposite protomer surrounds the metal-binding site (blue spheres) and includes the hydrophobic clip*

Nickel calls the tune

Ni(II) *vs.* Co(II) binding induce only sub-angström changes at the metal binding site, little more as far as protomers are concerned. In contrast, CnrXs dimers were significant different (**Fig. 29**).

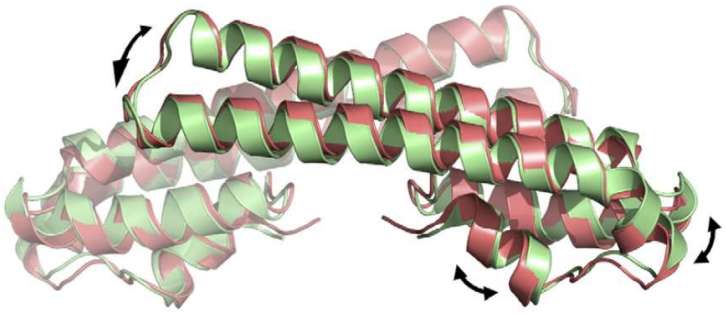

Figure 29. Metal-induced conformational changes outside the metal-binding site.

Superimposition of the dimeric form of Ni-bound CnrXs (green) and Co-bound CnrXs (salmon). The double arrows illustrate the metal-dependent breath of the protein.

This was a puzzle to everybody. Understanding how CnrX discriminates between the strong Ni(II) inducer and the weaker Co(II) inducer (Tibazarwa et al., 2001) has been the incentive that made me look into the core and cast the take-home message of Trepreau et al. (2011).

Starting from the metal-binding site, I recapitulated all the interactions taking place and documented how subtle changes induced by metal binding are able to affect (i) the helical bundle around the binding site, (ii) the α2–α3 helical hairpin protruding from the globular bundle, and (iii) the relative orientation of the protomers within a dimer.

In view of Ni conformation being the reference for maximal induction, it appears that the Co(II) conformation stabilizes only some of the features necessary for maximal induction and that Co(II)-bound CnrXs is structurally closer to inactive Zn-bound CnrXs. This correlates well with the fact that Co(II) is a weaker inducer of the cnr response than Ni(II) and may be due to a lower performance of Co(II) to promote local conformational changes that propagate as well as those induced by Ni(II).

The methionine 123 trigger

In CnrXs metal binding site, among the groups that chelate metals, Met123 thioether as the double peculiarity of being (i) specifically recruited by the agonist metals of the Cnr system but not by the non-inducing Zn(II) and of being (ii) very seldom present in cobalt or nickel specific binding sites.

The role of Met123 was assessed in *C. metallidurans* CH34 in collaboration with the group of Dietrich Nies (Halle, Germany). Met123 has been mutated to an alanyl residue. The M123A CnrX variant was effectively produced but the system was unresponsive to Co(II) or even Ni(II) (Trepreau et al., 2014). When characterized *in vitro* using the spectroscopic properties of Co(II) and chromogenic chelators to

compete with the protein, M123A-CnrXs *K*d was found to be four orders of magnitude higher than that of wild-type CnrXs but was still ~ 0.1µM (Trepreau et al., 2014).

M123A-CnrXs was crystallized in presence of Ni(II) and the structure was determined at 1.85 Å by Eric Girard. I compared the structures of Ni(II) bound wild type CnrXs and M123A-CnrXs and showed that Ni(II) location is almost the same whether M123 is here to chelate it or not (**Fig. 30B,C**) whereas protein conformation is actually that of apo CnrXs (**Fig. 30A**). This demonstrated that Met123 contributes to Ni(II) binding but is essential to the Ni(II) sensing by CnrXs.

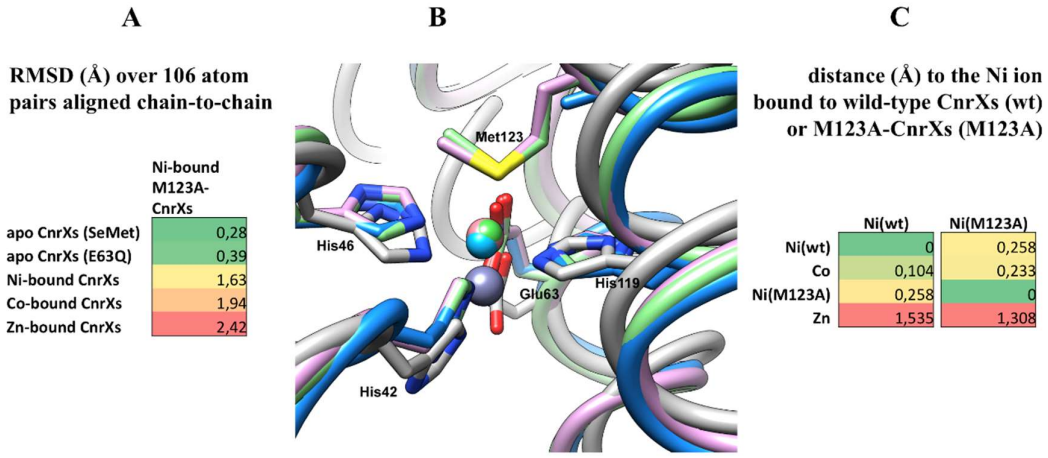

Figure 30. Ni(II) binding to M123A-CnrXs fails to promote a productive conformational change.

A, *Various metal-bound CnrXs dimers were superimposed. Reported is the RMSD measured between Ni-bound M123A-CnrXs (chain B) and the* apo*-form of a selenomethionine derivative of CnrXs (2y3g, chain C), the* apo*-form of E63Q-CnrXs (2y3h, chain C), Ni-bound CnrXs (2y39, chain A), Co-bound CnrXs (2y3b, chain A) or Zn-bound CnrXs (2y3d, chain B).* **B**, *Superimposition of the Cα of the residues common to all metal-binding sites highlights the similar location of Ni and Co ions as opposed to Zn(II). Note that the metal ions are almost aligned. Metal-chelating residues are named according to the three-letter code. Color code for proteins and metal ions: Ni-bound CnrXs, green; Ni-bound M123A-CnrXs, blue; Co-bound CnrXs, pink; Zn-bound CnrXs, grey.* **C,** *Distance between Ni(II) and other metal ions measured after metal-binding site superimposition. The Ni ion used as a reference was bound to either wild-type CnrXs (left column) or M123A-CnrXs (right column).*

Conformational sampling of CnrX sensing domain

As this story unfolds, the structure of fifteen different dimers of CnrXs has been determined in collaboration with Richard Kahn, Eric Girard and Anne Volbeda (Pompidor et al., 2008 ; Trepreau et al., 2011 ; Trepreau et al., 2014 ; Maillard et al., 2015).

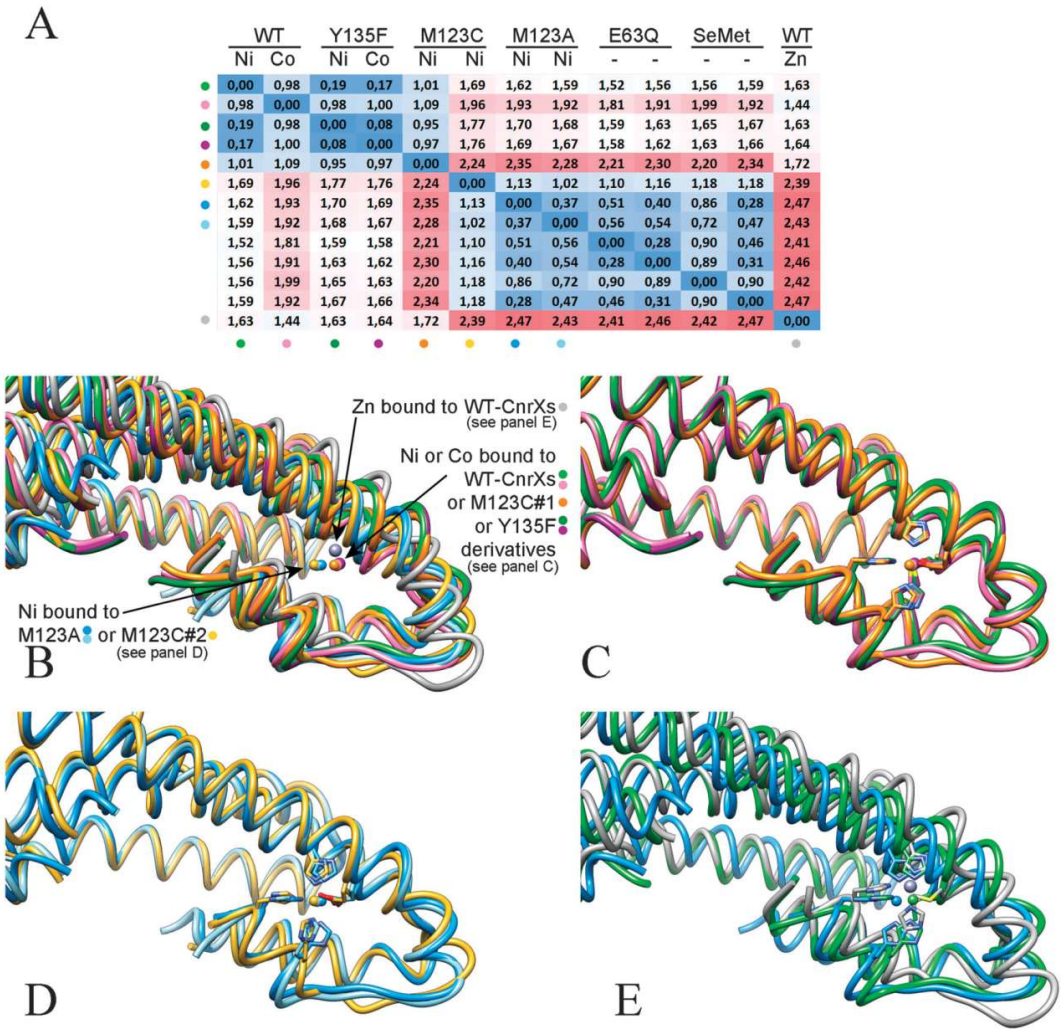

Figure 31. Structural superimposition of CnrXs establish three conformations.

Panel A*: CnrXs dimeric structures determined here and previously published have been superimposed. A structural alignment was produced for chains aligned with Ni-bound CnrXs chain B and the calculated rmsd's have been reported as a matrix. Blue-to-white-to-red shading was applied automatically with Excel over the complete table. Three ranges were identified. One gathered Ni-bound CnrXs, Co-bound CnrXs, Ni-bound Y135F-CnrXs, Co-bound Y135F-CnrXs and Ni-bound M123C-CnrXs-D (dimer 1 = chains AD). The second gathered the Ni-bound forms of M123C-C, M123A-A, M123A-C, and apo-forms of CnrXs as present in either E63Q-CnrXs or SeMet-CnrXs dimers. Finally, WT-Zn aligned poorly with all other structures. As a result, three conformational states are observed.* ***Panel B****: close-up view at the metal ions bound to superimposed CnrXs dimers. Each ion was colored as the protein chain. The color code is displayed in both entries of the table in panel A. Metal ions clustered the same way as the protein chains.* ***Panel C****: an ''active'' conformational state with Co or Ni in CnrXs WT, Y135F, and M123C dimer 1.* ***Panel D****: an ''artifactual'' conformational state observed in M123A and M123C mutants. Panel E: a Zn-bound conformational state (grey) displayed together with superimposed Ni-bound CnrXs and (green) and Ni-bound M123A-CnrXs (blue) for comparison.*

By extending the work that I had performed on M123A-CnrXs to this larger population, I have been able to define the conformational space of CnrXs, confirming that CnrXs crystallized under essentially three conformations that correspond to the apo-CnrXs, Ni(II)-CnrXs and Zn(II)-CnrXs states (Trepreau

et al., 2011). This conformational sampling of CnrXs indicates that CnrXs sensing function operates *via* a flexible scaffold that tend to reach three distinct conformations in equilibrium, the balance being shifted from the *apo* form to either metal-bound form, upon metal binding.

The principles that support conformational sensing by CnrX can be summarized as follows: (i) a small flexible protein binds (ii) two metal ions at symmetry-related sites, (iii) with metal-binding residues embedded in a bipartite hydrophobic core. Together, these properties allow subtle metal-induced changes to be propagated and amplified to the whole protein.

3.2.3. Conclusion

The characterization of structure:function relationships in CnrYXH has yielded significant discoveries about (i) sigma factor inhibiton and (ii) conformational-sensing.

The identification of the class II ASD, typified by CnrYc, highlights essential schemes underlying anti-σ-mediated inhibition of σ factors: (i) CnrYc minimal size makes sharper the observation that all anti-σs structurally documented so far target the same binding sites; (ii) closed conformation of the σ factor and conformational disorder in the anti-σ appear to correlate, suggesting that, for class II ASD at least, conformational disorder plays a role in regulating σ:anti-σ interaction; (iii) structural convergence of CnrH: CnrYc and PhyR:NepR questions the prevalence of proteolysis in transmembrane σECF activation since the latter operates a reversible titration switch (Francez-Charlot et al., 2009; Kaczmarczyk et al., 2014).

The class III ASD was recently documented with *Streptomyces venezuelae* RsbN (Schumacher et al., 2018). This 90-residue long protein has no intrinsic fold either and it illustrates a mixed strategy whereby two helices embrace the domain σ4 while the third helix wedges in-between domains σ2 and σ4. Having spent a lot of time trying to identify meaningful clusters in the collection of antisigma factor sequences published by Staroń et al. (2009), I had to step back and admit that no clear amino acid sequence signature should be expected for this module because of target diversity and relaxed tertiary structural constraints. This was confirmed as the class III ASD is a new example of a 'disordered' antisigma factor. A lot of additional information is needed before we can actually cluster antisigma factor sequences like the sigma factor sequences have been.

At the other end of the signaling pathway, CnrX has been a spectacular model to investigate structure:function relationships. Yet, it is not known how metal sensing by CnrX translates into CnrH release from CnrY. This has been investigated with Khouloud Maroug (BTS) then Widade Ziani at the

end of her PhD, who showed that CnrXs binds CnrY periplasmic domain in a metal dependent manner that echoed the metal specificity of the Cnr system *in vivo* (**Fig. 32**).

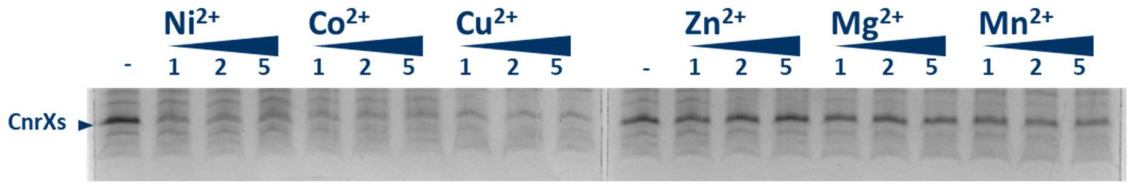

Figure 32. CnrXs coprecipitation with MBP fusion proteins containing the periplasmic domains of CnrY.

CnrXs was mixed with MBP-CnrYp and the indicated concentration (mM) of diverse cation salts. MBP-CnrYp was pulled down with amylose beads. Beads were washed then boiled in SDS-PAGE sample buffer.

The same assay was used to identify two CnrXs-binding determinants in CnrY periplasmic domain, the relevance of which was validated *in vivo*, as Rob van Houdt (Mol, Belgium) gave me tools that I could use to introduce recombinant *cnrYXH* in *C. metallidurans* CH34. Characterizing CnrY-binding determinants of CnrXs is much more delicate, because substituting residues in a conformational sensor could be dangerous. This was thus investigated by hydrogen/deuterium exchange coupled to mass spectrometry, in collaboration with Eric Forest. Widade Ziani identified segments of CnrXs that were slow to participate in H/D exchange. I confirmed these after she graduated but it is not clear whether slow exchange is due to direct protection by CnrY or to the effect of CnrY binding on CnrXs breathing dynamics at some other location.

Studying structure:function relationships in a conformational sensor met with unexpected (yet predictable) complications also when CnrX closest homolog, NccX, was crystallized as the full-length form after solubilization with dodecylphosphocholine, and the structure was determined at 3.1 Å resolution by Pierre Legrand (Soleil) using artful molecular replacement (Ziani et al., 2014). A critical assessment of the structure allowed me to point several artefactual features and to detail how the detergent and transmembrane segment actually disturbed the dimer interface, engaging separate pieces of the interface to play musical chairs (**Fig. 33**). The intrinsic flexibility of a conformational sensor which is also a single-pass transmembrane protein seems to have primed NccX for this to happen.

Perspective

The CnrYXH signal transduction system is original in several ways as it brings together (i) CnrY that combines a class II ASD with transmembrane anchorage (unlike NepR), (ii) CnrX which is structurally related to the chaperone Spy and to the protein CpxP, a negative regulator of the CpxAR two-

component system, and (iii) CnrH, a typical σECF. Elucidating the interaction between CnrX and CnrY would not only give clues on CnrYXH-mediated signaling, but also contribute to the characterization of the Spy/CpxP/CnrX superfamily of proteins.

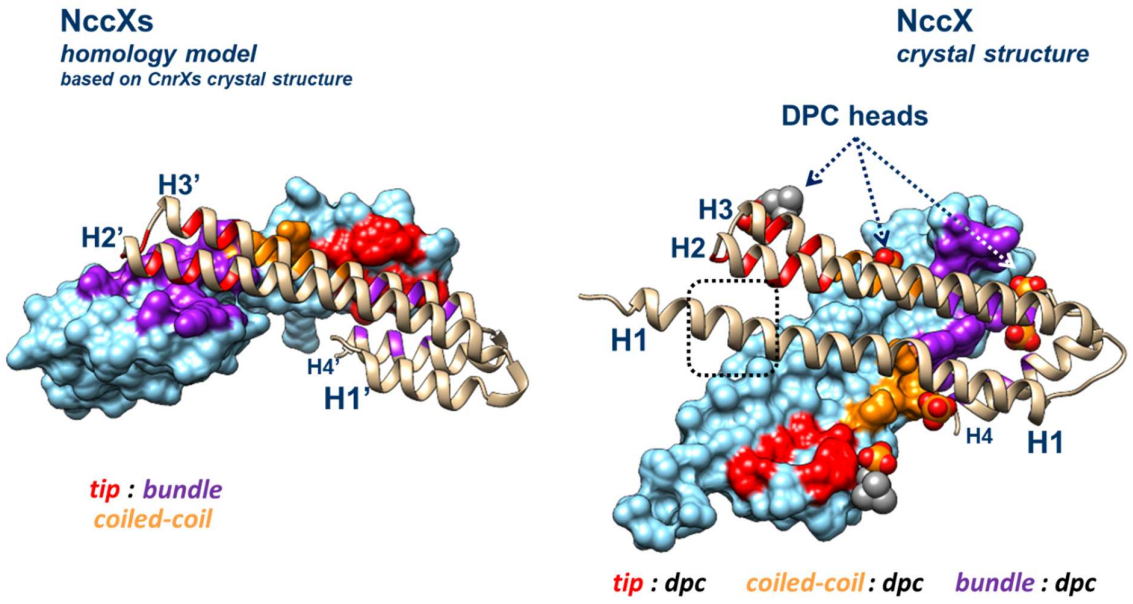

Figure 33. Effect of dodecylphosphocholine on the dimer interface of NccX.

*A homology model of NccXs, the periplasmic domain of NccX, was built using Zn(II)-bound CnrXs as a template. The dimer interface of each protomer of NccXs was considered as a collection of three pieces: the tip of the H2-H3 hairpin (**tip**, red), the body of helix H3 (**coiled-coil**, orange), and the platform built by H3-H4 (**bundle**, purple). Polar heads of dpc are shown as orange (phosphate moiety) and gray (choline moiety) spheres. (**Left**), in NccXs, two protomers stick together via tip-to-bundle contacts and helix-to-helix contacts (coiled-coil). (**Right**), in NccX, tip-to-bundle contacts have been replaced by bundle-to-bundle (with a docked dpc moiety, orange), tip-to-dpc contacts (**arrows**), and tip-to-transmembrane (**dashed box**) contacts. The helix-to-helix (coiled-coil) contacts have also been disrupted and replaced by helix-to-dpc contacts. As a result, the dimer interface in crystallized NccX has been completely remodeled as compared with that of NccXs with DPC and the transmembrane N-terminal half sticking in.*

4. Taming the outside world

With the exception of dormancy, life maintenance is supported by the exploitation of environmental resources (not to mention growth). While this is achieved by mere substrate degradation and metabolite uptake in a saprophytic lifestyle, pathogens, parasites and symbionts also perform a work of destruction or interference to invade their host or contact their partner. Such events are supported on either side by receptors as well as by secreted adhesins, enzymes, toxins…

By definition, a protein got secreted if it was released outside the cell. Several secretion systems do help protein substrates transit through membranes. The general protein secretion pathway, conserved across the three kingdoms of life, has been described in section 2. Working in parallel or in combination, specialized secretion systems endow bacterial cells with solutions for every need: secreting proteins that have folded in the cytoplasm, injecting effectors into target cells…

4.1. Ways & means of protein secretion in proteobacteria

This section briefly introduces the secretion systems that diderm bacteria use to release proteins out and leave those systems that deliver proteins directly into a target cell out of scope (see **Fig. 34** for the complete panel of bacterial export systems).

4.1.1. The general secretion pathway of proteins

The general secretion pathway has been described in **section 2.2**. It is performed by the Sec machinery which lets polypeptides transit through its channel or reach a lateral gate from which transmembrane segments partition into the inner membrane. Its early characterization was consubstantial to the discovery of the “signal hypothesis”, namely “the discovery that proteins have intrinsic signals that govern their transport and localization in the cell." which earned Günter Blobel the Nobel Prize in Physiology or Medicine in 1999. The signal hypothesis was born from fractionation and biochemical reconstitution experiments that led to define secretion-signal peptides (Blobel and Dobberstein, 1975) and was later generalized to explain how protein localization is determined in cells (Blobel, 1980). Not only signal specificity but also channel gating, energy source and oligomeric state are fundamental questions that apply to secretion systems in general and will be clarified where appropriate.

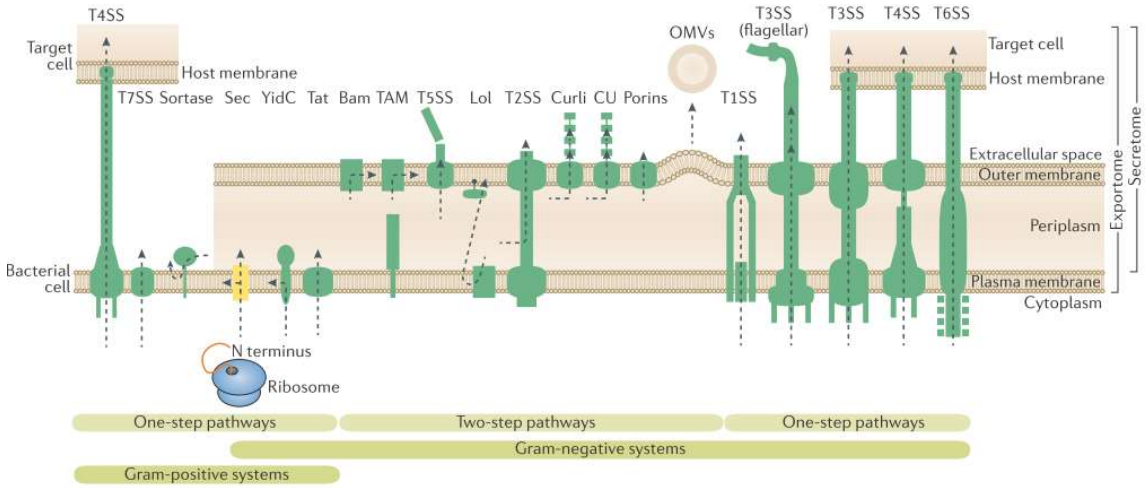

***Figure 34. Bacterial protein export systems In bacteria**.*

*Most exported proteins are transported across the plasma membrane through the **Sec** pathway (yellow). **YidC**, alone or in complex with SecYEG, functions as an insertase for some membrane proteins. A minority of proteins that first fold and/or associate with cytoplasmic cofactors before crossing the plasma membrane are transported through the twin-arginine translocation (**Tat**) pathway. **Gram-negative bacteria** have specialized export systems (**one-step pathways**, **right**): proteins that are involved in pathogenesis and nutrient scavenging are transported by the type 1 secretion system (**T1SS**). Flagellum proteins are transported by the **flagellar T3SS** and toxins are exported by the **pathogenic T3SS**. Proteins and nucleic acids are injected into other cells, as virulence factors or as a means of genetic exchange, through the **T4SS**. Pathogenic effectors are injected into a eukaryotic or bacterial target cell through the **T6SS**. **Gram-positive bacteria** have three specialized secretion systems (**one-step pathways, left**): virulence proteins cross the cytoplasmic membrane through the T7SS. Sortases recognize, cleave and attach proteins that have a carboxy-terminal sorting signal to the membrane and are responsible for the assembly of pilus structures. Virulence factors or genes are injected into other cells by T4SSs. Once the Gram-negative plasma membrane is crossed, secretory proteins can be diverted to secondary secretion pathways. Outer membrane proteins are assembled by the β-barrel assembly machine (**Bam**) complex or the translocation and assembly module (**TAM**). The soluble domains of outer membrane proteins can be secreted to the extracellular milieu through the T5SS. Lipoproteins are transported from the plasma membrane to the outer membrane through the localization of lipoproteins (Lol) pathway. Folded periplasmic proteins cross the outer membrane through the **T2SS**. Outer membrane-anchored structures, such as amyloids and pili, are secreted and/or assembled by the **curli secretion machinery** or the **chaperone–usher (CU) pathway**, respectively. Some extracellular proteins use either a complex of porins (for example, YebF) or outer-membrane vesicles (OMVs) to reach the extracellular milieu. (from Tsirigotaki et al., 2017 with some text modification)*

4.1.2. Secreting folded proteins

The general secretion machinery transports unfolded protein precursors. The case of LacZ chimeras showed that not any sequence is competent for secretion and folding in the periplasm (Dwyer et al., 2014). Besides the LacZ artifact, some proteins do require folding in the cytoplasm, e.g. because a metal or nucleotide cofactor has to be incorporated there: these proteins usually display a variant signal peptide with a twin-arginine motif that targets them to the twin-arginine translocase (TAT), that is present in bacteria, archaea and chloroplasts (Palmer and Berks, 2012). The TAT machinery is made of two-to-four transmembrane proteins that assemble dynamically into complexes that will

translocate substrates of up to 70 Å in size and the PMF is required as the power source (Hamsanathan and Musser, 2018). TAT-mediated translocation is not explained yet and the panel of substrates identified, some of which are known to impact bacterial virulence (De Buck et al., 2008), is still expanding (Ball et al., 2016; Gimenez et al., 2018).

Along the same lines, some proteins fold in the periplasm of diderm bacteria prior reaching their proper location outside, at the cell surface or in the extracellular milieu. In proteobacteria, such proteins are targeted to type 2 secretion systems (T2SS) in a process that is yet unresolved (Cianciotto and White, 2017). T2SS are assembled from a dozen different multimeric proteins, that together span the inner and the outer membranes. ATP hydrolysis in the cytoplasm powers translocation of an average number of 20 substrates for which a complex, conformational signal is suspected. Most of the T2SS substrates identified are hydrolytic enzymes whose action provides nutrients to saprophytic bacteria, or virulence factors like adhesins and toxins (Douzi et al., 2012; Nivaskumar and Francetic, 2014).

4.1.3. Autotransporters and two-partner secretion systems

Some of the proteins that reach the periplasm on their way out to the bacterial surface or the extracellular milieu require their very own channel to cross the outer membrane. Such is the case of various adhesins, toxins, enzymes or scavenging proteins of many pathogenic bacteria: despite system-to-system specificities, the several features that they share have prompted their grouping under the flag of type 5 secretion (Bernstein, 2019; Grijpstra et al., 2013; Guérin et al., 2017).

Type 5 secretion systems (T5SS) typically display two elements: the transporter and the passenger. Transporter and passenger polypeptides are encoded in one gene in the case of autotransporters (AT, four types to date) or two genes in the case of two-partner secretion (TPS or type 5b) systems. Transporter domains are 12-stranded (types 5a, 5c, 5e) or 16-stranded (types 5b, 5d) β-barrel proteins that need to be inserted into the OM to help the passenger getting across. Whether they perform this function alone differs among the five types, as a result of (i) β-barrel size heterogeneity, (ii) specific structural elements in the passenger (see below) and (iii) different topological arrangements of the transporter and the passenger, let them be fused together or not (**Fig. 35**).

The names AT and TPS reflect the original assumption that ATs and TPSSs are self-sufficient to achieve secretion through the OM, but this has been revised at least for ATs, as the Omp85 superfamily proteins TamA and BamA have been demonstrated to contribute to the assembly of various ATs *in vivo* (Ieva and Bernstein, 2009; Jain and Goldberg, 2007; Sauri et al., 2009; Selkrig et al., 2012; Voulhoux et

al., 2003) and *in vitro* (Roman-Hernandez et al., 2014). In contrast, the endogenous Omp85 protein of TPS systems (TpsB) has been shown to be a channel for TPS substrates (TpsA) by performing electrophysiology experiments, *in vitro* reconstitution and structure-informed cysteine scanning with *B. pertussis* FhaC (Baud et al., 2014; Fan et al., 2012; Méli et al., 2006).

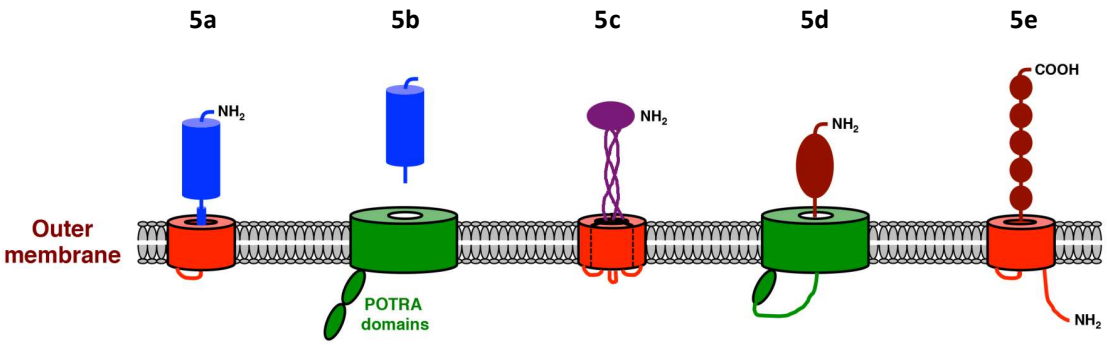

Figure 35. Schematic representation of proteins in type 5 secretion pathways.

T5SS proteins consist of a 12-stranded (red) or 16-stranded (green) β-barrel domain and an extracellular ("passenger") domain that typically folds into a β-helical (blue), mixed coiled-coil/β-roll/β-prism (purple) or immunoglobulin (brown) structure. The 16-stranded β-barrel domains are members of the Omp85 superfamily and contain one or two periplasmic POTRA domains. In most cases the β-barrel and passenger domains are covalently linked until the passenger gets out and proteolytic processing occurs, but in the type 5b pathway the β-barrel domain and the passenger substrate are separate polypeptides. In the type 5c pathway both domains are formed through the assembly of three identical subunits. The passenger domain is located at the N terminus of the protein in type 5a, 5b, 5c, and 5d pathways and at the C terminus in type 5e. (from Bernstein, 2019)

Although not elucidated yet, the secretion process has been shown to rely on specific domains: the autochaperone domain of ATs (Drobnak et al., 2015; Rojas-Lopez et al., 2017) and the TPS and POlypeptide TRansport Associated (POTRA) domains in TPSSs (Guérin et al., 2017). In the latter case, specific interactions have been shown to support targeting of TpsA proteins to their cognate TpsB transporter in *B. pertussis* FhaBC or *N. meningitidis* TpsBA1 and TpsBA2 (Delattre et al., 2011; ur Rahman et al., 2014). The channel-proximal POTRA of FHA was also found to play a role in channel gating as it regulates the occlusion of FhaC by the extracellular loop L6 (Guérin et al., 2015).

Despite the variety that is emerging in the structure of AT passenger domains (Batchelor et al., 2000; da Mata Madeira et al., 2016; Oberhettinger et al., 2012; Salacha et al., 2010), the structural hallmark of type 5 secreted proteins is the right-handed β helix that was predicted in 97% of type 5 passenger domains and in type 5b passenger substrates as well (Junker et al., 2006; Kajava and Steven, 2006). Such a fold is not exclusive to T5S passengers, but its high prevalence, including in proteins whose main function is carried out by an additional C-terminal domain - like ExlA or contact-dependent growth

inhibition toxins (Aoki et al., 2011; Guérin et al., 2017) - leads to wonder whether β helix domains are a part of the secretion system itself, i.e. they are needed for secretion. Indeed, because the periplasm has no nucleotide-based chemical energy supply and the OM cannot be energized with ionic gradients due to the presence of porins like OmpC and OmpF, it has been hypothesized that progressive folding of the helix outside the cell could drive translocation through the OM, by pulling the polypeptide chain out and preventing it from backsliding (Bernstein, 2019; Grijpstra et al., 2013; Guérin et al., 2017; Klauser et al., 1993). In support of this hypothesis, equilibrium refolding experiments with *B. pertussis* pertactin have shown that the folding of this β helix proceeds slowly, without a defined core (Junker and Clark, 2010; Junker et al., 2006). As for TpsA proteins, β helix folding could propagate from the TPS domain, whose secretion proceeds in a few discrete steps (Baud et al., 2014), in agreement with the complexity of the events taking place during the coupled secretion/activation process (Hodak et al., 2006; Ondraczek et al., 1992) and its multipartite core structure (Wimmer et al., 2015).

Until recently, the secretion of a TpsA protein through its TpsB partner was implicitly considered to be regulated by the binding of the TPS and POTRA domains together, *i.e.* at the initiation step. This has been recently challenged when Ruhe et al. (2018), combining cryoEM imaging with topological (accessibility) assays *in vivo*, have shown that the delivery of the contact-dependent growth inhibition toxin CdiA from *E. coli* was actually primed by a hairpin translocation intermediate in which a central domain serves to dock to CdiA receptor while the C-terminal, toxin domain still resides within the periplasm. Emphasizing the fact CdiA sequence harbors type 1 hemagglutinin repeats upstream the receptor domain and type 2 hemagglutinin repeats downstream to the toxin domain, Ruhe et al. (2018) further argued that the structure associated with type 2 hemagglutinin repeats is unknown and that helical folding is speculative (Kajava and Steven, 2006). Therefore Ruhe et al. (2018) suggested that their discovery could apply to other TpsA proteins with a similar arrangement of repeats, e.g. *B. pertussis* FhaB, with a major difference: the C-terminal domain is proteolytically processed in the periplasm, not secreted, to allow FHA release (Guérin et al., 2017; Nash and Cotter, 2019). Reconsidering previous data (Hoffman et al., 2017) a new function is proposed for FHA: delivering *B. pertussis* adenylate cyclase to target cells (Nash and Cotter, 2019).

This new controversy, along with open questions on the secretion process itself and the individual contribution of the different domains to secretion, illustrate how much progress is still expected in our understanding of T5SSs.

4.2. Focus on *P. aeruginosa* PA7 exolysin

P. aeruginosa virulence is mediated by multiple structures and factors even though it is dominated by the powerful and very much emblematic T3S toxins (Klockgether and Tümmler, 2017; Valentini et al., 2018). This plurality of factors determines graded fitness among different hosts (Hilker et al., 2015; Wiehlmann et al., 2015) which is probably instrumental in this pathogen's ubiquity. The type 5b secretion substrate exolysin (ExlA) is the latest addition to *P. aeruginosa* secreted virulence factors (Huber et al., 2016). It is the focus of a broad research effort at PBRC and has inspired my present research project.

The γ-proteobacterium *P. aeruginosa* is a ubiquitous bacillus that thrives in moisture environments and colonizes hosts from plants to insects to mammals (Klockgether and Tümmler, 2017; Moradali et al., 2017; Valentini et al., 2018). *P. aeruginosa* is well adapted to humans and readily infects a range of organs and tissues. It is often associated with nosocomial infections in Intensive Care Units and affects patients with underlying chronic diseases, e.g. patients with cystic fibrosis, for whom *P. aeruginosa* is the primary cause of morbidity and mortality (Winstanley et al., 2016).

A recent pan-genome analysis has led to discriminate *P. aeruginosa* isolates into five major groups (Freschi et al., 2019) of which groups 3 and 5 apparently coincide with previously described clonal outliers A and B, respectively (Huber et al., 2016). The most striking difference between clonal outliers and the bulk of *P. aeruginosa* strains (e.g. PA01 and PA14) is how cytotoxicity and virulence toward mammalian hosts are achieved, since isolates of groups 3 and 5 are typically devoid of a T3SS and related toxins altogether, which are the main virulence factors of other strains of *P. aeruginosa* (Diepold and Wagner, 2014; Freschi et al., 2019; Hilker et al., 2015). Instead, they rely on the exolysin (ExlA), a 170 kDa secreted toxin, to establish infection (Elsen et al., 2014; Reboud et al., 2016).

Exolysin has been first detected by non-targeted proteomics in the secreted medium of a highly cytotoxic strain, CLJ1, isolated from a patient with chronic obstructive pulmonary disease accompanied by signs of hemorrhage in the lungs (Elsen et al., 2014; Sentausa et al., 2019). The recombinant expression of *exlBA* was found to be sufficient to cause fatal outcome in a mouse model of acute pneumonia and both genes were necessary for cytotoxicity toward eukaryotic cells. The description of specific lesions in the lungs of mice infected by *P. aeruginosa* isolate CLJ1 as compared to the T3SS-positive strain PA01, suggested that ExlA supports the ability of this isolate to proliferate into and to disseminate from the lungs (Bouillot et al., 2017).

The *exlA* gene encodes a 1651 residue-long polypeptide that bears successive sequence signatures typical of (i) a signal peptide recognized by the general Sec machinery, (ii) a so-called Two-Partner Secretion (TPS) domain and (iii) several type 2 filamentous hemagglutinin (FHA2) repeats (**Fig. 36**). The

absence of any known sequence signature beyond residue 1364 defines a ~280 residue-long C-terminal domain that was proved necessary for ExlA activity toward eukaryotic cells (see below) (Basso et al., 2017a; Elsen et al., 2014). While the discovery of *exlA* in *P. aeruginosa* is very recent, it is orthologous to *Serratia marcescens* ShlA and *Proteus mirabilis* HpmA (Braun et al., 1987; König et al., 1987; Welch, 1987; see **section 4.2.4**).

Upstream *exlA* is *exlB* that encodes a 60 kDa protein channel of the Omp85 superfamily (Jacob-Dubuisson et al., 2013). Proteins of this superfamily possess a C-terminal 16-stranded OM-embedded β-barrel downstream a variable number of POlypeptide TRansport Associated (POTRA) domains (Heinz and Lithgow, 2014), of which ExlB has two. Together, *P. aeruginosa* ExlB and ExlA make a TPS secretion system. Although the TPS name was coined to account for the minimal set of proteins specifically involved in secretion, *i.e.* the effector and its cognate transporter (Jacob-Dubuisson et al., 2001), there are instances where additional dedicated partners may modify, neutralize or proteolyze the substrate (Jacob-Dubuisson et al., 2013) : none of this seems to happen to ExlA which was detected as a single ~170 kDa band after SDS-PAGE analysis of bacterial culture supernatants.

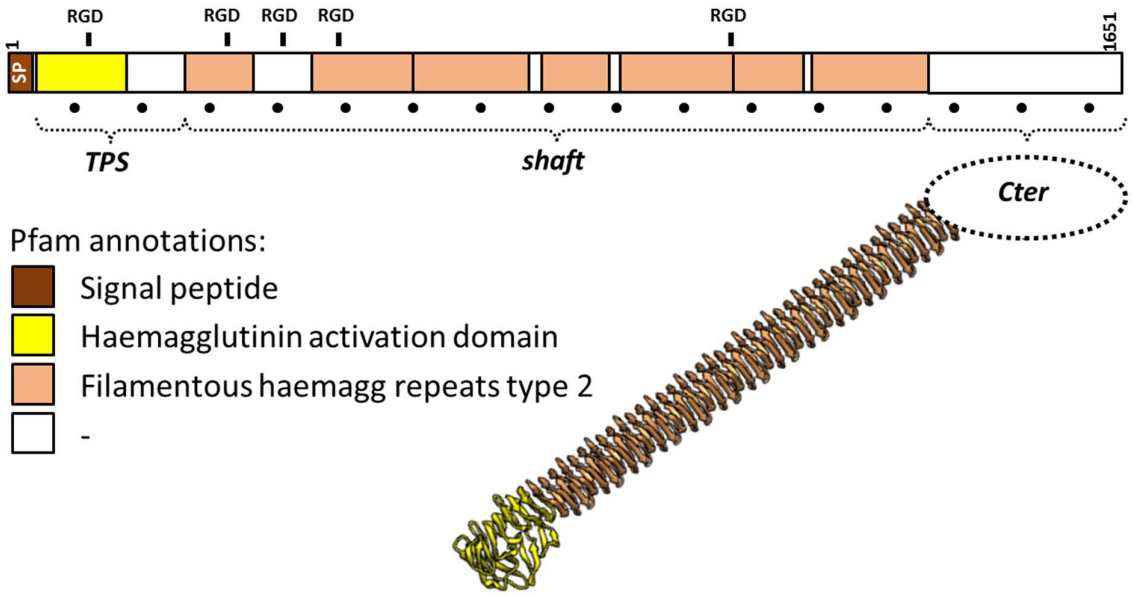

Figure 36. Pfam signatures in ExlA sequence and expected structural features.

(Top) *Linear representation of ExlA showing annotations corresponding to the signal peptide (SP) the TPS domain (yellow) and the alleged coiled repeats (salmon) in Pfam (Finn et al., 2014). A ruler is displayed below the diagram with a mark of every 100 residues. The five RGD motifs and the putative domains of ExlA are indicated.* ***(Bottom)*** *Hypothetical model of ExlA.. The TPS domain and first filamentous haemagglutinin repeats (yellow) were modeled by homology with* P. mirabilis *HpmA with which ExlA shares 35% identity. The shaft domain model was built by repeating the coils present in the HpmA template, assuming that the type 2 FHA repeats in ExlA shall fold like type 1 repeats in HpmA.*

ExlA was shown to carry out pore formation in red blood cell (RBC) membranes when these were challenged with bacteria. This activity has been associated with ExlA C-terminal domain, using a liposome leakage assay with recombinant protein domains produced in *E. coli* cytoplasm (Basso et al., 2017a). Also, absence of cytotoxicity in a transwell challenge as well as selection of low-cytotoxicity mutants where type IV pili had been inactivated by transposon mutagenesis (type IV pili are retractile hook appendages responsible for twitching motility (Leighton et al., 2015)) indicate clearly that ExlA efficiency is maximized when it is delivered fresh, next to the target cells (Basso et al., 2017a).

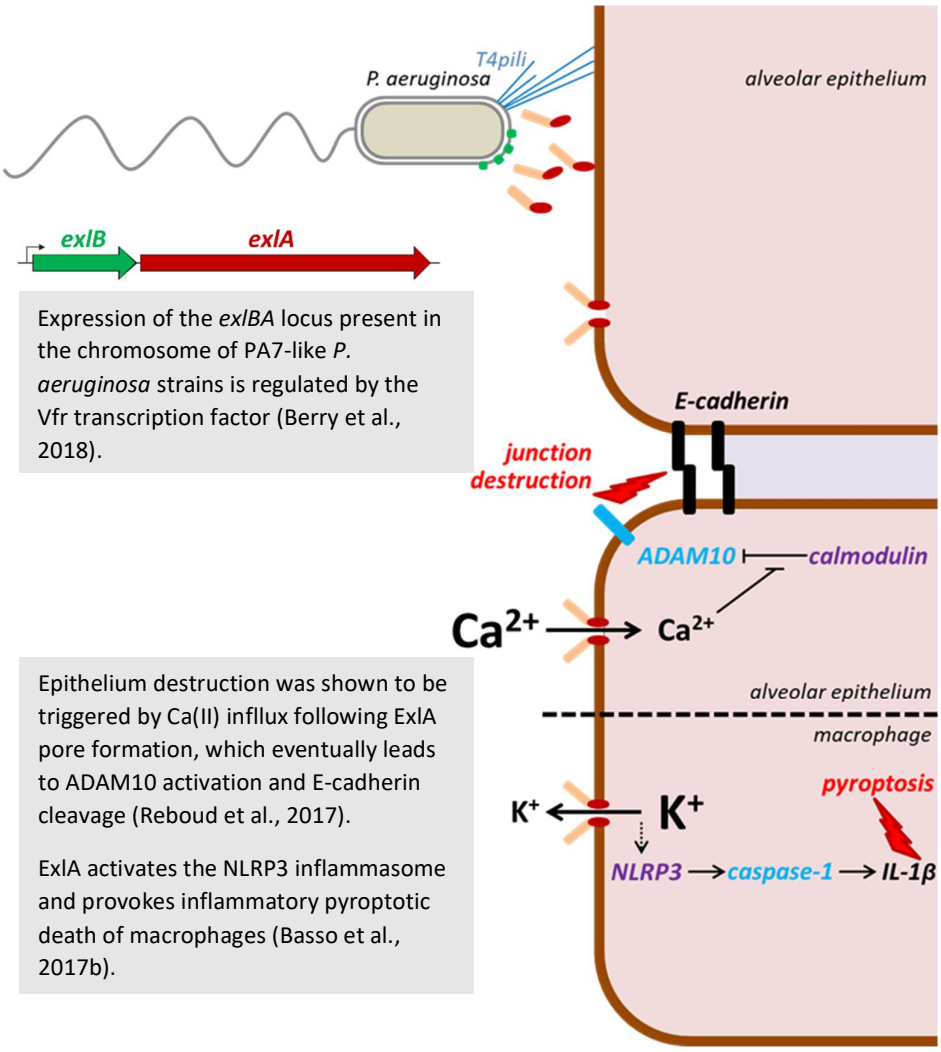

Figure 37. Modalities of ExlA-mediated virulence and cytotoxicity.

*(**top, above dash line**) in lung epithelium or (**bottom, below dash line**) in macrophage.*

Whereas e*x vivo* experiments on select cell types have led to significant progress in understanding the events that support ExlA cytotoxicity (Basso et al., 2017b; Reboud et al., 2017a, **Fig. 37**), the molecular bases of ExlA function are still unknown. It is the aim of the following project to decipher structure function relationships in *P. aeruginosa* ExlA and understand what kind of a pore-forming protein it is.

4.2.1. Looking for the molecular determinants of ExlA pore-forming activity

Pore forming toxins are soluble proteins that can oligomerize prior or upon interaction with target membranes and assemble into pores, leading to uncontrolled calcium influx and potassium efflux, possibly leading to cell death unless the membrane is repaired (Brito et al., 2019).

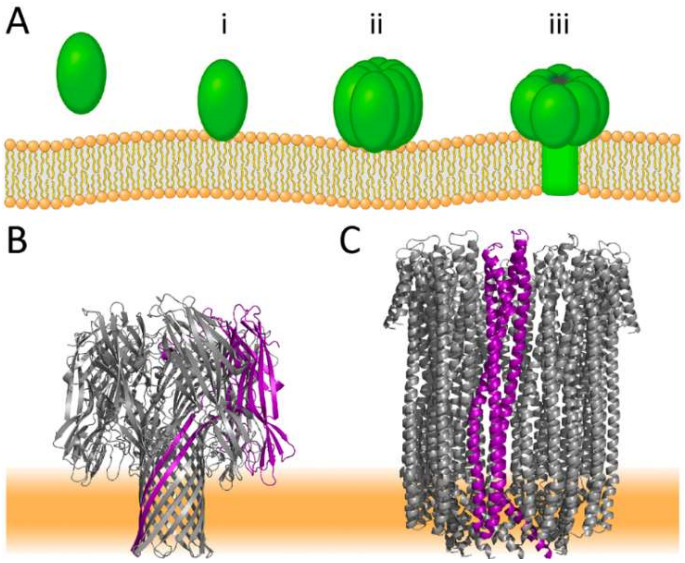

Figure 38. Both classes of PFTs damage membranes by a similar multistep mechanism.

*(**A**) Toxin binds the target membrane (i) possibly after binding a non-lipidic receptor, (ii) monomers oligomerize either during the process of membrane insertion (α-PFTs) or before, thus forming a prepore intermediate (β-PFTs); (iii) eventually a pore is formed. (**B**) α-hemolysin from* S. aureus *is an archetypal representative of β-PFTs, whose 2 nm-wide transmembrane pore is a β-barrel. (**C**) ClyA from* Escherichia coli *forms a 3.5 nm-wide pore with a cluster of helices and thus belongs to α-PFTs. One protomer is highlighted in purple in each pore. The orange rectangle denotes the lipid membrane. (modified from Rojko and Anderluh, 2015)*

To date, pore-forming toxins belong to six structural classes that are clustered in two groups according to the secondary structure of the peptide lining the pore: α-helical in α-PFTs and β-stranded in β-PFTs. (Dal Peraro and van der Goot, 2016). Each family also displays characteristic stoichiometry and pore size.

Active ShlA inserts in erythrocyte membranes (Schiebel and Braun, 1989) where it adopts a new conformation (Hertle et al., 2000; Schiebel et al., 1989; Walker et al., 2004) and makes 1-to-3 nm wide pores (Braun et al., 1987; Schönherr et al., 1994). Similarly, the measure of hemoglobin release from red blood cells in presence of osmoprotectants of select sizes allowed to infer that ExlA makes up ~1.6 nm wide pores (Basso et al., 2017a). It has been reported that hemolytic activity was virtually lost upon

C-terminal truncation of ShlA (Poole et al., 1988). C-terminal location of the activity is common in TPS substrates (Guérin et al., 2017) and consistently, ExlA-mediated-cytotoxicity was impaired when the last 295 residues of the protein were deleted (Basso et al., 2017a). This information is merely topological though: due to the lack of homology to any other protein and considering the lack of experimental data on pore formation by proteins of the ShlA/ExlA family, how ExlA pores assemble into target membranes is unknown.

Screening for impaired ExlA variants.

When looking for something unknown, genetic screens are the most reasonable way to proceed. Key to this is the proper selection of variants. ExlA hemolytic properties make blood agar plates an obvious way to screen for impaired function. Similarly to what has been described for ShlA (Braun et al., 1985; Hilger and Braun, 1995; Schiebel et al., 1989), RBC did not seem to be cleared around *P. aeruginosa* IHMA87 cells. In contrast, *E. coli* cells able to produce recombinant *exlBA* did show signs of hemolysis on blood agar plates (**Fig. 39**). Screening for impaired ExlB/ExlA function is possible. This means that a thinner or a larger halo could be due to mutations in either ExlB or ExlA (activation or secretion defect altogether). My intention is to perform targeted random mutagenesis in order to have mutants pre-sorted in some way. Several assays will be used to characterize the hemolysis defect (see below).

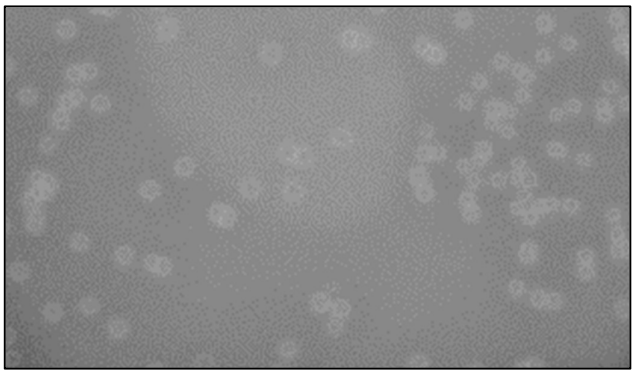

Figure 39. Expression of* exlBA *in* E. coli *yields hemolysis around colonies on blood agar plates.

ExlA function and disorder: when 'worse' works best.

When ExlA is harvested from *P. aeruginosa* culture broth supernatant or purified in a non-native form from *E. coli* cytoplasm, it is unable to lyse eukaryotic cells. This has imposed an infection set-up for most experiments (Basso et al., 2017a). While this has allowed significant advances (Reboud et al., 2017b), defined protein samples would be preferable to support the characterization of structure function relationships, where quantitative assays are essential.

This has been sought in two ways: preparing ExlA from the secretome of recombinant *E. coli* and adapting the procedures that have been developed for ShlA (Schiebel et al., 1989). I designed recombinant plasmids to boost ExlA secretion in *E. coli*: after induction and ammonium sulfate

precipitation of culture broth supernatant, the secreted ExlA protein is ~90% pure already. But conditions suitable for its concentration above 0.5-1 g/l have not been found yet. Plus it was inactive with respect to hemolysis and cytotoxicity (see below).

Applying protocols similar to those reported by Braun and colleagues as they characterized ShlA (Schiebel et al., 1989) proved to be useful for ExlA too. Switching from pure, secreted, native ExlA to raw urea extracts from bacterial pellets, I observed that the latter material was indeed compliant with functional studies (**Fig. 40, 41**). This had several implications: (i) it seems that ExlA needs to be at least partially denatured by urea to exert a hemolytic activity, and (ii) ExlA prepared that way is 50-75% pure and readily reaches concentrations higher than 5 g/l. The cleanest of such unorthodox samples actually led to the successful isolation of monoclonal hybridomas after mice immunization in a project led by Philippe Huber.

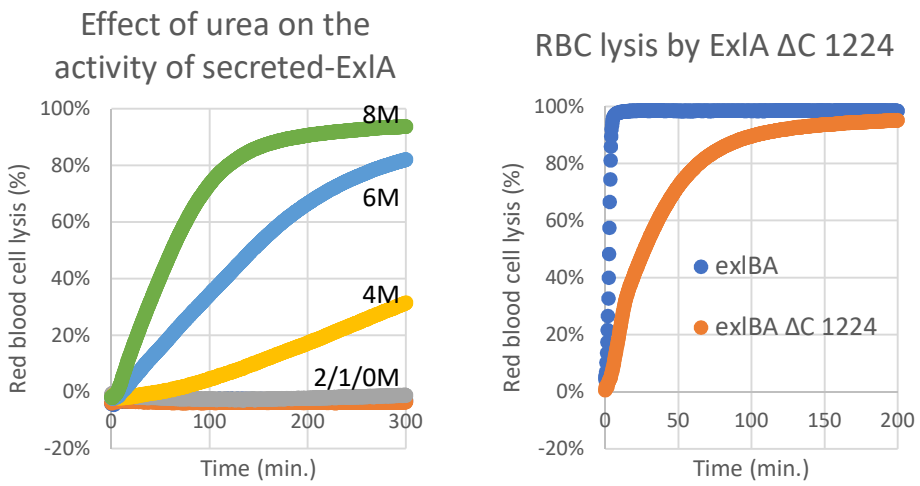

Figure 40. Kinetic assessment of ExlA-mediated hemolysis.

*(**Left**) Urea supplementation of filtered spent medium where ExlA has been secreted* via *ExlB. Urea final concentrations are indicated near the relevant curves. (**Right**) Hemolysis induced by 1.8nM full-length ExlA or 2.5nM truncated at residue 1224.*

The hypothesis that polypeptide disorder may be instrumental in ExlA function is consistent with the observation that ExlA cytotoxicity is higher when ExlA is delivered closer to target cells (Basso et al., 2017a). Indeed, refolding studies with the passenger domain of *B. pertussis* pertactin (type 5a) have suggested that β-helical domains be slow-folding units (Junker et al., 2006). In the case of ExlA, this might allow enough time for a productive encounter between disordered portions of the protein and the target membrane. This also provides an alternative, still hypothetic explanation to the rapid inactivation of ShlA after secretion, which was attributed to aggregation (Schiebel et al., 1989).

The C-terminal domain of ExlA was observed to carry ExlA cytotoxic and pore-forming activites (Basso et al., 2017a). The effect of pH and urea on the structure will be plotted as a function of their effect on the activity of the isolated C-terminal domain or full-length ExlA in order to substantiate the suspected correlation between denaturation and function. This will be performed with the anilinonaphtalene sulfonate fluorescent probe.

Hemolysis & cytotoxicity: different functions or different facets of ExlA function?

Hemolytic activity is how ExlA destroys red blood cells (RBC) while cytotoxicity is how ExlA kills cells and tissues. Although ExlA readily destroys RBC, hemolysis was not observed during infection with CLJ1 (Elsen et al., 2014). Still, RBC are widely accepted as a model to characterize pore forming toxins. This phenotype is immediately accessible on blood agar plates while cytotoxicity has long been costly and more tedious to investigate: this probably explains why so many toxins, including ShlA, have been dubbed 'hemolysin' even though cytotoxicity may be their primary function (Di Venanzio et al., 2017; Hertle et al., 1999; Reboud et al., 2017a; Scheffer et al., 1988).

Hemolytic and cytotoxic activities of ExlA are currently being assessed with microplate, kinetic assays, using human blood and lung carcinoma A549 cells. As discussed above, secreted native ExlA is inactive in both settings, unless it is supplemented with urea (hemolysis: **Fig. 40, left**). Partial denaturation is not the only key, as urea-denatured ExlA is inactive when produced in absence of its partner ExlB, like has been originally discovered on ShlBA (Ondraczek et al., 1992). Working with a collection of C-terminal truncated derivatives of ExlA, I have also observed that hemolysis determinants mapped to a broader region than cytotoxicity determinants (**Fig. 40, 41**). How hemolytic and cytotoxic activities are related is not clear. Do their determinants overlap or are they distinct? Should they be considered the same way, knowing that mature mammalian RBCs may not be able to display as efficient membrane repair responses as other cell types, e.g. due to the paucity of energy supply and lack of an internal membrane system? RBC could thus be more sensitive to PFTs than fibroblastic or epithelial cell types.

How many assays should be used to assess the function of ExlA variants?

Considering ExlA primary function, cytotoxicity assays are the most relevant to characterize ExlA activity *in vitro*. These assays allow to assess ExlA functionality and cellular responses altogether (Reboud et al., 2017a) even though the use of propidium iodide incorporation as a marker of cytotoxicity (Atale et al., 2014) prevails in routine assays or for screening purposes (Basso et al., 2017b).

Mammalian RBCs are highly differentiated cells that are produced from reticulocyte maturation in a process that involves enucleation and loss of an internal membrane system (Ovchynnikova et al., 2018). RBCs are likely not a pathophysiological model of ExlA activity, as no sign of hemolysis was

observed in the patient infected with *P. aeruginosa* CLJ1 (Elsen et al., 2014) but they are a straightforward biological system and are readily used to experiment with cytolysins / hemolysins (see above) with several advantages: (i) RBC are considered to behave essentially like liposomes even though they harbor membrane proteins and a cytoskeleton, (ii) their limited biosynthetic capacity allows to modify RBC surface e.g. by enzymatic treatment, in a more controlled manner than cultivable cell types, (iii) the preparation of RBC ghosts loaded with pore-forming proteins has supported numerous electromicroscopy imaging studies (see **section 4.2.4**). Thus the hemolysis assay is both complementary to cytotoxicity assays and a bridge to mechanistic and structural investigations.

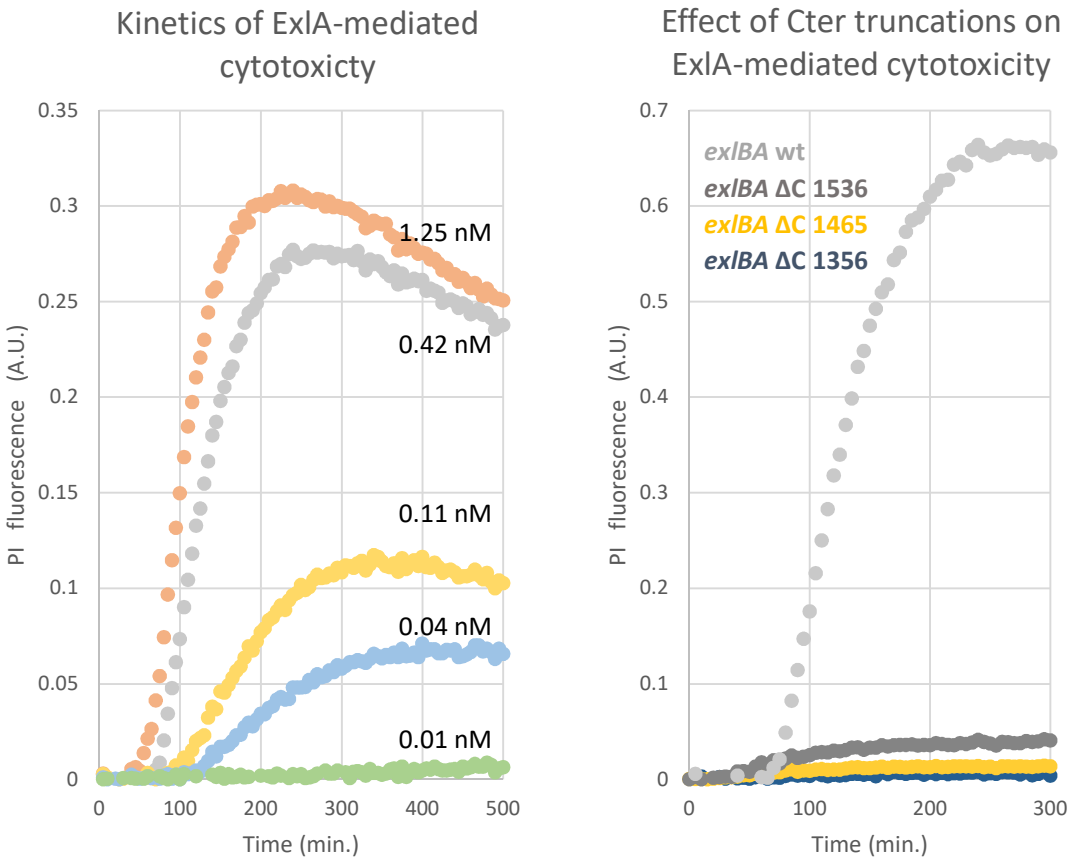

Figure 41. Kinetic assessment of ExlA-mediated cytotoxicity on cultivated lung carcinoma (A549) cells.

The assay measures propidium iodide fluorescence as a function of time, which allows to follow fluorophore incorporation in the nucleus, which is a measure of cytotoxicity. (Left) Dose response curves obtained with the indicated final concentrations of ExlA prepared as urea extracts. (Right) Cytoxicity of the full-length (wt) and C-terminal truncation constructs with the last residue as indicated. Fluorescence measurements have been normalized with respect to 1 nM protein concentration.

Finally, liposomes offer the best overall control, especially regarding membrane composition (Faudry et al., 2013). Initial experiments have been performed using ExlA derivatives produced in the cytoplasm of *E. coli*: this has allowed to observe liposome leakage in a C-terminal domain-dependent manner (Basso et al., 2017a). As the effect of pH was investigated, it was found that full-length ExlA promoted liposome leakage at pH 7 while the isolated C-terminal domain promoted leakage at pH 4. Although there is no obvious explanation to this, especially considering that the C-terminal domain has a theoretical pI of 9.3, one might reason that pH-dependent denaturation could play a role similar to that of urea with full-length ExlA. Making sense of the reciprocal effect of neutral and acidic pH on full-length and the C-terminal domain seems more challenging at this point.

As these three assays allow to assess complementary aspects of ExlA function over time, I will use them in parallel to characterize ExlA functional determinants *in vitro*.

4.2.2. Investigating ExlA interaction with target cells

PFTs classically dock to a receptor as they reach a target membrane, be it a protein, a sugar moiety or a lipid head group (Dal Peraro and van der Goot, 2016). Like ShlA and HpmA, ExlA was found to be active on RBCs as it is secreted from growing bacteria, although this seems to be irrelevant to pathogenesis (Elsen et al., 2014). The C-terminal domain of ExlA also induced liposome leakage in absence of any other protein (Basso et al., 2017a). This suggests that lipid binding is enough to drive membrane insertion of ExlA C-terminal domain. Accordingly, preliminary experiments with RBC, either trypsinized to shave proteins off the surface, or treated with peptide:N-glycosidase F to remove N-glycan moieties of glycoproteins, both showed no evidence that hemolysis was compromised or even delayed (not shown).

Does ExlA need docking to a specific receptor on target membranes?

The requirement for specific lipids in ExlA-mediated pore formation has been tested *in vitro* when Basso et al. (2017a) have set up their liposome leakage assay. Testing the effect of the lipids usually found in eukaryotic membranes (cholesterol, phosphatidylcholine, phosphatidylethanolamine , phosphatidylserine) on ExlA-induced liposome leakage, a specific requirement for phosphatidylserine (PS) was discovered. Similarly to ExlA, PS was found to be necessary to ShlA pore-forming activity in a liposome leakage assay, whereas PC and PE were not (Hertle, 2002). I have investigated the specificity of ExlA:lipid interaction by a protein overlay assay on so-called lipid strips, where specific lipids are spotted on a PVDF membrane. Preliminary results showed that ExlA has a clear preference for

negatively charged lipids and that this is mainly driven by the C-terminal domain, without which no binding could be observed (**Fig. 42**).

Although liposome and lipid binding studies point at similar lipids, especially PS, the physiological relevance of this preference is unclear since PS, phosphatidylinositol (PI) and phosphatidic acid (PA) are confined to the inner leaflet of the cytoplasmic membrane (Devaux, 1991; Zachowski, 1993) and cardiolipin is found in mitochondria (Schlame, 2008). All of these lipids are thus concealed within target cells. Therefore, the fact that ShlA and ExlA can perform their activity on protein-free lipid bilayers (Basso et al., 2017a; Hertle et al., 1997) does not imply that these proteins only require lipids as receptors. As a matter of fact, this is a common situation where protein receptors do not make a qualitative but quantitative contribution to PFT activity, supporting tissue specificity (DuMont and Torres, 2014).

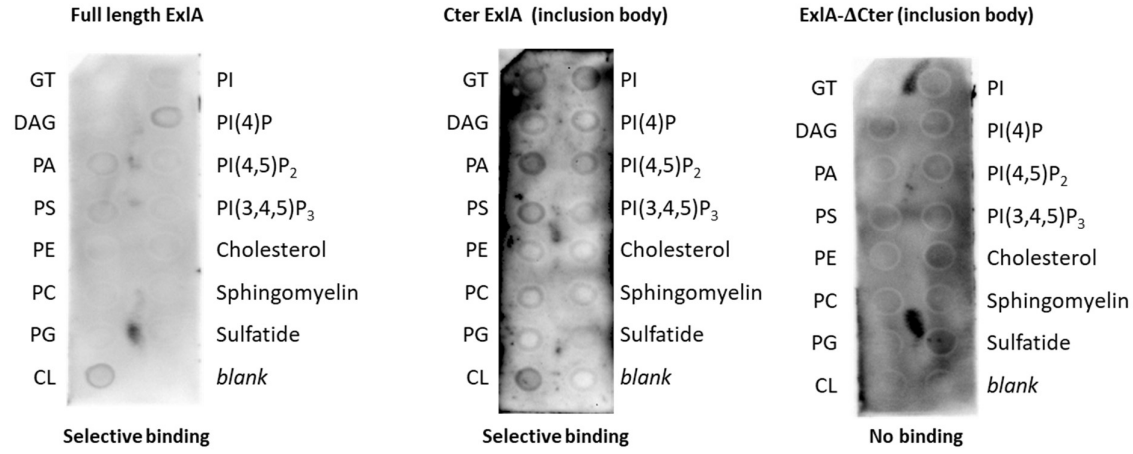

***Figure 42. Lipid binding properties of ExlA* in vitro**.

Full length ExlA and each domain were tested in parallel for their ability to bind spots of lipids, which was revealed with an anti-ExlA polyclonal antibody. ***Top legend****: ExlA material used. Full-length ExlA was first denatured with 6M urea, otherwise no signal was observed.* ***Side legend****: lipid spot identification Glyceryl tripalmitate (GT), Diacylglycerol (DAG), Phosphatidic Acid (PA), Phosphatidylserine (PS), Phosphatidylethanolamine (PE), Phosphatidylcholine (PC), Phosphatidylglycerol (PG), Cardiolipin (CL), Phosphatidylinositol (PI), and its derivatives PI(4)P, PI(4,5)P_2,PI(3,4,5)P_3 phosphorylated as indicated.)* ***Bottom legend****: partial conclusion.*

How does ExlA behave upon lipid binding?

Pore formation requires membrane insertion of a portion of ExlA and likely involves an oligomerization step (for the latter see **section 4.2.4**).

Identifying the region of a protein that is embedded into the lipid phase used to be carried out by photoactivable crosslinking of a radioactive lipophilic probe to the protein followed by site-specific proteolysis (Brunner, 1989). Such a technique is based on a carbene moiety that generates a highly reactive radical species upon irradiation. It has allowed to spot the signal peptide as the only part of a secretory protein to be exposed to the lipid phase during translocation (Martoglio et al., 1995) or to localize membrane interacting domains of diverse proteins in a proteolytic peptide map (Durrer et al., 1995; Kennedy et al., 1989). This offers the advantage to be free from preconceived ideas but it requires skills and equipment that were never wide-spread and, from a literature point of view, this seems outdated. Yet the same 'carbene-based' chemistry is now coupled to MS/MS analyses to map protein:protein interactions *via* the identification of the non-reactive residues (Manzi et al., 2016) and the development of a lipid-partitioning labeling probe could make it a pertinent approach to determine ExlA pore lining residues (Manzi et al., 2017).

Yet another approach is classical and much more accessible. To identify and characterize protein:lipid phase interactions, the use of site-directed protein variants where a probe is used to modify e.g. a cysteinyl residue, has found multiple applications. The accessibility of cysteines to the hydrophilic maleimide-biotin reagent can be used to identify membrane-embedded residues as those residues that are not modified (Anderluh et al., 1999). Also, the derivatization of single cysteine mutants with a polarity-sensitive fluorophore like acrylodan allows to map positions that are sensitive to the presence of lipid vesicles (Anderluh et al., 1999; Promdonkoy and Ellar, 2000). Finally, site-directed spin labeling of cysteinyl residues allows to collect informations about the mobility, the solvent accessibility and the polarity of the immediate environment of the spin labelled side chain (Bordignon and Steinhoff, 2007) although contradictory results occasionally may be produced (Pulagam and Steinhoff, 2013, and references therein).

```
     AEGVK VNVDARLGVE KNQPGLVNKL ASKTGPLKDK LETKAENAFD
KHRGKLENGI DRNVERLGKA GDNLLAKAEK AKERLGEKLV RSGSYEVNPE
PRGAFASKLD RARGYLAEKG EALGDRLSGL KQRLSPNKTG SYVVNDKQTA
GAKVGNAAEN VLFGDKSGEA SVTPTLYLDV SHVSRNYVTE ASGITGRQGV
NLQVGAATQL TGARISASDG KVDLGGSRVE TRALAGKDYR ADLGLNVSRS
PVDLAFGIKD EFSQEHDQAT RDDQAFNLGA LRVGGRNRDQ QLQAGIEQKAD
```

Figure 43. C-terminal sequence of ExlA.

*The sequence corresponds to residues 1356 to 1651 of the entry **PSPA7_4642**. The sequence starts right after the end of the last annotated feature in Pfam. Single letter code was used. Basic and acidic aminoacyl residues in blue and red, respectively. Serinyl residues (underlined) are good candidates for a conservative change to a cysteinyl side-chain.*

Alternatively, the intrinsic fluorescence of tryptophanyl residues can be used, with brominated lipids available to report on the depth of membrane insertion of the indole ring, since bromine quenches indole fluorescence within a short range (Bolen and Holloway, 1990; Duché et al., 1996; Li et al., 2019; Pfefferkorn et al., 2015).

The C-terminal domain is necessary to, and possibly carries ExlA pore-forming activity (Basso et al., 2017a). It is highly charged and does not display any obvious hydrophobic stretch (**Fig. 43**). It is also devoid of cysteinyl and tryptophanyl residues. Single cysteine mutants will be made, e.g. by substituting select serinyl residues and tested for accessibility or membrane insertion such as identify which residues do insert into the target membrane.

How to track ExlA?

Besides the description of the structural changes that ExlA experiences when meeting the target membrane, it is desirable to be able to track a fluorescently labeled ExlA at the cells' surface. A fluorescent derivative of ExlA could be advantageous also to monitor protein translocation into vesicles in real time (see **section 4.2.3**) or to detect the protein spectroscopically at low concentration, which could be useful to carry out structural characterization (**section 4.2.4**). Labeling of lysyl or cysteinyl residues by N-hydroxy-succinimidyl or maleimidyl esters, respectively, is a common way of modifying proteins, e.g. with fluorescent moieties (Nanda and Lorsch, 2014a, 2014b).

Investigating the fate of ExlA requires the possibility to stabilize intermediate states. In a chemical reaction, this can be achieved by shifting physicochemical parameters, e.g. low temperature. Conformational changes intermediates may be trapped in the same way (Markosyan et al., 2001; Nguyen et al., 2002), but this is most surely obtained mechanistically, by introducing road blocks i.e. sizable moieties or covalent links, as exemplified in diverse ways during the characterization of SecY-mediated translocation (Erlandson et al., 2008; Li et al., 2016; Park et al., 2014).

This is why split-GFP constructs will be designed in which the C-terminal strand of GFP will be added C-terminally or N-terminally to the sequence of mature ExlA, hoping that a functional fusion protein will be obtained either way after mixing with the rest of the GFP barrel, either coproduced in the periplasm to block transfer or produced separately for functionalization (Cabantous et al., 2005; Kamiyama et al., 2016). For the latter, covalent attachment of a reporter on the secreted protein could also be attempted with the SpyTag which similarly consists in a single β strand (Reddington and Howarth, 2015; Zakeri et al., 2012), or by sortagging, which also has minimal requirements regarding tag sequence except for accessibility and flexibility (Ritzefeld, 2014) and has already been used to discover new receptors of the *Aeromonas hydrophila* PFT aerolysin (Wuethrich et al., 2014).

***Seeking ExlA receptor on target cells* in vivo**

ExlA needs no protein to bind lipids and form a pore (see above), but looking for (additional) receptor(s) of ExlA is of prime importance with respect to the elucidation of ExlA-associated pathogenesis. This is actually part of the PhD project of Vincent Déruelle (Philippe Huber, supervisor). My contribution to this project is based on pull down experiments using wild-type ExlA and a FLAG tag derivative of ExlA. Pulled-down eluates are then submitted to MS-MS for differential protein content identification (collaboration with Yohann Couté, BGE).

So far, two experiments have yielded about 20 non-consensual hits. The present plan is to perform strictly parallel experiments with another cell-type such as to cross identify which proteins do interact significantly with ExlA. The use of a membrane-impermeant, reversible cross-linker like DTSSP is also tested (Bennett et al., 2000).

At least one alternative strategy may be used. Hypothesizing that a functional, pore-forming active ExlA will exist as several non-synchronized states in the target cell membrane, thereby yielding complex profiles, I am willing to test whether functional, pore-forming inactive ExlA could support the hunt for a receptor. Secreted ExlA, which is non-cytotoxic unless supplemented with urea (see above), will be tested for binding to target cells. ExlA could be fluorescently labeled, or immunodetected with a recently obtained immunofluorescence-compliant monoclonal anti-ExlA antibody, to screen for binding at the cell surface. Should ExlA be bound at the cell surface then the pull down procedure would be performed as described above, including a crosslinking step or not.

Discovering a receptor for ExlA would be significant from the pathophysiological point of view. It may also reveal some unexpected feature about ExlA molecular mechanism and open a new perspective for ExlA-like toxins characterization.

4.2.3. Biogenesis of *P. aeruginosa* ExlA

ExlA gets activated during translocation through ExlB, similarly to what has been reported for *S. marcescens* ShlA (Schiebel et al., 1989). Many results obtained with ShlA await to be tested with other models, of which ExlA is presently the only to be actively studied, to my knowledge.

What happens to ExlA on its way out from* P. aeruginosa*?

Some founding members of the TPSS group are well characterized homologs of ExlBA, like *B. pertussis* FhaCB and, of course, *S. marcescens* ShlBA (Jacob-Dubuisson et al., 2009). With analogy to these well-studied TPS systems, ExlA secretion is predicted to occur in two steps: (i) the 34 residue-long, cleavable

signal peptide at the N-terminus of ExlA targets the precursor to the general secretion pathway, which delivers ExlA to the periplasm after signal peptide processing and (ii) mature ExlA gets translocated across the outer membrane through ExlB **(Fig. 44)**. ExlA targeting to ExlB across the periplasm probably requires the TPS domain of ExlA to interact with ExlB POTRA domains 1 and 2 (Delattre et al., 2011; ur Rahman et al., 2014), making them indispensable for ExlA secretion (Basso et al., 2017a).

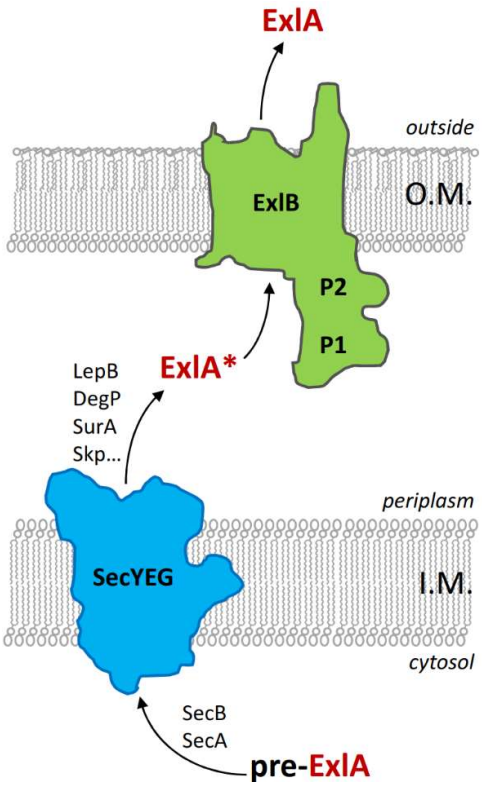

Figure 44. Schematic representation of the ExlA secretion pathway, as pictured from ShlA data.

ExlB and ExlA precursors are targeted to the periplasm via the general secretion pathway by recognition of their N-terminal signal peptides. With analogy to the ShlBA TPS, ExlB inserts into the outer-membrane where it forms the translocation pore to which the non-functional periplasmic intermediate ExlA is targeted via the interaction between its TPS domain and ExlB POTRA domains P1 and P2. Some chaperones usually involved in protein secretion are mentioned (SecB, SurA, Skp, DegP)*

On its way out, pre-ExlA may meet chaperones like the secretion dedicated chaperone SecB, and SecA in the cytoplasm (see **section 2.1**) and ExlA* may reach ExlB with the help of the chaperones SurA, Skp and/or DegP in the periplasm. A role for DegP has already been shown in the case of FHA (Baud et al., 2009, 2011). The role of chaperones in ExlA secretion will be investigated *in vivo* and *in vitro*.

Looking for partners by coexpression in vivo

ExlA can be produced by *E. coli* and precipitated from spent medium (**section 4.2.1**). In the heterologous expression system presently in use, ExlA and ExlB encoding genes are carried by pET and pACYC184 plasmids, respectively. My goal is to make a generic tool that would help testing the effect of periplasmic chaperones as well as SecB on protein secretion in *E. coli*. For this, the pCOLA backbone, which is compatible with pET and pACYC has been selected, together with a tunable expression system like arabinose- or cumate-inducible promoters (Choi et al., 2010; Guzman et al., 1995). With this system, it should be possible to observe if overexpression of either gene increases the yield of ExlA production. As this takes place in *E. coli*, the information will primarily be used to improve the yield of recombinant proteins. This will also prime *in vitro* reconstitution experiments.

In vitro reconstitution of ExlA secretion

In vitro reconstitution of TPS secretion through the OM has been published (Fan et al., 2012; Norell et al., 2014). The assay uses spheroplasts to produce FHA *in situ* and radioactive labeling to detect the products that have moved into outer membrane vesicles, which makes it somewhat cumbersome. My goal is to set up an assay for ExlA translocation across the OM, that would be performed in the same way as SecYEG-mediated translocation is assessed (**section 2**) with urea-denatured ExlA* (periplasmic intermediate produced in absence of ExlB), periplasmic cofactors and ExlB-loaded outer membrane vesicles or proteoliposomes. Recent progress in the reconstitution of AT translocation (Hagan et al., 2010; Roman-Hernandez et al., 2014) do support that direction. Should immunodetection of translocated ExlA fail to give satisfaction, fluorescent detection could be sought as described by De Keyzer et al., (2002) who set up a fluorescent assay of SecY-mediated translocation (see also **section 4.2.2**).

State of the art in brief and selection of present questions

FhaC has been shown to be the channel through which FHA precursor, FhaB, is threaded and folded outside (Baud et al., 2014; Fan et al., 2012). Targeting of FhaB to FhaC involves the TPS domain of FhaB and some signals nearby downstream (Hodak et al., 2006) as well as the two POTRA domains of FhaC, which may use β augmentation to interact with FhaB (Delattre et al., 2011). Refering to several structures of FhaC, either in the translocation-competent idle state, or in a translocation-incompetent double mutant (Clantin et al., 2007; Maier et al., 2015), and using functional assays ranging from binding to secretion to channel conductivity to EPR (Delattre et al., 2010; Guérin et al., 2014, 2015), the intramolecular motions of FhaC have been scrutinized and interpreted to suggest that gating is supported by the competition of the incoming substrate for the barrel proximal POTRA domain (POTRA 2) of FhaC that is engaged in intramolecular interactions.

Question 1: How a TpsA is threaded through the cognate TpsB is not known but likely supposes conformational changes in both proteins. These events probably support the secretion-coupled activation of ShlA (Hertle et al., 1997, 2000; Schiebel et al., 1989; Walker et al., 2004), which has been characterized at the genetic level mostly, yielding mutants with secretion and/or activation impaired (Poole et al., 1988; Pramanik et al., 2014; Schönherr et al., 1993; Yang and Braun, 2000) or enhanced (Hilger and Braun, 1995).

Select mutations from the literature ought to be introduced in ExlBA to be tested for translocation and activation in order to make sound comparisons between both systems. So far, C-terminal truncated variants of ExlA have already been tested for secretion, yielding results as expected (see **section 4.2.1**). Given the dynamic process at work, I would like to probe possible molecular rearrangements by

introducing intramolecular disulfide bridges, along the line that was mine as I was working on SecYEG. The difficulty here is that there is no focal point to support a clear hypothesis like the plug hypothesis back in 2004, so this cannot be a priority yet.

Question 2: Where does the energy that fuels secretion come from? This question is ever present at the OM (see **section 1.1.4**). Now demonstrated for ATs (see **section 4.1.3**) it is reasonable to assume that TpsA folding suffices to provide outward directionality, be it by preventing backsliding through TpsB or by pulling the chain out, which would be more efficient.

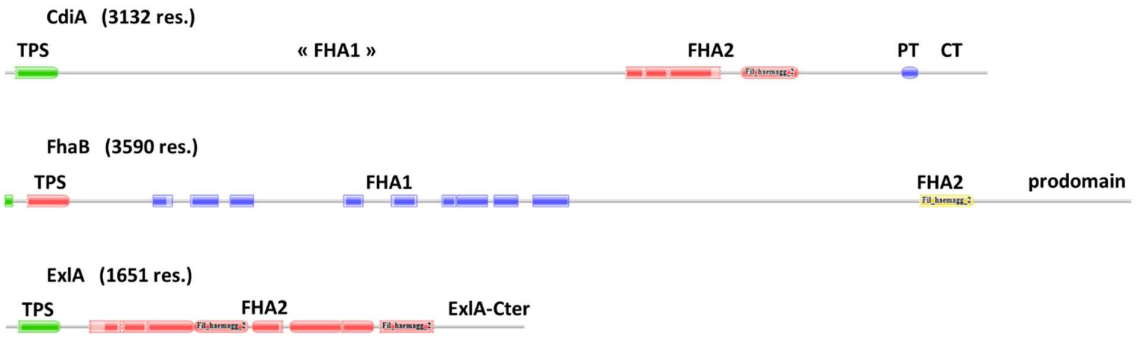

Figure 45. Schematic representation of E. coli CdiA, B. pertussis FhaB and P. aeruginosa ExlA.

Graphics from Pfam (Finn et al., 2014), with TPS domain (TPS), filamentous hemagglutinin repeats type 1 (FHA1), filamentous hemagglutinin repeats type 2 (FHA2) emphasized. Curiously, FHA1 repeats are not displayed by Pfam in any of E. coli CdiA toxins I have looked up.

Question 3: ExlA was originally detected in the bacterial culture supernatant, but it is not clear whether the secreted form is the active one. Its poor solubility could severely restrain diffusion of the toxin in the milieu, perhaps tethering it to the envelope. Indeed, the fact that ExlA-mediated virulence was potentiated by type 4 pili (Basso et al., 2017a), which are contractile appendages working like a grapple hook, also suggests that the diffusion of secreted ExlA is confined around *P. aeruginosa*. This is in agreement with the limited diffusion reported for *S. marcescens* ShlA (Ondraczek et al., 1992), with whom ExlA shares 34% overall identity. A recent publication on another TPSS, *E. coli* contact-dependent growth inhibition toxin CdiA, suggested that in this case at least the secretion process would stall at some point, with the receptor binding domain displayed at the tip of a helix made of type 1 filamentous hemagglutinin repeats (Ruhe et al., 2018). The polypeptide chain would go back into the periplasm, with a previously undescribed Tyr-Pro rich domain and type 2 filamentous hemagglutinin repeats leading to the toxin domain. Secretion would resume upon receptor binding.

While type 1 and type 2 repeats have both been proposed to fold as triangle-shaped, right-handed β-helices (Kajava and Steven, 2006), Ruhe et al. (2018) have suggested that this may not be the case, based on their cryoEM and functional data. This is relevant to ExlA whose passenger domain is exclusively made of type 2 repeats (**Fig. 45**), for which indeed there is no template in the Protein Data Bank. As a consequence, building a model for ExlA may not be as straightforward as initially suggested (Reboud et al., 2017b).

4.2.4. Characterizing the structure of *P. aeruginosa* ExlA

Getting a family picture of* P. aeruginosa *ExlA

P. aeruginosa ExlA is 170kDa large and does not seem to be further matured by limited proteolysis or a covalent modification, in contrast with other TPS proteins like *B. pertussis* FHA or *Haemophilus influenzae* HMW1A and HMW2A. The most relevant homologs present in the literature are *S. marcescens* ShlA and *P. mirabilis* HpmA which share 34% and 29% overall identity with mature ExlA, respectively.

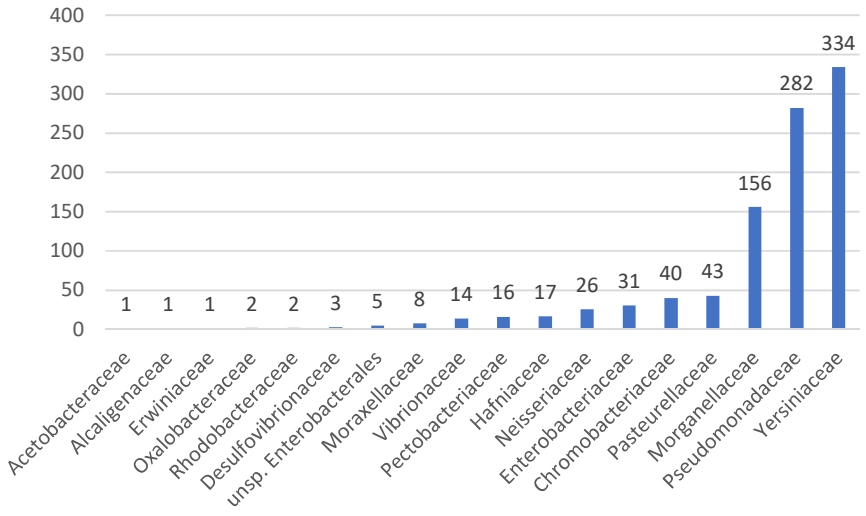

Figure 46. Taxonomic distribution of ExlA-like sequences with respect to families.

Yersiniaceae: Yersinia sp., Serratia sp.

Pseudomonadaceae: Pseudomonas sp.

Morganellaceae: Proteus sp., Photorhabdus sp., Xenorhabdus sp.

As structural information on ExlA is scarce, I have used NCBI-BLAST (Altschul et al., 1990, 1994) to collect 980+ non-redundant sequences from NCBI-Protein, KEGG, JGI and Pseudomonas.com genome databases (Chen et al., 2019; Kanehisa et al., 2016; Winsor et al., 2016) in order to explore taxonomic distribution and to detect sequence conservation within ExlA-like sequences. Pfam annotations of the collected sequences allow to spot 80 CDI toxins which should be filtered out, and a thoughtful assessment of particular sequences showing extreme parameters, e.g. with respect to polypeptidic

chain length, is still needed before the collection can be used to generate a profile signature (Söding, 2005). In the present state, three families cover 80% of ExlA-like sequences, each displaying a known prototype: *S. marcescens* ShlA, *P. aeruginosa* ExlA and *P. mirabilis* HpmA (**Fig. 46**). This apparent concentration into a few pathogen families may reflect the prevalence of pathogens in bacterial genome sequencing projects.

When the ExlA-like sequences collected have been aligned, the non-obvious repeats in the so-called shaft domain were delineated (**Fig. 47**). This information will be used to modify the shaft domain, making it shorter (internal truncation) or longer (internal duplication). With such constructs, it will be possible to investigate the effect of shaft domain-size on ExlA translocation and on *P. aeruginosa* virulence. Increasing the size of ExlA could also serve a practical goal: assuming a β helix fold, the actual size of ExlA was estimated to 23 nm (Reboud et al., 2017b) and larger constructs would favor imaging by electromicroscopy (see below).

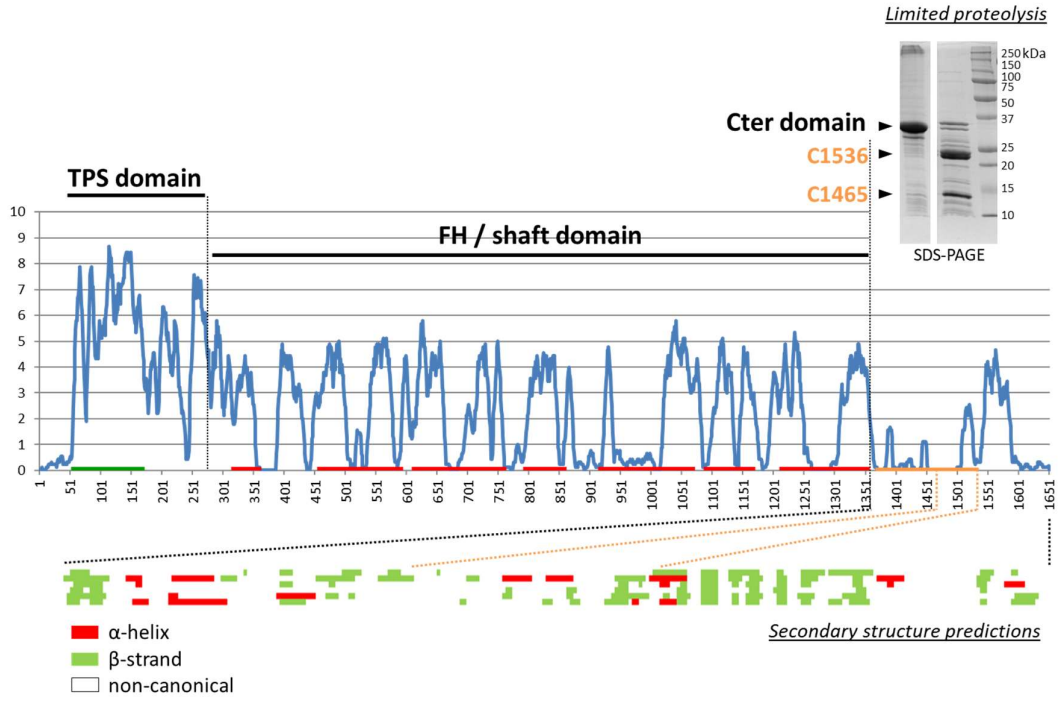

Figure 47. Aminoacid conservation along ExlA sequence and predicted features of the C-terminal domain.

*(**Top**) The 984 sequences were aligned with MAFFT using global alignment parameters (Katoh et al., 2017) and the alignment of 44 sequences from the* Pseudomonas *genus was extracted. The graph represents sequence conservation, as scored by Jalview (Waterhouse et al., 2009). Positions of Pfam TPS and FHA2 signatures are indicated by green and red segments, respectively. The orange segment encompasses the two overlapping fragments produced by limited proteolysis of the isolated C-terminal domain, which have an intact N-terminus and were found by mass spectrometry to end at positions 1465 and 1536 (inset). (**Bottom**) The sequence of ExlA corresponding to the longer of these fragments was submitted to several secondary structure algorithms (see text) to find non canonical and extended (β) structure elements.*

What does ExlA look like before it meets a target membrane?

The C-terminal domain set aside, the structure of ExlA-like proteins seems to be accessible by structural homology. TPS domains are very well conserved in sequence and in structure; sequence alignments allowing to discriminate between at least two groups of TPS domains, depending on whether their closest homolog is *B. pertussis* FHA, which is the case of ExlA, or *H. influenzae* HMW1A (Guérin et al., 2017). Several TPS domains have been crystallized and their structure solved at high resolution, including that of *P. mirabilis* HpmA which shares 47% identity with ExlA's (Weaver et al., 2009) (**Fig 36**). Based on the structure of a complete TPS substrate (Zambolin et al., 2016), it is possible to envision how the helix primed in the TPS domain extends into the filamentous repeats-rich domain of ExlA to yield a fiber like structure of 1000-1200 residues called the shaft domain (**Fig 36**). Assuming β helical folding of type 2 hemagglutinin repeats , the secretion of mature ExlA by *P. aeruginosa* would release the ~30 kDa cytotoxicity domain at the tip of a-more-than-230 Å-long fiber (**Fig 36**). As for the C-terminal domain, in absence of any detectable signature, its sequence was submitted to secondary structure prediction algorithms (including JNET, YASPIN, SCRATCH, PREDICTPROTEIN, PSIPRED and ALI2). The output was synthesized in **Fig 47** which shows no clear structural tendency except for sparse extended (β-sheet) elements in the second half. As mentioned above, PFTs are classified according to the secondary structure element that lines the pore once the protein has oligomerized and inserted into the membrane (see **section 4.2.1**). Identifying the so-called pore-forming domain (Basso et al., 2017a) as a member of the α or β class of PFTs is a major goal in ExlA characterization.

Investigation of ExlA secondary structure

The homology model introduced above needs to be challenged and completed with respect to the C-terminal domain. To this purpose, the most accessible technique is circular dichroism spectroscopy (CD), which only requires µM amounts of protein. The first experiments have been carried out with the purified C-terminal domain of ExlA and fragments thereof, by Amandine Morand during her M1 internship. Although producing a portion of a TPS substrate in the cytoplasm of *E. coli* as a heterologous system is irrelevant to the physiological secretion pathway of such proteins, this was justified by the observation of a pH-induced pore-forming activity with this product (Basso et al., 2017a). No canonical structure was detected at pH 7 (not shown). New experiments will be performed in order to test the pH-dependency reported by Basso et al. (2017a) and the possible effect of known lipid binding properties (see **section 4.2.2**). Addition of a cosolvent like trifluoroethanol, reputedly mimicking a membrane environment in solution, could be tested with precaution (Maillard et al., 2003).

Although CD recordings are exquisitely sensitive, I will also investigate CD absorption by secreted ExlA and truncated derivatives thereof, carefully prepared in the same buffers, such as to check the

signature of the TPS and shaft domains which should show a strong b sheet signal, and possibly estimate the contribution of the C-terminal domain to the overall CD signal, using an appropriate deconvolution tool (Whitmore and Wallace, 2004, 2008).

Investigation of ExlA quaternary structure

PFTs oligomerization is essential to function; oligomerization occurs either on the membrane or in solution (Dal Peraro and van der Goot, 2016). I have observed SDS-resistant oligomers of ExlA which should be identified by comparison with the migration profiles of fully denatured cross-linked adducts. Repeating these experiments with ExlA variants, e.g. truncated proteins, the oligomerization domain could be localized within the sequence of ExlA.

The quaternary structure of the isolated C-terminal domain of ExlA has been investigated with size exclusion chromatography coupled to multi angle light scattering (SEC-MALS). Amandine Morand (M1) found it to be monomeric although it elutes like a globular protein four times its size. This somehow confirms the observation of non-canonical structure in CD: this product is not folded, although it has been shown to induce liposome leakage in a pH-dependent fashion.

What has been performed with the C-terminal domain is presently not possible with secreted ExlA due to the concentration issue described above. This will be circumvented with fluorescent labeling of ExlA, either with chemical modification or split-GFP fusion, as described in section **4.2.2**. Such a tool would allow quaternary structure of ExlA to be characterized in solution by analytical ultracentrifugation (C. Ebel, IBS).

Structural investigation of membrane-embedded ExlA

Electromicroscopy is a technique of choice to characterize the pore of a PFTs and we are fortunate to collaborate with Guy Schoehn (IBS). Imaging of membrane-embedded PFTs is commonly performed with RBC or liposomes. Building on the hemolysis assay that I have developed with urea solubilized ExlA and on *ad hoc* publications (Ikigai et al., 1996; Sekiya et al., 1993), Daphna Fenel (IBS/MEM) has successfully adapted the ghosts imaging protocol (**Fig.48**).

So far, in spite of methodic variations in the load of ExlA, no ExlA-specific shape could be identified. As advised by our collaborators the next step is to perform immunogold labeling to localize ExlA and possibly identify some pattern. This and size-shifted ExlA variants, with a modified number of repeats or a globular protein grafted at one end, (see above) will further help identify ExlA in electromicroscopy samples.

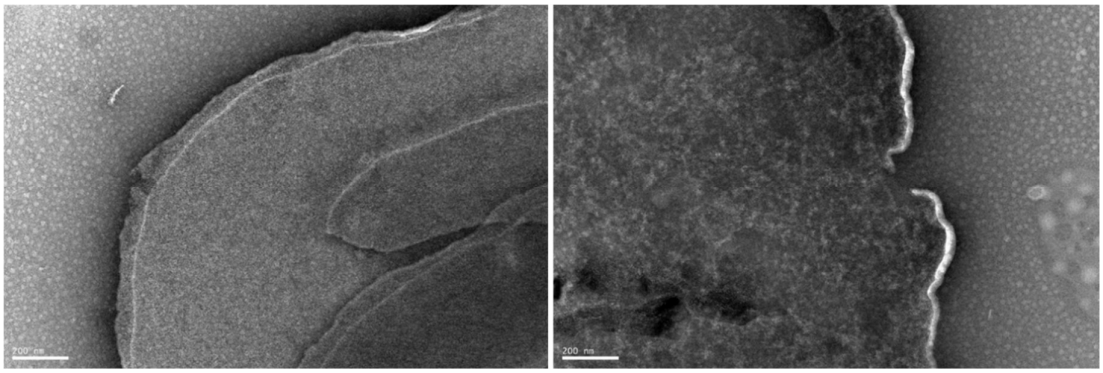

Figure 48. Negative stain electron microscopy imaging of RBC ghosts challenged with urea extracted ExlA

*Ghosts were prepared from RBC prior (**left**) or after (**right**) they have been challenged with ExlA. Samples were prepared according to Ikigai et al. (1996) and pictures were taken by Daphna Fenel (IBS/MEM).*

Conclusion & outlook

Structure and function like chance and necessity.

From the hierarchical organization of physical elements and chemical groups to biology.

Studying how the peptidoglycan gets assembled has introduced me to the specifics of bacterial organization, bacterial life, and societal impact *via* the spread of antibiotic resistance. This experience has turned me into a biochemist with a particular interest in bacterial objects and functions: I moved from considering the bacteria as a mere factory to consider them as a host, as a model and as a (re)source. Moving to the field of protein translocation has promoted a functional point of view on envelope biogenesis, opening a window on the diversity of the devices and functions associated with the envelope.

Now renewing my interest in toxins and protein translocation in the same time, I am happy to have joined the research group led by Ina Attrée. Virulence determinants of *P. aeruginosa* offer a considerable array of structures and functions that tweak or disrupt host homeostasis. That means opportunities to get a picture that includes molecules, cells, tissues, sometimes animals. That means opportunities to work and share, to discover and learn. And opportunities to enjoy my colleagues' proficiency and company!

Science is a passion - if it feels like fun, you've probably got it right.

Tom A Rapoport

References

Allen, W.J., Corey, R.A., Oatley, P., Sessions, R.B., Baldwin, S.A., Radford, S.E., Tuma, R., and Collinson, I. (2016). Two-way communication between SecY and SecA suggests a Brownian ratchet mechanism for protein translocation. ELife *5*.

Altschul, S.F., Gish, W., Miller, W., Myers, E.W., and Lipman, D.J. (1990). Basic local alignment search tool. J. Mol. Biol. *215*, 403–410.

Altschul, S.F., Boguski, M.S., Gish, W., and Wootton, J.C. (1994). Issues in searching molecular sequence databases. Nat. Genet. *6*, 119–129.

Anderluh, G., Barlic, A., Podlesek, Z., Macek, P., Pungercar, J., Gubensek, F., Zecchini, M.L., Serra, M.D., and Menestrina, G. (1999). Cysteine-scanning mutagenesis of an eukaryotic pore-forming toxin from sea anemone: topology in lipid membranes. Eur. J. Biochem. *263*, 128–136.

Aoki, S.K., Poole, S.J., Hayes, C.S., and Low, D.A. (2011). Toxin on a stick: modular CDI toxin delivery systems play roles in bacterial competition. Virulence *2*, 356–359.

Archibald, J.M. (2015). Endosymbiosis and Eukaryotic Cell Evolution. Curr. Biol. CB *25*, R911-921.

Arthur, T.M., Anthony, L.C., and Burgess, R.R. (2000). Mutational analysis of beta '260-309, a sigma 70 binding site located on Escherichia coli core RNA polymerase. J. Biol. Chem. *275*, 23113–23119.

Atale, N., Gupta, S., Yadav, U.C.S., and Rani, V. (2014). Cell-death assessment by fluorescent and nonfluorescent cytosolic and nuclear staining techniques. J. Microsc. *255*, 7–19.

Ball, G., Antelmann, H., Imbert, P.R.C., Gimenez, M.R., Voulhoux, R., and Ize, B. (2016). Contribution of the Twin Arginine Translocation system to the exoproteome of Pseudomonas aeruginosa. Sci. Rep. *6*, 27675.

Barik, S., Sureka, K., Mukherjee, P., Basu, J., and Kundu, M. (2010). RseA, the SigE specific anti-sigma factor of Mycobacterium tuberculosis, is inactivated by phosphorylation-dependent ClpC1P2 proteolysis. Mol. Microbiol. *75*, 592–606.

Basso, P., Ragno, M., Elsen, S., Reboud, E., Golovkine, G., Bouillot, S., Huber, P., Lory, S., Faudry, E., and Attrée, I. (2017a). Pseudomonas aeruginosa Pore-Forming Exolysin and Type IV Pili Cooperate To Induce Host Cell Lysis. MBio *8*.

Basso, P., Wallet, P., Elsen, S., Soleilhac, E., Henry, T., Faudry, E., and Attrée, I. (2017b). Multiple Pseudomonas species secrete exolysin-like toxins and provoke Caspase-1-dependent macrophage death. Environ. Microbiol. *19*, 4045–4064.

Batchelor, M., Prasannan, S., Daniell, S., Reece, S., Connerton, I., Bloomberg, G., Dougan, G., Frankel, G., and Matthews, S. (2000). Structural basis for recognition of the translocated intimin receptor (Tir) by intimin from enteropathogenic Escherichia coli. EMBO J. *19*, 2452–2464.

Baud, C., Hodak, H., Willery, E., Drobecq, H., Locht, C., Jamin, M., and Jacob-Dubuisson, F. (2009). Role of DegP for two-partner secretion in Bordetella. Mol. Microbiol. *74*, 315–329.

Baud, C., Gutsche, I., Willery, E., de Paepe, D., Drobecq, H., Gilleron, M., Locht, C., Jamin, M., and Jacob-Dubuisson, F. (2011). Membrane-associated DegP in Bordetella chaperones a repeat-rich secretory protein. Mol. Microbiol. *80*, 1625–1636.

Baud, C., Guérin, J., Petit, E., Lesne, E., Dupré, E., Locht, C., and Jacob-Dubuisson, F. (2014). Translocation path of a substrate protein through its Omp85 transporter. Nat. Commun. *5*, 5271.

Bauer, B.W., Shemesh, T., Chen, Y., and Rapoport, T.A. (2014). A "push and slide" mechanism allows sequence-insensitive translocation of secretory proteins by the SecA ATPase. Cell *157*, 1416–1429.

Bennett, K.L., Kussmann, M., Björk, P., Godzwon, M., Mikkelsen, M., Sørensen, P., and Roepstorff, P. (2000). Chemical cross-linking with thiol-cleavable reagents combined with differential mass spectrometric peptide mapping--a novel approach to assess intermolecular protein contacts. Protein Sci. Publ. Protein Soc. *9*, 1503–1518.

Benson, T.E., Prince, D.B., Mutchler, V.T., Curry, K.A., Ho, A.M., Sarver, R.W., Hagadorn, J.C., Choi, G.H., and Garlick, R.L. (2002). X-ray crystal structure of Staphylococcus aureus FemA. Struct. Lond. Engl. 1993 *10*, 1107–1115.

Berlow, R.B., Dyson, H.J., and Wright, P.E. (2015). Functional advantages of dynamic protein disorder. FEBS Lett. *589*, 2433–2440.

Bernstein, H.D. (2019). Type V Secretion in Gram-Negative Bacteria. EcoSal Plus *8*.

Bertani, B., and Ruiz, N. (2018). Function and Biogenesis of Lipopolysaccharides. EcoSal Plus *8*.

Biarrotte-Sorin, S., Maillard, A.P., Delettré, J., Sougakoff, W., Blanot, D., Blondeau, K., Hugonnet, J.-E., Mayer, C., and Arthur, M. (2003). Crystallization and preliminary X-ray analysis of Weissella viridescens FemX UDP-MurNAc-pentapeptide:l-alanine ligase. Acta Crystallogr. D Biol. Crystallogr. *59*, 1055–1057.

Biarrotte-Sorin, S., Maillard, A.P., Delettré, J., Sougakoff, W., Arthur, M., and Mayer, C. (2004). Crystal structures of Weissella viridescens FemX and its complex with UDP-MurNAc-pentapeptide: insights into FemABX family substrates recognition. Struct. Lond. Engl. 1993 *12*, 257–267.

Bieker, K.L., Phillips, G.J., and Silhavy, T.J. (1990). The sec and prl genes of Escherichia coli. J. Bioenerg. Biomembr. *22*, 291–310.

Blobel, G. (1980). Intracellular protein topogenesis. Proc. Natl. Acad. Sci. U. S. A. *77*, 1496–1500.

Blobel, G., and Dobberstein, B. (1975). Transfer of proteins across membranes. I. Presence of proteolytically processed and unprocessed nascent immunoglobulin light chains on membrane-bound ribosomes of murine myeloma. J. Cell Biol. *67*, 835–851.

Bogdanov, M., Dowhan, W., and Vitrac, H. (2014). Lipids and topological rules governing membrane protein assembly. Biochim. Biophys. Acta *1843*, 1475–1488.

Bolen, E.J., and Holloway, P.W. (1990). Quenching of tryptophan fluorescence by brominated phospholipid. Biochemistry (Mosc.) *29*, 9638–9643.

Bordignon, E., and Steinhoff, H.-J. (2007). Membrane Protein Structure and Dynamics Studied by Site-Directed Spin-Labeling ESR. In ESR Spectroscopy in Membrane Biophysics, M.A. Hemminga, and L.J. Berliner, eds. (Boston, MA: Springer US), pp. 129–164.

Botte, M., Zaccai, N.R., Nijeholt, J.L.À., Martin, R., Knoops, K., Papai, G., Zou, J., Deniaud, A., Karuppasamy, M., Jiang, Q., et al. (2016). A central cavity within the holo-translocon suggests a mechanism for membrane protein insertion. Sci. Rep. *6*, 38399.

Bouhss, A., Josseaume, N., Allanic, D., Crouvoisier, M., Gutmann, L., Mainardi, J.L., Mengin-Lecreulx, D., van Heijenoort, J., and Arthur, M. (2001). Identification of the UDP-MurNAc-pentapeptide:L-alanine ligase for synthesis of branched peptidoglycan precursors in Enterococcus faecalis. J. Bacteriol. *183*, 5122–5127.

Bouhss, A., Josseaume, N., Severin, A., Tabei, K., Hugonnet, J.-E., Shlaes, D., Mengin-Lecreulx, D., Van Heijenoort, J., and Arthur, M. (2002). Synthesis of the L-alanyl-L-alanine cross-bridge of Enterococcus faecalis peptidoglycan. J. Biol. Chem. *277*, 45935–45941.

Bouillot, S., Munro, P., Gallet, B., Reboud, E., Cretin, F., Golovkine, G., Schoehn, G., Attrée, I., Lemichez, E., and Huber, P. (2017). Pseudomonas aeruginosa Exolysin promotes bacterial growth in lungs, alveolar damage and bacterial dissemination. Sci. Rep. *7*, 2120.

Braun, V., and Rehn, K. (1969). Chemical characterization, spatial distribution and function of a lipoprotein (murein-lipoprotein) of the E. coli cell wall. The specific effect of trypsin on the membrane structure. Eur. J. Biochem. *10*, 426–438.

Braun, V., Günther, H., Neuss, B., and Tautz, C. (1985). Hemolytic activity of Serratia marcescens. Arch. Microbiol. *141*, 371–376.

Braun, V., Neuss, B., Ruan, Y., Schiebel, E., Schöffler, H., and Jander, G. (1987). Identification of the Serratia marcescens hemolysin determinant by cloning into Escherichia coli. J. Bacteriol. *169*, 2113–2120.

Breyton, C., Haase, W., Rapoport, T.A., Kühlbrandt, W., and Collinson, I. (2002). Three-dimensional structure of the bacterial protein-translocation complex SecYEG. Nature *418*, 662–665.

Brito, C., Cabanes, D., Sarmento Mesquita, F., and Sousa, S. (2019). Mechanisms protecting host cells against bacterial pore-forming toxins. Cell. Mol. Life Sci. CMLS *76*, 1319–1339.

Brundage, L., Hendrick, J.P., Schiebel, E., Driessen, A.J., and Wickner, W. (1990). The purified E. coli integral membrane protein SecY/E is sufficient for reconstitution of SecA-dependent precursor protein translocation. Cell *62*, 649–657.

Brunner, J. (1989). Photochemical labeling of apolar phase of membranes. Methods Enzymol. *172*, 628–687.

Byrd, A.L., Belkaid, Y., and Segre, J.A. (2018). The human skin microbiome. Nat. Rev. Microbiol. *16*, 143–155.

Cabantous, S., Terwilliger, T.C., and Waldo, G.S. (2005). Protein tagging and detection with engineered self-assembling fragments of green fluorescent protein. Nat. Biotechnol. *23*, 102–107.

Campagne, S., Damberger, F.F., Kaczmarczyk, A., Francez-Charlot, A., Allain, F.H.-T., and Vorholt, J.A. (2012). Structural basis for sigma factor mimicry in the general stress response of Alphaproteobacteria. Proc. Natl. Acad. Sci. U. S. A. *109*, E1405-1414.

Campbell, E.A., Muzzin, O., Chlenov, M., Sun, J.L., Olson, C.A., Weinman, O., Trester-Zedlitz, M.L., and Darst, S.A. (2002). Structure of the bacterial RNA polymerase promoter specificity sigma subunit. Mol. Cell *9*, 527–539.

Campbell, E.A., Tupy, J.L., Gruber, T.M., Wang, S., Sharp, M.M., Gross, C.A., and Darst, S.A. (2003). Crystal structure of Escherichia coli sigmaE with the cytoplasmic domain of its anti-sigma RseA. Mol. Cell *11*, 1067–1078.

Campbell, E.A., Greenwell, R., Anthony, J.R., Wang, S., Lim, L., Das, K., Sofia, H.J., Donohue, T.J., and Darst, S.A. (2007). A conserved structural module regulates transcriptional responses to diverse stress signals in bacteria. Mol. Cell *27*, 793–805.

Campbell, E.A., Westblade, L.F., and Darst, S.A. (2008). Regulation of bacterial RNA polymerase sigma factor activity: a structural perspective. Curr. Opin. Microbiol. *11*, 121–127.

Cannon, K.S., Or, E., Clemons, W.M., Shibata, Y., and Rapoport, T.A. (2005). Disulfide bridge formation between SecY and a translocating polypeptide localizes the translocation pore to the center of SecY. J. Cell Biol. *169*, 219–225.

Capra, E.J., and Laub, M.T. (2012). Evolution of two-component signal transduction systems. Annu. Rev. Microbiol. *66*, 325–347.

Catipovic, M.A., Bauer, B.W., Loparo, J.J., and Rapoport, T.A. (2019). Protein translocation by the SecA ATPase occurs by a power-stroke mechanism. EMBO J.

Caveney, N.A., Li, F.K., and Strynadka, N.C. (2018). Enzyme structures of the bacterial peptidoglycan and wall teichoic acid biogenesis pathways. Curr. Opin. Struct. Biol. *53*, 45–58.

Cerdà-Costa, N., and Gomis-Rüth, F.X. (2014). Architecture and function of metallopeptidase catalytic domains. Protein Sci. Publ. Protein Soc. *23*, 123–144.

Chen, I.-M.A., Chu, K., Palaniappan, K., Pillay, M., Ratner, A., Huang, J., Huntemann, M., Varghese, N., White, J.R., Seshadri, R., et al. (2019). IMG/M v.5.0: an integrated data management and comparative analysis system for microbial genomes and microbiomes. Nucleic Acids Res. *47*, D666–D677.

Choi, Y.J., Morel, L., Le François, T., Bourque, D., Bourget, L., Groleau, D., Massie, B., and Míguez, C.B. (2010). Novel, versatile, and tightly regulated expression system for Escherichia coli strains. Appl. Environ. Microbiol. *76*, 5058–5066.

Cianciotto, N.P., and White, R.C. (2017). Expanding Role of Type II Secretion in Bacterial Pathogenesis and Beyond. Infect. Immun. *85*.

Clantin, B., Delattre, A.-S., Rucktooa, P., Saint, N., Méli, A.C., Locht, C., Jacob-Dubuisson, F., and Villeret, V. (2007). Structure of the membrane protein FhaC: a member of the Omp85-TpsB transporter superfamily. Science *317*, 957–961.

Clare, D.K., and Saibil, H.R. (2013). ATP-driven molecular chaperone machines. Biopolymers *99*, 846–859.

Clark, P.L., and Elcock, A.H. (2016). Molecular chaperones: providing a safe place to weather a midlife protein-folding crisis. Nat. Struct. Mol. Biol. *23*, 621–623.

Collard, J.M., Provoost, A., Taghavi, S., and Mergeay, M. (1993). A new type of Alcaligenes eutrophus CH34 zinc resistance generated by mutations affecting regulation of the cnr cobalt-nickel resistance system. J. Bacteriol. *175*, 779–784.

Dal Peraro, M., and van der Goot, F.G. (2016). Pore-forming toxins: ancient, but never really out of fashion. Nat. Rev. Microbiol. *14*, 77–92.

Daughdrill, G.W., Chadsey, M.S., Karlinsey, J.E., Hughes, K.T., and Dahlquist, F.W. (1997). The C-terminal half of the anti-sigma factor, FlgM, becomes structured when bound to its target, sigma 28. Nat. Struct. Biol. *4*, 285–291.

De Buck, E., Lammertyn, E., and Anné, J. (2008). The importance of the twin-arginine translocation pathway for bacterial virulence. Trends Microbiol. *16*, 442–453.

De Keyzer, J., Van Der Does, C., and Driessen, A.J.M. (2002). Kinetic analysis of the translocation of fluorescent precursor proteins into Escherichia coli membrane vesicles. J. Biol. Chem. *277*, 46059–46065.

Delattre, A.-S., Clantin, B., Saint, N., Locht, C., Villeret, V., and Jacob-Dubuisson, F. (2010). Functional importance of a conserved sequence motif in FhaC, a prototypic member of the TpsB/Omp85 superfamily. FEBS J. *277*, 4755–4765.

Delattre, A.-S., Saint, N., Clantin, B., Willery, E., Lippens, G., Locht, C., Villeret, V., and Jacob-Dubuisson, F. (2011). Substrate recognition by the POTRA domains of TpsB transporter FhaC. Mol. Microbiol. *81*, 99–112.

Denks, K., Vogt, A., Sachelaru, I., Petriman, N.-A., Kudva, R., and Koch, H.-G. (2014). The Sec translocon mediated protein transport in prokaryotes and eukaryotes. Mol. Membr. Biol. *31*, 58–84.

Devaux, P.F. (1991). Static and dynamic lipid asymmetry in cell membranes. Biochemistry (Mosc.) *30*, 1163–1173.

Deville, K., Gold, V.A.M., Robson, A., Whitehouse, S., Sessions, R.B., Baldwin, S.A., Radford, S.E., and Collinson, I. (2011). The oligomeric state and arrangement of the active bacterial translocon. J. Biol. Chem. *286*, 4659–4669.

Di Venanzio, G., Lazzaro, M., Morales, E.S., Krapf, D., and García Véscovi, E. (2017). A pore-forming toxin enables Serratia a nonlytic egress from host cells. Cell. Microbiol. *19*.

Diepold, A., and Wagner, S. (2014). Assembly of the bacterial type III secretion machinery. FEMS Microbiol. Rev. *38*, 802–822.

Douzi, B., Filloux, A., and Voulhoux, R. (2012). On the path to uncover the bacterial type II secretion system. Philos. Trans. R. Soc. Lond. B. Biol. Sci. *367*, 1059–1072.

Drobnak, I., Braselmann, E., Chaney, J.L., Leyton, D.L., Bernstein, H.D., Lithgow, T., Luirink, J., Nataro, J.P., and Clark, P.L. (2015). Of linkers and autochaperones: an unambiguous nomenclature to identify common and uncommon themes for autotransporter secretion. Mol. Microbiol. *95*, 1–16.

Duché, D., Izard, J., González-Mañas, J.M., Parker, M.W., Crest, M., Chartier, M., and Baty, D. (1996). Membrane topology of the colicin A pore-forming domain analyzed by disulfide bond engineering. J. Biol. Chem. *271*, 15401–15406.

DuMont, A.L., and Torres, V.J. (2014). Cell targeting by the Staphylococcus aureus pore-forming toxins: it's not just about lipids. Trends Microbiol. *22*, 21–27.

Duong, F., and Wickner, W. (1997). The SecDFyajC domain of preprotein translocase controls preprotein movement by regulating SecA membrane cycling. EMBO J. *16*, 4871–4879.

Duong, F., and Wickner, W. (1999). The PrlA and PrlG phenotypes are caused by a loosened association among the translocase SecYEG subunits. EMBO J. *18*, 3263–3270.

Durrer, P., Gaudin, Y., Ruigrok, R.W., Graf, R., and Brunner, J. (1995). Photolabeling identifies a putative fusion domain in the envelope glycoprotein of rabies and vesicular stomatitis viruses. J. Biol. Chem. *270*, 17575–17581.

Dwyer, R.S., Malinverni, J.C., Boyd, D., Beckwith, J., and Silhavy, T.J. (2014). Folding LacZ in the periplasm of Escherichia coli. J. Bacteriol. *196*, 3343–3350.

Dyda, F., Klein, D.C., and Hickman, A.B. (2000). GCN5-related N-acetyltransferases: a structural overview. Annu. Rev. Biophys. Biomol. Struct. *29*, 81–103.

Economou, A., and Wickner, W. (1994). SecA promotes preprotein translocation by undergoing ATP-driven cycles of membrane insertion and deinsertion. Cell *78*, 835–843.

Elsen, S., Huber, P., Bouillot, S., Couté, Y., Fournier, P., Dubois, Y., Timsit, J.-F., Maurin, M., and Attrée, I. (2014). A type III secretion negative clinical strain of Pseudomonas aeruginosa employs a two-partner secreted exolysin to induce hemorrhagic pneumonia. Cell Host Microbe *15*, 164–176.

Erlandson, K.J., Or, E., Osborne, A.R., and Rapoport, T.A. (2008). Analysis of polypeptide movement in the SecY channel during SecA-mediated protein translocation. J. Biol. Chem. *283*, 15709–15715.

Errington, J., Mickiewicz, K., Kawai, Y., and Wu, L.J. (2016). L-form bacteria, chronic diseases and the origins of life. Philos. Trans. R. Soc. Lond. B. Biol. Sci. *371*.

van der Es, D., Hogendorf, W.F.J., Overkleeft, H.S., van der Marel, G.A., and Codée, J.D.C. (2017). Teichoic acids: synthesis and applications. Chem. Soc. Rev. *46*, 1464–1482.

Facey, S.J., and Kuhn, A. (2010). Biogenesis of bacterial inner-membrane proteins. Cell. Mol. Life Sci. CMLS *67*, 2343–2362.

Fan, E., Fiedler, S., Jacob-Dubuisson, F., and Müller, M. (2012). Two-partner secretion of gram-negative bacteria: a single β-barrel protein enables transport across the outer membrane. J. Biol. Chem. *287*, 2591–2599.

Faudry, E., Perdu, C., and Attrée, I. (2013). Pore formation by T3SS translocators: liposome leakage assay. Methods Mol. Biol. Clifton NJ *966*, 173–185.

Feklistov, A., and Darst, S.A. (2011). Structural basis for promoter-10 element recognition by the bacterial RNA polymerase σ subunit. Cell *147*, 1257–1269.

Filipe, S.R., Severina, E., and Tomasz, A. (2001). The role of murMN operon in penicillin resistance and antibiotic tolerance of Streptococcus pneumoniae. Microb. Drug Resist. Larchmt. N *7*, 303–316.

Finn, R.D., Bateman, A., Clements, J., Coggill, P., Eberhardt, R.Y., Eddy, S.R., Heger, A., Hetherington, K., Holm, L., Mistry, J., et al. (2014). Pfam: the protein families database. Nucleic Acids Res. *42*, D222-230.

Fisher, J.F., and Mobashery, S. (2016). Endless Resistance. Endless Antibiotics? MedChemComm *7*, 37–49.

Fonvielle, M., Li de La Sierra-Gallay, I., El-Sagheer, A.H., Lecerf, M., Patin, D., Mellal, D., Mayer, C., Blanot, D., Gale, N., Brown, T., et al. (2013). The structure of FemX(Wv) in complex with a peptidyl-RNA conjugate: mechanism of aminoacyl transfer from Ala-tRNA(Ala) to peptidoglycan precursors. Angew. Chem. Int. Ed Engl. *52*, 7278–7281.

Francez-Charlot, A., Frunzke, J., Reichen, C., Ebneter, J.Z., Gourion, B., and Vorholt, J.A. (2009). Sigma factor mimicry involved in regulation of general stress response. Proc. Natl. Acad. Sci. U. S. A. *106*, 3467–3472.

Freschi, L., Vincent, A.T., Jeukens, J., Emond-Rheault, J.-G., Kukavica-Ibrulj, I., Dupont, M.-J., Charette, S.J., Boyle, B., and Levesque, R.C. (2019). The Pseudomonas aeruginosa Pan-Genome Provides New Insights on Its Population Structure, Horizontal Gene Transfer, and Pathogenicity. Genome Biol. Evol. *11*, 109–120.

Gan, L., Chen, S., and Jensen, G.J. (2008). Molecular organization of Gram-negative peptidoglycan. Proc. Natl. Acad. Sci. U. S. A. *105*, 18953–18957.

Gensollen, T., Iyer, S.S., Kasper, D.L., and Blumberg, R.S. (2016). How colonization by microbiota in early life shapes the immune system. Science *352*, 539–544.

Geszvain, K., Gruber, T.M., Mooney, R.A., Gross, C.A., and Landick, R. (2004). A hydrophobic patch on the flap-tip helix of E.coli RNA polymerase mediates sigma(70) region 4 function. J. Mol. Biol. *343*, 569–587.

Gimenez, M.R., Chandra, G., Van Overvelt, P., Voulhoux, R., Bleves, S., and Ize, B. (2018). Genome wide identification and experimental validation of Pseudomonas aeruginosa Tat substrates. Sci. Rep. *8*, 11950.

Goemans, C., Denoncin, K., and Collet, J.-F. (2014). Folding mechanisms of periplasmic proteins. Biochim. Biophys. Acta *1843*, 1517–1528.

Gold, V.A.M., Robson, A., Bao, H., Romantsov, T., Duong, F., and Collinson, I. (2010). The action of cardiolipin on the bacterial translocon. Proc. Natl. Acad. Sci. U. S. A. *107*, 10044–10049.

Grass, G., Grosse, C., and Nies, D.H. (2000). Regulation of the cnr cobalt and nickel resistance determinant from Ralstonia sp. strain CH34. J. Bacteriol. *182*, 1390–1398.

Grass, G., Fricke, B., and Nies, D.H. (2005). Control of expression of a periplasmic nickel efflux pump by periplasmic nickel concentrations. Biometals Int. J. Role Met. Ions Biol. Biochem. Med. *18*, 437–448.

Greene, N.G., Fumeaux, C., and Bernhardt, T.G. (2018). Conserved mechanism of cell-wall synthase regulation revealed by the identification of a new PBP activator in Pseudomonas aeruginosa. Proc. Natl. Acad. Sci. U. S. A. *115*, 3150–3155.

Grijpstra, J., Arenas, J., Rutten, L., and Tommassen, J. (2013). Autotransporter secretion: varying on a theme. Res. Microbiol. *164*, 562–582.

Grosse, C., Anton, A., Hoffmann, T., Franke, S., Schleuder, G., and Nies, D.H. (2004). Identification of a regulatory pathway that controls the heavy-metal resistance system Czc via promoter czcNp in Ralstonia metallidurans. Arch. Microbiol. *182*, 109–118.

Grosse, C., Friedrich, S., and Nies, D.H. (2007). Contribution of extracytoplasmic function sigma factors to transition metal homeostasis in Cupriavidus metallidurans strain CH34. J. Mol. Microbiol. Biotechnol. *12*, 227–240.

Gruber, T.M., and Gross, C.A. (2003). Multiple sigma subunits and the partitioning of bacterial transcription space. Annu. Rev. Microbiol. *57*, 441–466.

Guérin, J., Baud, C., Touati, N., Saint, N., Willery, E., Locht, C., Vezin, H., and Jacob-Dubuisson, F. (2014). Conformational dynamics of protein transporter FhaC: large-scale motions of plug helix. Mol. Microbiol. *92*, 1164–1176.

Guérin, J., Saint, N., Baud, C., Meli, A.C., Etienne, E., Locht, C., Vezin, H., and Jacob-Dubuisson, F. (2015). Dynamic interplay of membrane-proximal POTRA domain and conserved loop L6 in Omp85 transporter FhaC. Mol. Microbiol. *98*, 490–501.

Guérin, J., Bigot, S., Schneider, R., Buchanan, S.K., and Jacob-Dubuisson, F. (2017). Two-Partner Secretion: Combining Efficiency and Simplicity in the Secretion of Large Proteins for Bacteria-Host and Bacteria-Bacteria Interactions. Front. Cell. Infect. Microbiol. *7*, 148.

Guzman, L.M., Belin, D., Carson, M.J., and Beckwith, J. (1995). Tight regulation, modulation, and high-level expression by vectors containing the arabinose PBAD promoter. J. Bacteriol. *177*, 4121–4130.

Hagan, C.L., Kim, S., and Kahne, D. (2010). Reconstitution of outer membrane protein assembly from purified components. Science *328*, 890–892.

Hakenbeck, R. (2001). Detection of Low Affinity Penicillin-Binding Protein Variants in Streptococcus pneumoniae. Methods Mol. Med. *48*, 265–271.

Hamsanathan, S., and Musser, S.M. (2018). The Tat protein transport system: intriguing questions and conundrums. FEMS Microbiol. Lett. *365*.

Harris, C.R., and Silhavy, T.J. (1999). Mapping an interface of SecY (PrlA) and SecE (PrlG) by using synthetic phenotypes and in vivo cross-linking. J. Bacteriol. *181*, 3438–3444.

Hegde, S.S., and Blanchard, J.S. (2003). Kinetic and mechanistic characterization of recombinant Lactobacillus viridescens FemX (UDP-N-acetylmuramoyl pentapeptide-lysine N6-alanyltransferase). J. Biol. Chem. *278*, 22861–22867.

Hegde, S.S., and Shrader, T.E. (2001). FemABX family members are novel nonribosomal peptidyltransferases and important pathogen-specific drug targets. J. Biol. Chem. *276*, 6998–7003.

Heinz, E., and Lithgow, T. (2014). A comprehensive analysis of the Omp85/TpsB protein superfamily structural diversity, taxonomic occurrence, and evolution. Front. Microbiol. *5*, 370.

Herrou, J., Rotskoff, G., Luo, Y., Roux, B., and Crosson, S. (2012). Structural basis of a protein partner switch that regulates the general stress response of α-proteobacteria. Proc. Natl. Acad. Sci. U. S. A. *109*, E1415-1423.

Hertle, R. (2002). Serratia marcescens hemolysin (ShlA) binds artificial membranes and forms pores in a receptor-independent manner. J. Membr. Biol. *189*, 1–14.

Hertle, R., Brutsche, S., Groeger, W., Hobbie, S., Koch, W., Könninger, U., and Braun, V. (1997). Specific phosphatidylethanolamine dependence of Serratia marcescens cytotoxin activity. Mol. Microbiol. *26*, 853–865.

Hertle, R., Hilger, M., Weingardt-Kocher, S., and Walev, I. (1999). Cytotoxic action of Serratia marcescens hemolysin on human epithelial cells. Infect. Immun. *67*, 817–825.

Hertle, R., Süssmuth, R., Braun, V., and Jung, G. (2000). Two-step fast protein liquid chromatographic purification of the Serratia marcescens hemolysin and peptide mapping with mass spectrometry. J. Chromatogr. B. Biomed. Sci. App. *737*, 13–23.

Hilger, M., and Braun, V. (1995). Superlytic hemolysin mutants of Serratia marcescens. J. Bacteriol. *177*, 7202–7209.

Hilker, R., Munder, A., Klockgether, J., Losada, P.M., Chouvarine, P., Cramer, N., Davenport, C.F., Dethlefsen, S., Fischer, S., Peng, H., et al. (2015). Interclonal gradient of virulence in the Pseudomonas aeruginosa pangenome from disease and environment. Environ. Microbiol. *17*, 29–46.

Hodak, H., Clantin, B., Willery, E., Villeret, V., Locht, C., and Jacob-Dubuisson, F. (2006). Secretion signal of the filamentous haemagglutinin, a model two-partner secretion substrate. Mol. Microbiol. *61*, 368–382.

Hoffman, C., Eby, J., Gray, M., Heath Damron, F., Melvin, J., Cotter, P., and Hewlett, E. (2017). Bordetella adenylate cyclase toxin interacts with filamentous haemagglutinin to inhibit biofilm formation in vitro. Mol. Microbiol. *103*, 214–228.

Höltje, J.V. (1998). Growth of the stress-bearing and shape-maintaining murein sacculus of Escherichia coli. Microbiol. Mol. Biol. Rev. MMBR *62*, 181–203.

Huber, P., Basso, P., Reboud, E., and Attrée, I. (2016). Pseudomonas aeruginosa renews its virulence factors. Environ. Microbiol. Rep. *8*, 564–571.

Hughes, K.T., and Mathee, K. (1998). The anti-sigma factors. Annu. Rev. Microbiol. *52*, 231–286.

Hugonnet, J.-E., Mengin-Lecreulx, D., Monton, A., den Blaauwen, T., Carbonnelle, E., Veckerlé, C., Brun, Y.V., van Nieuwenhze, M., Bouchier, C., Tu, K., et al. (2016). Factors essential for L,D-transpeptidase-mediated peptidoglycan cross-linking and β-lactam resistance in Escherichia coli. ELife *5*.

Ieva, R., and Bernstein, H.D. (2009). Interaction of an autotransporter passenger domain with BamA during its translocation across the bacterial outer membrane. Proc. Natl. Acad. Sci. U. S. A. *106*, 19120–19125.

Ikigai, H., Akatsuka, A., Tsujiyama, H., Nakae, T., and Shimamura, T. (1996). Mechanism of membrane damage by El Tor hemolysin of Vibrio cholerae O1. Infect. Immun. *64*, 2968–2973.

Jacob-Dubuisson, F., Locht, C., and Antoine, R. (2001). Two-partner secretion in Gram-negative bacteria: a thrifty, specific pathway for large virulence proteins. Mol. Microbiol. *40*, 306–313.

Jacob-Dubuisson, F., Villeret, V., Clantin, B., Delattre, A.-S., and Saint, N. (2009). First structural insights into the TpsB/Omp85 superfamily. Biol. Chem. *390*, 675–684.

Jacob-Dubuisson, F., Guérin, J., Baelen, S., and Clantin, B. (2013). Two-partner secretion: as simple as it sounds? Res. Microbiol. *164*, 583–595.

Jacob-Dubuisson, F., Mechaly, A., Betton, J.-M., and Antoine, R. (2018). Structural insights into the signalling mechanisms of two-component systems. Nat. Rev. Microbiol. *16*, 585–593.

Jacobitz, A.W., Kattke, M.D., Wereszczynski, J., and Clubb, R.T. (2017). Sortase Transpeptidases: Structural Biology and Catalytic Mechanism. Adv. Protein Chem. Struct. Biol. *109*, 223–264.

Jain, S., and Goldberg, M.B. (2007). Requirement for YaeT in the outer membrane assembly of autotransporter proteins. J. Bacteriol. *189*, 5393–5398.

Janssen, P.J., Van Houdt, R., Moors, H., Monsieurs, P., Morin, N., Michaux, A., Benotmane, M.A., Leys, N., Vallaeys, T., Lapidus, A., et al. (2010). The complete genome sequence of Cupriavidus metallidurans strain CH34, a master survivalist in harsh and anthropogenic environments. PloS One *5*, e10433.

Jung, K., Fabiani, F., Hoyer, E., and Lassak, J. (2018). Bacterial transmembrane signalling systems and their engineering for biosensing. Open Biol. *8*.

Junker, M., and Clark, P.L. (2010). Slow formation of aggregation-resistant beta-sheet folding intermediates. Proteins *78*, 812–824.

Junker, M., Schuster, C.C., McDonnell, A.V., Sorg, K.A., Finn, M.C., Berger, B., and Clark, P.L. (2006). Pertactin beta-helix folding mechanism suggests common themes for the secretion and folding of autotransporter proteins. Proc. Natl. Acad. Sci. U. S. A. *103*, 4918–4923.

Junne, T., Schwede, T., Goder, V., and Spiess, M. (2006). The plug domain of yeast Sec61p is important for efficient protein translocation, but is not essential for cell viability. Mol. Biol. Cell *17*, 4063–4068.

Kaczmarczyk, A., Hochstrasser, R., Vorholt, J.A., and Francez-Charlot, A. (2014). Complex two-component signaling regulates the general stress response in Alphaproteobacteria. Proc. Natl. Acad. Sci. U. S. A. *111*, E5196-5204.

Kajava, A.V., and Steven, A.C. (2006). The turn of the screw: variations of the abundant beta-solenoid motif in passenger domains of Type V secretory proteins. J. Struct. Biol. *155*, 306–315.

Kamiyama, D., Sekine, S., Barsi-Rhyne, B., Hu, J., Chen, B., Gilbert, L.A., Ishikawa, H., Leonetti, M.D., Marshall, W.F., Weissman, J.S., et al. (2016). Versatile protein tagging in cells with split fluorescent protein. Nat. Commun. *7*, 11046.

Kanehisa, M., Sato, Y., Kawashima, M., Furumichi, M., and Tanabe, M. (2016). KEGG as a reference resource for gene and protein annotation. Nucleic Acids Res. *44*, D457-462.

Katoh, K., Rozewicki, J., and Yamada, K.D. (2017). MAFFT online service: multiple sequence alignment, interactive sequence choice and visualization. Brief. Bioinform.

Kawai, Y., Mercier, R., and Errington, J. (2014). Bacterial cell morphogenesis does not require a preexisting template structure. Curr. Biol. CB *24*, 863–867.

Kennedy, L., DeAngelis, P.L., and Glabe, C.G. (1989). Analysis of the membrane-interacting domain of the sea urchin sperm adhesive protein bindin. Biochemistry (Mosc.) *28*, 9153–9158.

Klauser, T., Pohlner, J., and Meyer, T.F. (1993). The secretion pathway of IgA protease-type proteins in gram-negative bacteria. BioEssays News Rev. Mol. Cell. Dev. Biol. *15*, 799–805.

Klockgether, J., and Tümmler, B. (2017). Recent advances in understanding Pseudomonas aeruginosa as a pathogen. F1000Research *6*, 1261.

König, W., Faltin, Y., Scheffer, J., Schöffler, H., and Braun, V. (1987). Role of cell-bound hemolysin as a pathogenicity factor for Serratia infections. Infect. Immun. *55*, 2554–2561.

Konovalova, A., Kahne, D.E., and Silhavy, T.J. (2017). Outer Membrane Biogenesis. Annu. Rev. Microbiol. *71*, 539–556.

Kopp, U., Roos, M., Wecke, J., and Labischinski, H. (1996). Staphylococcal peptidoglycan interpeptide bridge biosynthesis: a novel antistaphylococcal target? Microb. Drug Resist. Larchmt. N *2*, 29–41.

Krojer, T., Pangerl, K., Kurt, J., Sawa, J., Stingl, C., Mechtler, K., Huber, R., Ehrmann, M., and Clausen, T. (2008a). Interplay of PDZ and protease domain of DegP ensures efficient elimination of misfolded proteins. Proc. Natl. Acad. Sci. U. S. A. *105*, 7702–7707.

Krojer, T., Sawa, J., Schäfer, E., Saibil, H.R., Ehrmann, M., and Clausen, T. (2008b). Structural basis for the regulated protease and chaperone function of DegP. Nature *453*, 885–890.

Kuhn, A., Koch, H.-G., and Dalbey, R.E. (2017). Targeting and Insertion of Membrane Proteins. EcoSal Plus *7*.

Langevin, S., Vincelette, J., Bekal, S., and Gaudreau, C. (2011). First Case of Invasive Human Infection Caused by Cupriavidus metallidurans. J. Clin. Microbiol. *49*, 744–745.

Leduc, M., Fréhel, C., Siegel, E., and Van Heijenoort, J. (1989). Multilayered distribution of peptidoglycan in the periplasmic space of Escherichia coli. J. Gen. Microbiol. *135*, 1243–1254.

Leighton, T.L., Buensuceso, R.N.C., Howell, P.L., and Burrows, L.L. (2015). Biogenesis of Pseudomonas aeruginosa type IV pili and regulation of their function. Environ. Microbiol. *17*, 4148–4163.

Li, L., Park, E., Ling, J., Ingram, J., Ploegh, H., and Rapoport, T.A. (2016). Crystal structure of a substrate-engaged SecY protein-translocation channel. Nature *531*, 395–399.

Li, P., Wang, J., Zou, Y., Sun, Z., Zhang, M., Geng, Z., Xu, W., and Wang, D. (2019). Interaction of Hsp90AA1 with phospholipids stabilizes membranes under stress conditions. Biochim. Biophys. Acta Biomembr. *1861*, 457–465.

Li, W., Schulman, S., Boyd, D., Erlandson, K., Beckwith, J., and Rapoport, T.A. (2007). The plug domain of the SecY protein stabilizes the closed state of the translocation channel and maintains a membrane seal. Mol. Cell *26*, 511–521.

Liesegang, H., Lemke, K., Siddiqui, R.A., and Schlegel, H.G. (1993). Characterization of the inducible nickel and cobalt resistance determinant cnr from pMOL28 of Alcaligenes eutrophus CH34. J. Bacteriol. *175*, 767–778.

Lin, M.-H., Li, C.-C., Shu, J.-C., Chu, H.-W., Liu, C.-C., and Wu, C.-C. (2018). Exoproteome Profiling Reveals the Involvement of the Foldase PrsA in the Cell Surface Properties and Pathogenesis of Staphylococcus aureus. Proteomics *18*, e1700195.

Lonetto, M.A., Brown, K.L., Rudd, K.E., and Buttner, M.J. (1994). Analysis of the Streptomyces coelicolor sigE gene reveals the existence of a subfamily of eubacterial RNA polymerase sigma factors involved in the regulation of extracytoplasmic functions. Proc. Natl. Acad. Sci. U. S. A. *91*, 7573–7577.

Maier, T., Clantin, B., Gruss, F., Dewitte, F., Delattre, A.-S., Jacob-Dubuisson, F., Hiller, S., and Villeret, V. (2015). Conserved Omp85 lid-lock structure and substrate recognition in FhaC. Nat. Commun. *6*, 7452.

Maillard, A., Domanski, M., Brunet, P., Chaffotte, A., Guittet, E., and Gaudin, Y. (2003). Spectroscopic characterization of two peptides derived from the stem of rabies virus glycoprotein. Virus Res. *93*, 151–158.

Maillard, A.P., Biarrotte-Sorin, S., Villet, R., Mesnage, S., Bouhss, A., Sougakoff, W., Mayer, C., and Arthur, M. (2005). Structure-based site-directed mutagenesis of the UDP-MurNAc-pentapeptide-binding cavity of the FemX alanyl transferase from Weissella viridescens. J. Bacteriol. *187*, 3833–3838.

Maillard, A.P., Lalani, S., Silva, F., Belin, D., and Duong, F. (2007). Deregulation of the SecYEG translocation channel upon removal of the plug domain. J. Biol. Chem. *282*, 1281–1287.

Maillard, A.P., Girard, E., Ziani, W., Petit-Härtlein, I., Kahn, R., and Covès, J. (2014). The crystal structure of the anti-σ factor CnrY in complex with the σ factor CnrH shows a new structural class of anti-σ factors targeting extracytoplasmic function σ factors. J. Mol. Biol. *426*, 2313–2327.

Mainardi, J.-L., Villet, R., Bugg, T.D., Mayer, C., and Arthur, M. (2008). Evolution of peptidoglycan biosynthesis under the selective pressure of antibiotics in Gram-positive bacteria. FEMS Microbiol. Rev. *32*, 386–408.

Malinverni, J.C., and Silhavy, T.J. (2009). An ABC transport system that maintains lipid asymmetry in the gram-negative outer membrane. Proc. Natl. Acad. Sci. U. S. A. *106*, 8009–8014.

Man, W.H., de Steenhuijsen Piters, W.A.A., and Bogaert, D. (2017). The microbiota of the respiratory tract: gatekeeper to respiratory health. Nat. Rev. Microbiol. *15*, 259–270.

Manzi, L., Barrow, A.S., Scott, D., Layfield, R., Wright, T.G., Moses, J.E., and Oldham, N.J. (2016). Carbene footprinting accurately maps binding sites in protein-ligand and protein-protein interactions. Nat. Commun. *7*, 13288.

Manzi, L., Barrow, A.S., Hopper, J.T.S., Kaminska, R., Kleanthous, C., Robinson, C.V., Moses, J.E., and Oldham, N.J. (2017). Carbene Footprinting Reveals Binding Interfaces of a Multimeric Membrane-Spanning Protein. Angew. Chem. Int. Ed Engl. *56*, 14873–14877.

Markosyan, R.M., Melikyan, G.B., and Cohen, F.S. (2001). Evolution of intermediates of influenza virus hemagglutinin-mediated fusion revealed by kinetic measurements of pore formation. Biophys. J. *80*, 812–821.

Martoglio, B., Hofmann, M.W., Brunner, J., and Dobberstein, B. (1995). The protein-conducting channel in the membrane of the endoplasmic reticulum is open laterally toward the lipid bilayer. Cell *81*, 207–214.

Mas, G., and Hiller, S. (2018). Conformational plasticity of molecular chaperones involved in periplasmic and outer membrane protein folding. FEMS Microbiol. Lett. *365*.

Mascher, T. (2013). Signaling diversity and evolution of extracytoplasmic function (ECF) σ factors. Curr. Opin. Microbiol. *16*, 148–155.

Mascher, T., Helmann, J.D., and Unden, G. (2006). Stimulus perception in bacterial signal-transducing histidine kinases. Microbiol. Mol. Biol. Rev. MMBR *70*, 910–938.

da Mata Madeira, P.V., Zouhir, S., Basso, P., Neves, D., Laubier, A., Salacha, R., Bleves, S., Faudry, E., Contreras-Martel, C., and Dessen, A. (2016). Structural Basis of Lipid Targeting and Destruction by the Type V Secretion System of Pseudomonas aeruginosa. J. Mol. Biol. *428*, 1790–1803.

Matias, V.R.F., and Beveridge, T.J. (2006). Native cell wall organization shown by cryo-electron microscopy confirms the existence of a periplasmic space in Staphylococcus aureus. J. Bacteriol. *188*, 1011–1021.

Matias, V.R.F., and Beveridge, T.J. (2008). Lipoteichoic acid is a major component of the Bacillus subtilis periplasm. J. Bacteriol. *190*, 7414–7418.

May, K.L., and Silhavy, T.J. (2017). Making a membrane on the other side of the wall. Biochim. Biophys. Acta Mol. Cell Biol. Lipids *1862*, 1386–1393.

McCarthy, R.R., Mazon-Moya, M.J., Moscoso, J.A., Hao, Y., Lam, J.S., Bordi, C., Mostowy, S., and Filloux, A. (2017). Cyclic-di-GMP regulates lipopolysaccharide modification and contributes to Pseudomonas aeruginosa immune evasion. Nat. Microbiol. *2*, 17027.

Méli, A.C., Hodak, H., Clantin, B., Locht, C., Molle, G., Jacob-Dubuisson, F., and Saint, N. (2006). Channel properties of TpsB transporter FhaC point to two functional domains with a C-terminal protein-conducting pore. J. Biol. Chem. *281*, 158–166.

Meltzer, M., Hasenbein, S., Hauske, P., Kucz, N., Merdanovic, M., Grau, S., Beil, A., Jones, D., Krojer, T., Clausen, T., et al. (2008). Allosteric activation of HtrA protease DegP by stress signals during bacterial protein quality control. Angew. Chem. Int. Ed Engl. *47*, 1332–1334.

Mergeay, M., Nies, D., Schlegel, H.G., Gerits, J., Charles, P., and Van Gijsegem, F. (1985). Alcaligenes eutrophus CH34 is a facultative chemolithotroph with plasmid-bound resistance to heavy metals. J. Bacteriol. *162*, 328–334.

Miller, M.L., Soufi, B., Jers, C., Blom, N., Macek, B., and Mijakovic, I. (2009). NetPhosBac - a predictor for Ser/Thr phosphorylation sites in bacterial proteins. Proteomics *9*, 116–125.

Monchy, S., Benotmane, M.A., Janssen, P., Vallaeys, T., Taghavi, S., van der Lelie, D., and Mergeay, M. (2007). Plasmids pMOL28 and pMOL30 of Cupriavidus metallidurans are specialized in the maximal viable response to heavy metals. J. Bacteriol. *189*, 7417–7425.

Moradali, M.F., Ghods, S., and Rehm, B.H.A. (2017). Pseudomonas aeruginosa Lifestyle: A Paradigm for Adaptation, Survival, and Persistence. Front. Cell. Infect. Microbiol. *7*, 39.

Morris, D.M., and Jensen, G.J. (2008). Toward a biomechanical understanding of whole bacterial cells. Annu. Rev. Biochem. *77*, 583–613.

Nanda, J.S., and Lorsch, J.R. (2014a). Labeling a protein with fluorophores using NHS ester derivitization. Methods Enzymol. *536*, 87–94.

Nanda, J.S., and Lorsch, J.R. (2014b). Labeling of a protein with fluorophores using maleimide derivitization. Methods Enzymol. *536*, 79–86.

Nash, Z.M., and Cotter, P.A. (2019). Bordetella Filamentous Hemagglutinin, a Model for the Two-Partner Secretion Pathway. Microbiol. Spectr. *7*.

Nguyen, V.T., Higuchi, H., and Kamio, Y. (2002). Controlling pore assembly of staphylococcal gamma-haemolysin by low temperature and by disulphide bond formation in double-cysteine LukF mutants. Mol. Microbiol. *45*, 1485–1498.

Nicolson, G.L. (2014). The Fluid-Mosaic Model of Membrane Structure: still relevant to understanding the structure, function and dynamics of biological membranes after more than 40 years. Biochim. Biophys. Acta *1838*, 1451–1466.

Nies, A., Nies, D.H., and Silver, S. (1989). Cloning and expression of plasmid genes encoding resistances to chromate and cobalt in Alcaligenes eutrophus. J. Bacteriol. *171*, 5065–5070.

Nikolaidis, I., Favini-Stabile, S., and Dessen, A. (2014). Resistance to antibiotics targeted to the bacterial cell wall. Protein Sci. Publ. Protein Soc. *23*, 243–259.

Nishiyama, K., Hanada, M., and Tokuda, H. (1994). Disruption of the gene encoding p12 (SecG) reveals the direct involvement and important function of SecG in the protein translocation of Escherichia coli at low temperature. EMBO J. *13*, 3272–3277.

Nivaskumar, M., and Francetic, O. (2014). Type II secretion system: a magic beanstalk or a protein escalator. Biochim. Biophys. Acta *1843*, 1568–1577.

Noinaj, N., Guillier, M., Barnard, T.J., and Buchanan, S.K. (2010). TonB-dependent transporters: regulation, structure, and function. Annu. Rev. Microbiol. *64*, 43–60.

Noinaj, N., Gumbart, J.C., and Buchanan, S.K. (2017). The β-barrel assembly machinery in motion. Nat. Rev. Microbiol. *15*, 197–204.

Norell, D., Heuck, A., Tran-Thi, T.-A., Götzke, H., Jacob-Dubuisson, F., Clausen, T., Daley, D.O., Braun, V., Müller, M., and Fan, E. (2014). Versatile in vitro system to study translocation and functional integration of bacterial outer membrane proteins. Nat. Commun. *5*, 5396.

Nouwen, N., de Kruijff, B., and Tommassen, J. (1996). prlA suppressors in Escherichia coli relieve the proton electrochemical gradient dependency of translocation of wild-type precursors. Proc. Natl. Acad. Sci. U. S. A. *93*, 5953–5957.

Oberhettinger, P., Schütz, M., Leo, J.C., Heinz, N., Berger, J., Autenrieth, I.B., and Linke, D. (2012). Intimin and invasin export their C-terminus to the bacterial cell surface using an inverse mechanism compared to classical autotransport. PloS One *7*, e47069.

Ondraczek, R., Hobbie, S., and Braun, V. (1992). In vitro activation of the Serratia marcescens hemolysin through modification and complementation. J. Bacteriol. *174*, 5086–5094.

Osborne, R.S., and Silhavy, T.J. (1993). PrlA suppressor mutations cluster in regions corresponding to three distinct topological domains. EMBO J. *12*, 3391–3398.

Otten, C., Brilli, M., Vollmer, W., Viollier, P.H., and Salje, J. (2018). Peptidoglycan in obligate intracellular bacteria. Mol. Microbiol. *107*, 142–163.

Ovchynnikova, E., Aglialoro, F., von Lindern, M., and van den Akker, E. (2018). The Shape Shifting Story of Reticulocyte Maturation. Front. Physiol. *9*, 829.

Owji, H., Nezafat, N., Negahdaripour, M., Hajiebrahimi, A., and Ghasemi, Y. (2018). A comprehensive review of signal peptides: Structure, roles, and applications. Eur. J. Cell Biol. *97*, 422–441.

Palmer, T., and Berks, B.C. (2012). The twin-arginine translocation (Tat) protein export pathway. Nat. Rev. Microbiol. *10*, 483–496.

Park, E., Ménétret, J.-F., Gumbart, J.C., Ludtke, S.J., Li, W., Whynot, A., Rapoport, T.A., and Akey, C.W. (2014). Structure of the SecY channel during initiation of protein translocation. Nature *506*, 102–106.

Patikoglou, G.A., Westblade, L.F., Campbell, E.A., Lamour, V., Lane, W.J., and Darst, S.A. (2007). Crystal structure of the Escherichia coli regulator of sigma70, Rsd, in complex with sigma70 domain 4. J. Mol. Biol. *372*, 649–659.

Peters, E.A., Schatz, P.J., Johnson, S.S., and Dower, W.J. (1994). Membrane insertion defects caused by positive charges in the early mature region of protein pIII of filamentous phage fd can be corrected by prlA suppressors. J. Bacteriol. *176*, 4296–4305.

Pfefferkorn, C.M., Walker, R.L., He, Y., Gruschus, J.M., and Lee, J.C. (2015). Tryptophan probes reveal residue-specific phospholipid interactions of apolipoprotein C-III. Biochim. Biophys. Acta *1848*, 2821–2828.

Plapp, R., and Strominger, J.L. (1970a). Biosynthesis of the peptidoglycan of bacterial cell walls. 18. Purification and properties of L-alanyl transfer ribonucleic acid-uridine diphosphate-N-acetylmuramyl-pentapeptide transferase from Lactobacillus viridescens. J. Biol. Chem. *245*, 3675–3682.

Plapp, R., and Strominger, J.L. (1970b). Biosynthesis of the peptidoglycan of bacterial cell walls. XVII. Biosynthesis of peptidoglycan and of interpeptide bridges in Lactobacillus viridescens. J. Biol. Chem. *245*, 3667–3674.

Plath, K., Mothes, W., Wilkinson, B.M., Stirling, C.J., and Rapoport, T.A. (1998). Signal sequence recognition in posttranslational protein transport across the yeast ER membrane. Cell *94*, 795–807.

du Plessis, D.J.F., Berrelkamp, G., Nouwen, N., and Driessen, A.J.M. (2009). The lateral gate of SecYEG opens during protein translocation. J. Biol. Chem. *284*, 15805–15814.

Pompidor, G., Maillard, A.P., Girard, E., Gambarelli, S., Kahn, R., and Covès, J. (2008). X-ray structure of the metal-sensor CnrX in both the apo- and copper-bound forms. FEBS Lett. *582*, 3954–3958.

Pompidor, G., Girard, E., Maillard, A., Ramella-Pairin, S., Bersch, B., Kahn, R., and Covès, J. (2009). Biostructural analysis of the metal-sensor domain of CnrX from Cupriavidus metallidurans CH34. Antonie Van Leeuwenhoek *96*, 141–148.

Poole, K., Schiebel, E., and Braun, V. (1988). Molecular characterization of the hemolysin determinant of Serratia marcescens. J. Bacteriol. *170*, 3177–3188.

Pramanik, A., Könninger, U., Selvam, A., and Braun, V. (2014). Secretion and activation of the Serratia marcescens hemolysin by structurally defined ShlB mutants. Int. J. Med. Microbiol. IJMM *304*, 351–359.

Prinz, W.A., Boyd, D.H., Ehrmann, M., and Beckwith, J. (1998). The protein translocation apparatus contributes to determining the topology of an integral membrane protein in Escherichia coli. J. Biol. Chem. *273*, 8419–8424.

Promdonkoy, B., and Ellar, D.J. (2000). Membrane pore architecture of a cytolytic toxin from Bacillus thuringiensis. Biochem. J. *350 Pt 1*, 275–282.

Pulagam, L.P., and Steinhoff, H.-J. (2013). Acidic pH-induced membrane insertion of colicin A into E. coli natural lipids probed by site-directed spin labeling. J. Mol. Biol. *425*, 1782–1794.

Puziss, J.W., Strobel, S.M., and Bassford, P.J. (1992). Export of maltose-binding protein species with altered charge distribution surrounding the signal peptide hydrophobic core in Escherichia coli cells harboring prl suppressor mutations. J. Bacteriol. *174*, 92–101.

ur Rahman, S., Arenas, J., Öztürk, H., Dekker, N., and van Ulsen, P. (2014). The polypeptide transport-associated (POTRA) domains of TpsB transporters determine the system specificity of two-partner secretion systems. J. Biol. Chem. *289*, 19799–19809.

Rapoport, T.A., Li, L., and Park, E. (2017). Structural and Mechanistic Insights into Protein Translocation. Annu. Rev. Cell Dev. Biol. *33*, 369–390.

Ray, A., Cot, M., Puzo, G., Gilleron, M., and Nigou, J. (2013). Bacterial cell wall macroamphiphiles: pathogen-/microbe-associated molecular patterns detected by mammalian innate immune system. Biochimie *95*, 33–42.

Reboud, E., Elsen, S., Bouillot, S., Golovkine, G., Basso, P., Jeannot, K., Attrée, I., and Huber, P. (2016). Phenotype and toxicity of the recently discovered exlA-positive Pseudomonas aeruginosa strains collected worldwide. Environ. Microbiol. *18*, 3425–3439.

Reboud, E., Bouillot, S., Patot, S., Béganton, B., Attrée, I., and Huber, P. (2017a). Pseudomonas aeruginosa ExlA and Serratia marcescens ShlA trigger cadherin cleavage by promoting calcium influx and ADAM10 activation. PLoS Pathog. *13*, e1006579.

Reboud, E., Basso, P., Maillard, A.P., Huber, P., and Attrée, I. (2017b). Exolysin Shapes the Virulence of Pseudomonas aeruginosa Clonal Outliers. Toxins *9*.

Reddington, S.C., and Howarth, M. (2015). Secrets of a covalent interaction for biomaterials and biotechnology: SpyTag and SpyCatcher. Curr. Opin. Chem. Biol. *29*, 94–99.

Reith, F., Etschmann, B., Grosse, C., Moors, H., Benotmane, M.A., Monsieurs, P., Grass, G., Doonan, C., Vogt, S., Lai, B., et al. (2009). Mechanisms of gold biomineralization in the bacterium Cupriavidus metallidurans. Proc. Natl. Acad. Sci. U. S. A. *106*, 17757–17762.

Ritzefeld, M. (2014). Sortagging: a robust and efficient chemoenzymatic ligation strategy. Chem. Weinh. Bergstr. Ger. *20*, 8516–8529.

Rohrer, S., and Berger-Bächi, B. (2003). FemABX peptidyl transferases: a link between branched-chain cell wall peptide formation and beta-lactam resistance in gram-positive cocci. Antimicrob. Agents Chemother. *47*, 837–846.

Rojas-Lopez, M., Zorgani, M.A., Kelley, L.A., Bailly, X., Kajava, A.V., Henderson, I.R., Polticelli, F., Pizza, M., Rosini, R., and Desvaux, M. (2017). Identification of the Autochaperone Domain in the Type Va Secretion System (T5aSS): Prevalent Feature of Autotransporters with a β-Helical Passenger. Front. Microbiol. *8*, 2607.

Rojko, N., and Anderluh, G. (2015). How Lipid Membranes Affect Pore Forming Toxin Activity. Acc. Chem. Res. *48*, 3073–3079.

Roman-Hernandez, G., Peterson, J.H., and Bernstein, H.D. (2014). Reconstitution of bacterial autotransporter assembly using purified components. ELife *3*, e04234.

von Rozycki, T., and Nies, D.H. (2009). Cupriavidus metallidurans: evolution of a metal-resistant bacterium. Antonie Van Leeuwenhoek *96*, 115–139.

Ruhe, Z.C., Subramanian, P., Song, K., Nguyen, J.Y., Stevens, T.A., Low, D.A., Jensen, G.J., and Hayes, C.S. (2018). Programmed Secretion Arrest and Receptor-Triggered Toxin Export during Antibacterial Contact-Dependent Growth Inhibition. Cell *175*, 921-933.e14.

Salacha, R., Kovacić, F., Brochier-Armanet, C., Wilhelm, S., Tommassen, J., Filloux, A., Voulhoux, R., and Bleves, S. (2010). The Pseudomonas aeruginosa patatin-like protein PlpD is the archetype of a novel Type V secretion system. Environ. Microbiol. *12*, 1498–1512.

Sauri, A., Soprova, Z., Wickström, D., de Gier, J.-W., Van der Schors, R.C., Smit, A.B., Jong, W.S.P., and Luirink, J. (2009). The Bam (Omp85) complex is involved in secretion of the autotransporter haemoglobin protease. Microbiol. Read. Engl. *155*, 3982–3991.

Schäffer, C., and Messner, P. (2017). Emerging facets of prokaryotic glycosylation. FEMS Microbiol. Rev. *41*, 49–91.

Scheffer, J., König, W., Braun, V., and Goebel, W. (1988). Comparison of four hemolysin-producing organisms (Escherichia coli, Serratia marcescens, Aeromonas hydrophila, and Listeria monocytogenes) for release of inflammatory mediators from various cells. J. Clin. Microbiol. *26*, 544–551.

Schiebel, E., and Braun, V. (1989). Integration of the Serratia marcescens haemolysin into human erythrocyte membranes. Mol. Microbiol. *3*, 445–453.

Schiebel, E., Schwarz, H., and Braun, V. (1989). Subcellular location and unique secretion of the hemolysin of Serratia marcescens. J. Biol. Chem. *264*, 16311–16320.

Schlame, M. (2008). Cardiolipin synthesis for the assembly of bacterial and mitochondrial membranes. J. Lipid Res. *49*, 1607–1620.

Schleifer, K.H., and Kandler, O. (1972). Peptidoglycan types of bacterial cell walls and their taxonomic implications. Bacteriol. Rev. *36*, 407–477.

Schmidt, T., and Schlegel, H.G. (1994). Combined nickel-cobalt-cadmium resistance encoded by the ncc locus of Alcaligenes xylosoxidans 31A. J. Bacteriol. *176*, 7045–7054.

Schneider, T., Senn, M.M., Berger-Bächi, B., Tossi, A., Sahl, H.-G., and Wiedemann, I. (2004). In vitro assembly of a complete, pentaglycine interpeptide bridge containing cell wall precursor (lipid II-Gly5) of Staphylococcus aureus. Mol. Microbiol. *53*, 675–685.

Schönherr, R., Tsolis, R., Focareta, T., and Braun, V. (1993). Amino acid replacements in the Serratia marcescens haemolysin ShlA define sites involved in activation and secretion. Mol. Microbiol. *9*, 1229–1237.

Schönherr, R., Hilger, M., Broer, S., Benz, R., and Braun, V. (1994). Interaction of Serratia marcescens hemolysin (ShlA) with artificial and erythrocyte membranes. Demonstration of the formation of aqueous multistate channels. Eur. J. Biochem. *223*, 655–663.

Schulze, R.J., Komar, J., Botte, M., Allen, W.J., Whitehouse, S., Gold, V.A.M., Lycklama A Nijeholt, J.A., Huard, K., Berger, I., Schaffitzel, C., et al. (2014). Membrane protein insertion and proton-motive-force-dependent secretion through the bacterial holo-translocon SecYEG-SecDF-YajC-YidC. Proc. Natl. Acad. Sci. U. S. A. *111*, 4844–4849.

Schumacher, M.A., Bush, M.J., Bibb, M.J., Ramos-León, F., Chandra, G., Zeng, W., and Buttner, M.J. (2018). The crystal structure of the RsbN-σBldN complex from Streptomyces venezuelae defines a new structural class of anti-σ factor. Nucleic Acids Res. *46*, 7405–7417.

Scotti, P.A., Urbanus, M.L., Brunner, J., de Gier, J.W., von Heijne, G., van der Does, C., Driessen, A.J., Oudega, B., and Luirink, J. (2000). YidC, the Escherichia coli homologue of mitochondrial Oxa1p, is a component of the Sec translocase. EMBO J. *19*, 542–549.

Sekiya, K., Satoh, R., Danbara, H., and Futaesaku, Y. (1993). A ring-shaped structure with a crown formed by streptolysin O on the erythrocyte membrane. J. Bacteriol. *175*, 5953–5961.

Selkrig, J., Mosbahi, K., Webb, C.T., Belousoff, M.J., Perry, A.J., Wells, T.J., Morris, F., Leyton, D.L., Totsika, M., Phan, M.-D., et al. (2012). Discovery of an archetypal protein transport system in bacterial outer membranes. Nat. Struct. Mol. Biol. *19*, 506–510, S1.

Sentausa, E., Basso, P., Berry, A., Adrait, A., Bellement, G., Couté, Y., Lory, S., Elsen, S., and Attrée, I. (2019). Insertion sequences drive the emergence of a highly adapted human pathogen. Microb. Genomics.

Sharp, M.M., Chan, C.L., Lu, C.Z., Marr, M.T., Nechaev, S., Merritt, E.W., Severinov, K., Roberts, J.W., and Gross, C.A. (1999). The interface of sigma with core RNA polymerase is extensive, conserved, and functionally specialized. Genes Dev. *13*, 3015–3026.

Silhavy, T.J., Kahne, D., and Walker, S. (2010). The bacterial cell envelope. Cold Spring Harb. Perspect. Biol. *2*, a000414.

Simon, S.M., and Blobel, G. (1992). Signal peptides open protein-conducting channels in E. coli. Cell *69*, 677–684.

Sineva, E., Savkina, M., and Ades, S.E. (2017). Themes and variations in gene regulation by extracytoplasmic function (ECF) sigma factors. Curr. Opin. Microbiol. *36*, 128–137.

Smith, M.A., Clemons, W.M., DeMars, C.J., and Flower, A.M. (2005). Modeling the effects of prl mutations on the Escherichia coli SecY complex. J. Bacteriol. *187*, 6454–6465.

Söding, J. (2005). Protein homology detection by HMM-HMM comparison. Bioinforma. Oxf. Engl. *21*, 951–960.

Sonnenburg, J.L., and Bäckhed, F. (2016). Diet-microbiota interactions as moderators of human metabolism. Nature *535*, 56–64.

Sorenson, M.K., Ray, S.S., and Darst, S.A. (2004). Crystal structure of the flagellar sigma/anti-sigma complex sigma(28)/FlgM reveals an intact sigma factor in an inactive conformation. Mol. Cell *14*, 127–138.

Spann, D., Pross, E., Chen, Y., Dalbey, R.E., and Kuhn, A. (2018). Each protomer of a dimeric YidC functions as a single membrane insertase. Sci. Rep. *8*, 589.

Spiess, C., Beil, A., and Ehrmann, M. (1999). A temperature-dependent switch from chaperone to protease in a widely conserved heat shock protein. Cell *97*, 339–347.

Staroń, A., Sofia, H.J., Dietrich, S., Ulrich, L.E., Liesegang, H., and Mascher, T. (2009). The third pillar of bacterial signal transduction: classification of the extracytoplasmic function (ECF) sigma factor protein family. Mol. Microbiol. *74*, 557–581.

Strahl, H., and Errington, J. (2017). Bacterial Membranes: Structure, Domains, and Function. Annu. Rev. Microbiol. *71*, 519–538.

Strandén, A.M., Ehlert, K., Labischinski, H., and Berger-Bächi, B. (1997). Cell wall monoglycine cross-bridges and methicillin hypersusceptibility in a femAB null mutant of methicillin-resistant Staphylococcus aureus. J. Bacteriol. *179*, 9–16.

Stubenrauch, C.J., and Lithgow, T. (2019). The TAM: A Translocation and Assembly Module of the β-Barrel Assembly Machinery in Bacterial Outer Membranes. EcoSal Plus *8*.

Sutterlin, H.A., Zhang, S., and Silhavy, T.J. (2014). Accumulation of phosphatidic acid increases vancomycin resistance in Escherichia coli. J. Bacteriol. *196*, 3214–3220.

Sutterlin, H.A., Shi, H., May, K.L., Miguel, A., Khare, S., Huang, K.C., and Silhavy, T.J. (2016). Disruption of lipid homeostasis in the Gram-negative cell envelope activates a novel cell death pathway. Proc. Natl. Acad. Sci. U. S. A. *113*, E1565-1574.

Tam, P.C.K., Maillard, A.P., Chan, K.K.Y., and Duong, F. (2005). Investigating the SecY plug movement at the SecYEG translocation channel. EMBO J. *24*, 3380–3388.

Tibazarwa, C., Wuertz, S., Mergeay, M., Wyns, L., and van Der Lelie, D. (2000). Regulation of the cnr cobalt and nickel resistance determinant of Ralstonia eutropha (Alcaligenes eutrophus) CH34. J. Bacteriol. *182*, 1399–1409.

Tibazarwa, C., Corbisier, P., Mench, M., Bossus, A., Solda, P., Mergeay, M., Wyns, L., and van der Lelie, D. (2001). A microbial biosensor to predict bioavailable nickel in soil and its transfer to plants. Environ. Pollut. Barking Essex 1987 *113*, 19–26.

Tocheva, E.I., López-Garrido, J., Hughes, H.V., Fredlund, J., Kuru, E., Vannieuwenhze, M.S., Brun, Y.V., Pogliano, K., and Jensen, G.J. (2013). Peptidoglycan transformations during Bacillus subtilis sporulation. Mol. Microbiol. *88*, 673–686.

Trepreau, J., Girard, E., Maillard, A.P., de Rosny, E., Petit-Haertlein, I., Kahn, R., and Covès, J. (2011). Structural basis for metal sensing by CnrX. J. Mol. Biol. *408*, 766–779.

Trepreau, J., Grosse, C., Mouesca, J.-M., Sarret, G., Girard, E., Petit-Haertlein, I., Kuennemann, S., Desbourdes, C., de Rosny, E., Maillard, A.P., et al. (2014). Metal sensing and signal transduction by CnrX from Cupriavidus metallidurans CH34: role of the only methionine assessed by a functional, spectroscopic, and theoretical study. Met. Integr. Biometal Sci. *6*, 263–273.

Tsirigotaki, A., De Geyter, J., Šoštaric, N., Economou, A., and Karamanou, S. (2017). Protein export through the bacterial Sec pathway. Nat. Rev. Microbiol. *15*, 21–36.

Tsukazaki, T. (2018). Structure-based working model of SecDF, a proton-driven bacterial protein translocation factor. FEMS Microbiol. Lett. *365*.

Turner, R.D., Mesnage, S., Hobbs, J.K., and Foster, S.J. (2018). Molecular imaging of glycan chains couples cell-wall polysaccharide architecture to bacterial cell morphology. Nat. Commun. *9*, 1263.

Typas, A., Banzhaf, M., van den Berg van Saparoea, B., Verheul, J., Biboy, J., Nichols, R.J., Zietek, M., Beilharz, K., Kannenberg, K., von Rechenberg, M., et al. (2010). Regulation of peptidoglycan synthesis by outer-membrane proteins. Cell *143*, 1097–1109.

Typas, A., Banzhaf, M., Gross, C.A., and Vollmer, W. (2011). From the regulation of peptidoglycan synthesis to bacterial growth and morphology. Nat. Rev. Microbiol. *10*, 123–136.

Ulrich, L.E., and Zhulin, I.B. (2010). The MiST2 database: a comprehensive genomics resource on microbial signal transduction. Nucleic Acids Res. *38*, D401-407.

Ulrich, L.E., Koonin, E.V., and Zhulin, I.B. (2005). One-component systems dominate signal transduction in prokaryotes. Trends Microbiol. *13*, 52–56.

Uversky, V.N., and Dunker, A.K. (2010). Understanding protein non-folding. Biochim. Biophys. Acta *1804*, 1231–1264.

Valentini, M., Gonzalez, D., Mavridou, D.A., and Filloux, A. (2018). Lifestyle transitions and adaptive pathogenesis of Pseudomonas aeruginosa. Curr. Opin. Microbiol. *41*, 15–20.

Van den Berg, B., Clemons, W.M., Collinson, I., Modis, Y., Hartmann, E., Harrison, S.C., and Rapoport, T.A. (2004). X-ray structure of a protein-conducting channel. Nature *427*, 36–44.

Vandamme, P., and Coenye, T. (2004). Taxonomy of the genus Cupriavidus: a tale of lost and found. Int. J. Syst. Evol. Microbiol. *54*, 2285–2289.

Vassylyev, D.G., Sekine, S., Laptenko, O., Lee, J., Vassylyeva, M.N., Borukhov, S., and Yokoyama, S. (2002). Crystal structure of a bacterial RNA polymerase holoenzyme at 2.6 A resolution. Nature *417*, 712–719.

Veenhoff, L.M., Heuberger, E.H.M.L., and Poolman, B. (2002). Quaternary structure and function of transport proteins. Trends Biochem. Sci. *27*, 242–249.

Verwer, R.W., Nanninga, N., Keck, W., and Schwarz, U. (1978). Arrangement of glycan chains in the sacculus of Escherichia coli. J. Bacteriol. *136*, 723–729.

Vetting, M.W., S de Carvalho, L.P., Yu, M., Hegde, S.S., Magnet, S., Roderick, S.L., and Blanchard, J.S. (2005). Structure and functions of the GNAT superfamily of acetyltransferases. Arch. Biochem. Biophys. *433*, 212–226.

Villet, R., Fonvielle, M., Busca, P., Chemama, M., Maillard, A.P., Hugonnet, J.-E., Dubost, L., Marie, A., Josseaume, N., Mesnage, S., et al. (2007). Idiosyncratic features in tRNAs participating in bacterial cell wall synthesis. Nucleic Acids Res. *35*, 6870–6883.

Vogel, C., and Morea, V. (2006). Duplication, divergence and formation of novel protein topologies. BioEssays News Rev. Mol. Cell. Dev. Biol. *28*, 973–978.

Voulhoux, R., Bos, M.P., Geurtsen, J., Mols, M., and Tommassen, J. (2003). Role of a highly conserved bacterial protein in outer membrane protein assembly. Science *299*, 262–265.

Wahlström, E., Vitikainen, M., Kontinen, V.P., and Sarvas, M. (2003). The extracytoplasmic folding factor PrsA is required for protein secretion only in the presence of the cell wall in Bacillus subtilis. Microbiol. Read. Engl. *149*, 569–577.

Walker, G., Hertle, R., and Braun, V. (2004). Activation of Serratia marcescens hemolysin through a conformational change. Infect. Immun. *72*, 611–614.

Wang, H., Li, Q., Fang, Y., Yu, S., Tang, B., Na, L., Yu, B., Zou, Q., Mao, X., and Gu, J. (2016). Biochemical and functional characterization of the periplasmic domain of the outer membrane protein A from enterohemorrhagic Escherichia coli. Microbiol. Res. *182*, 109–115.

Weaver, T.M., Smith, J.A., Hocking, J.M., Bailey, L.J., Wawrzyn, G.T., Howard, D.R., Sikkink, L.A., Ramirez-Alvarado, M., and Thompson, J.R. (2009). Structural and functional studies of truncated hemolysin A from Proteus mirabilis. J. Biol. Chem. *284*, 22297–22309.

Welch, R.A. (1987). Identification of two different hemolysin determinants in uropathogenic Proteus isolates. Infect. Immun. *55*, 2183–2190.

Westblade, L.F., Ilag, L.L., Powell, A.K., Kolb, A., Robinson, C.V., and Busby, S.J.W. (2004). Studies of the Escherichia coli Rsd-sigma70 complex. J. Mol. Biol. *335*, 685–692.

Whitmore, L., and Wallace, B.A. (2004). DICHROWEB, an online server for protein secondary structure analyses from circular dichroism spectroscopic data. Nucleic Acids Res. *32*, W668-673.

Whitmore, L., and Wallace, B.A. (2008). Protein secondary structure analyses from circular dichroism spectroscopy: methods and reference databases. Biopolymers *89*, 392–400.

Wickner, W., and Schekman, R. (2005). Protein translocation across biological membranes. Science *310*, 1452–1456.

Wiehlmann, L., Cramer, N., and Tümmler, B. (2015). Habitat-associated skew of clone abundance in the Pseudomonas aeruginosa population. Environ. Microbiol. Rep. *7*, 955–960.

Wimmer, M.R., Woods, C.N., Adamczak, K.J., Glasgow, E.M., Novak, W.R.P., Grilley, D.P., and Weaver, T.M. (2015). Sequential unfolding of the hemolysin two-partner secretion domain from Proteus mirabilis. Protein Sci. Publ. Protein Soc. *24*, 1841–1855.

Winsor, G.L., Griffiths, E.J., Lo, R., Dhillon, B.K., Shay, J.A., and Brinkman, F.S.L. (2016). Enhanced annotations and features for comparing thousands of Pseudomonas genomes in the Pseudomonas genome database. Nucleic Acids Res. *44*, D646-653.

Winstanley, C., O'Brien, S., and Brockhurst, M.A. (2016). Pseudomonas aeruginosa Evolutionary Adaptation and Diversification in Cystic Fibrosis Chronic Lung Infections. Trends Microbiol. *24*, 327–337.

Woese, C.R., Kandler, O., and Wheelis, M.L. (1990). Towards a natural system of organisms: proposal for the domains Archaea, Bacteria, and Eucarya. Proc. Natl. Acad. Sci. U. S. A. *87*, 4576–4579.

van der Wolk, J.P., Fekkes, P., Boorsma, A., Huie, J.L., Silhavy, T.J., and Driessen, A.J. (1998). PrlA4 prevents the rejection of signal sequence defective preproteins by stabilizing the SecA-SecY interaction during the initiation of translocation. EMBO J. *17*, 3631–3639.

Wuethrich, I., Peeters, J.G.C., Blom, A.E.M., Theile, C.S., Li, Z., Spooner, E., Ploegh, H.L., and Guimaraes, C.P. (2014). Site-specific chemoenzymatic labeling of aerolysin enables the identification of new aerolysin receptors. PloS One *9*, e109883.

Wuichet, K., Cantwell, B.J., and Zhulin, I.B. (2010). Evolution and phyletic distribution of two-component signal transduction systems. Curr. Opin. Microbiol. *13*, 219–225.

Yan, Y., Barlev, N.A., Haley, R.H., Berger, S.L., and Marmorstein, R. (2000). Crystal structure of yeast Esa1 suggests a unified mechanism for catalysis and substrate binding by histone acetyltransferases. Mol. Cell *6*, 1195–1205.

Yang, F.L., and Braun, V. (2000). ShlB mutants of Serratia marcescens allow uncoupling of activation and secretion of the ShlA hemolysin. Int. J. Med. Microbiol. IJMM *290*, 529–538.

Yuan, A.H., Gregory, B.D., Sharp, J.S., McCleary, K.D., Dove, S.L., and Hochschild, A. (2008). Rsd family proteins make simultaneous interactions with regions 2 and 4 of the primary sigma factor. Mol. Microbiol. *70*, 1136–1151.

Zachowski, A. (1993). Phospholipids in animal eukaryotic membranes: transverse asymmetry and movement. Biochem. J. *294 (Pt 1)*, 1–14.

Zakeri, B., Fierer, J.O., Celik, E., Chittock, E.C., Schwarz-Linek, U., Moy, V.T., and Howarth, M. (2012). Peptide tag forming a rapid covalent bond to a protein, through engineering a bacterial adhesin. Proc. Natl. Acad. Sci. U. S. A. *109*, E690-697.

Zambolin, S., Clantin, B., Chami, M., Hoos, S., Haouz, A., Villeret, V., and Delepelaire, P. (2016). Structural basis for haem piracy from host haemopexin by Haemophilus influenzae. Nat. Commun. *7*, 11590.

Zhang, Y.-M., and Rock, C.O. (2008). Membrane lipid homeostasis in bacteria. Nat. Rev. Microbiol. *6*, 222–233.

Zhao, H., Patel, V., Helmann, J.D., and Dörr, T. (2017). Don't let sleeping dogmas lie: new views of peptidoglycan synthesis and its regulation. Mol. Microbiol. *106*, 847–860.

Ziani, W., Maillard, A.P., Petit-Härtlein, I., Garnier, N., Crouzy, S., Girard, E., and Covès, J. (2014). The X-ray structure of NccX from Cupriavidus metallidurans 31A illustrates potential dangers of detergent solubilization when generating and interpreting crystal structures of membrane proteins. J. Biol. Chem. *289*, 31160–31172.

Zou, Z., Qin, H., Brenner, A.E., Raghavan, R., Millar, J.A., Gu, Q., Xie, Z., Kreth, J., and Merritt, J. (2018). LytTR Regulatory Systems: A potential new class of prokaryotic sensory system. PLoS Genet. *14*, e1007709.

Zschiedrich, C.P., Keidel, V., and Szurmant, H. (2016). Molecular Mechanisms of Two-Component Signal Transduction. J. Mol. Biol. *428*, 3752–3775.

Zückert, W.R. (2014). Secretion of bacterial lipoproteins: through the cytoplasmic membrane, the periplasm and beyond. Biochim. Biophys. Acta *1843*, 1509–1516.

Stories from the wall:

Envelope-associated functions in bacteria

Focus on cell wall synthesis, protein secretion & signal transduction machineries.

Abstract

Bacterial cells are enclosed within an envelope that displays several layers: the cytoplasmic membrane, the periplasmic space or equivalent and the peptidoglycan-based cell wall, made complete with teichoic acids or an outer membrane. The bacterial envelope serves as a physical scaffold, a selective diffusion barrier and a functional hub altogether. By electing projects on peptidoglycan synthesis, protein translocation and signal transduction, I have made my research experience relate to all of these properties. My present project aims at understanding how the exolysin that is the main virulence factor of *P. aeruginosa* clonal outliers and a pore-forming toxin, acquires its functional properties upon secretion and achieves function upon target membrane encounter. This somehow sounds like an echo of my predoctoral research, when I investigated fungal or snake toxins and a viral membrane-fusion protein. I have always been attracted to questions revolving about structure:function relationships. In my experience, it feels even better when there's a border to cross.